2014

Use Of Rna Aptamers For Enhanced Drug Therapy And Imaging

Supipi Liyamali Auwardt
Iowa State University

Use of RNA aptamers for enhanced drug therapy and imaging

by

Supipi Auwardt

A thesis submitted to the graduate faculty

in partial fulfillment of the requirements for the degree of

MASTER OF SCIENCE

Major: Chemistry

Program of Study Committee:
Marit Nilsen-Hamilton, Co-Major Professor
Arthur Winter, Co-Major Professor
George Kraus

Iowa State University

Ames, Iowa

2014

To My Family and Teachers.

TABLE OF CONTENTS

LIST OF FIGURES

LIST OF TABLES

CHAPTER 1: GENERAL INTRODUCTION: DISSERTATIONAL ORGANISATION

This dissertation has 3 chapters.

Chapter 1 includes a general introduction to the organization of the dissertation and the significance of the study included in the dissertation.

The second chapter of this dissertation is a literature review that describes the work related to reported experimental studies. Aptamers are introduced in the first section of the second chapter. Then, a survey of the literature regarding therapeutically important aptamers and aptamers expressed *in vivo* are discussed. In this section, aptamers in all stages of clinical development and also aptamers utilized in various diseases such as cancer, diabetes are described. In the next section, on the topic of *in-vivo* expressed aptamers, other aptamers, such as those selected against the human immunodeficiency virus proteins are also discussed. How these various aptamers might aid in disease prevention or cure is also discussed in detail. In the next section of the literature review aminoglycoside antibiotics are described. The section starts with an introduction to aminoglycoside antibiotics. Then the aminoglycoside structure is described. This is followed by a discussion of how the aminoglycosides elicit their antibacterial effects. In addition, mechanisms that bacteria use to resist the effects of aminoglycoside antibiotics are also discussed.

The current study is based on a mathematical model for the intracellular activity of aptamers, which proposes that aptamers or other small receptors for drugs can be used to increase the intracellular concentration of free (not aptamer-bound) drugs in target cells. This is discussed in the next section. In this study the model was tested using aptamers that recognize aminoglycosides. Therefore, aptamers selected to bind aminoglycoside antibiotics are introduced and the binding mechanisms of ligand with the aptamers are described. Natural and synthetic RNA that can bind with aminoglycosides are described in this section. The next section reviews bacterial cell structure, their growth phases and the inoculum effect. Throughout the entire study reported here, *Escherichia coli* bacterial cells were used for experimentation. Therefore, the review focuses on the growth characteristics of *E. coli*. First, the *Escherichia coli* morphology

and extracellular and the intracellular structural elements are described. Then, the growth of the *E. coli* is reviewed with reference to the various growth phases. In addition, the inoculum effect is described, which applies to the response of bacteria to certain aminoglycosides and other drugs. The mathematical model proposes that the mobility of the drug receptors is important. Therefore, the mobility of molecules in cells is reviewed. In this section first physical theories behind the mobility of molecules inside the cells are considered. Then techniques utilized to observe and measure mobility of molecules inside the cell are described. Two of the most mobile molecules in the cell are RNA and proteins. In this dissertation we concentrate on RNA aptamers. Therefore studies in of RNA mobility are discussed and related aspects of protein mobility inside the cells are also reviewed. Finally, the chapter of literature review ends with a discussion of research results related the study described in the dissertation.

Chapter three describes studies in which aptamers were used to increase the intracellular drug concentrations in order to obtain more effective killing of cells. This study is focused on cancer cells, which require a very high drug concentration in order to obtain an effective killing of cancer cells. A major challenge in cancer treatment today is to provide a high enough drug concentration in order to obtain an effective killing of cancer cells. Cancer, medically known as malignant neoplasm is a disease that involves unregulated cell growth. Cancer cells have biological mechanisms that allow them to resist drug treatments, such as by increasing the expression of multi drug efflux pumps. Therefore, when undergoing chemotherapy, cancer patients should be given concentrations of drugs as high as possible in order to effectively destroy all the cancer cells. But, most drugs used in cancer chemotherapy are generally cytotoxic. Thus, providing these drugs in high concentrations without targeted delivery can also be harmful to healthy cells. Since general toxicity of chemotherapy treatments is one of the major causes for deaths among cancer patients, increasing the effective intracellular drug concentration is extremely important. For this reason, the current study to test the ability of aptamers to increase the intracellular concentrations of drugs was initiated. Before testing this idea in cancer cells, the simpler *Escherichia coli* bacterial cells were used as a model system. In this model system aminoglycoside aptamers that had been selected to bind with aminoglycosides with high specificity and affinity were used. These aminoglycoside RNA aptamers were cloned downstream of the T7 RNA polymerase promoter in an expression vector and used to test the questions: 1) can intracellular aptamers increase the concentration of drug in a cell?. And 2) can

intracellular aptamers increase the concentration of free drug (not bound to the aptamers) in the cell?. The first question was tested with Cy3-paromomycin that was used to determine the effect of expressing aptamers on the intracellular concentration of the drug. The second question was tested by determining the effect of aptamer expression on the growth of *E. coli* cells. If the expression of aptamers in the cells increases the concentration of free drug (which is not bound to the aptamer) that can bind to the ribosome and kill the cell, then the IC50 (half maximal inhibitory concentration) and the MIC (minimum inhibitory concentration) for the drug should decrease with aptamer expression. Both questions were answered in the affirmatory as demonstrated with the data shown in Chapter 3.

CHAPTER 2: LITERATURE REVIEW

Aptamers

Introduction to aptamers

Aptamers are synthetic, single stranded nucleic acid molecules that fold into unique 3D structures allowing them to bind specifically and with a high affinity to their target molecules. There are also peptide aptamers although this discussion will focus on nucleic acid aptamers. The name aptamer comes from the latin *aptus* meaning to fit and Greek *meros* meaning regions (1). Therefore the word aptamer describes the oligonucleotide or peptide as having high specificity and affinity towards its target. In this sense, aptamers are the chemical equivalents of antibodies. In the therapeutic front, aptamers are always in competition with small molecules and antibodies. Aptamers can be used for therapeutic purposes in the same way as monoclonal antibodies. There are both advantages and limitations for the use of aptamers (1). One advantage of aptamers compared to antibodies is that aptamers can be produced chemically by readily scalable processes whereas antibody production requires traditional methods involving living organisms or cultured mammalian cells. Because of the biological mode production of antibodies, it is difficult to scale up production without affecting the product quality and characteristics. Antibody production is more prone to viral and bacterial contaminations that affect the product quality. On the other hand, the chemical production process of aptamers is not prone to bacterial and viral contamination. Aptamers are non- immunogenic whereas antibodies often elicit immunogenic reactions. The smaller sizes of aptamers allow them efficient entry into many biological compartments. But it also makes them susceptible to renal filtration which leads to a shorter blood half-life. On the other hand, although the larger size of antibodies prevents renal filtration giving them a longer half-life it also prevents their access to many biological compartments thus reducing their bioavailability. The short half-life of aptamers has been overcome by the addition of conjugation partners such as polyethylene glycol or cholesterol to increase the half-life. Also, the chemistries required for the addition of such conjugation partners to antibodies are nonspecific and therefore can produce mixtures of derivatives and reduced activity. Another advantage of aptamers is that they can be reversibly denatured and the phosphodiester bond is chemically very stable. Antibodies are irreversibly denatured and the shelf life is limited. But antibodies are not susceptible to nuclease degradation in the serum

whereas unmodified aptamers are highly inclined to nuclease degradation. Chemical modifications incorporated into the sugars or internucleotide phosphodiester linkages enhance nuclease resistance and such modifications of aptamers can be readily introduced during synthesis.

Aptamers exhibit high affinities for their targets with Kd values often in the low nanomolar to picomolar range (2). Aptamers are very selective for their targets. In some instances, the specificity of aptamers enables their discrimination between closely related isoforms or different conformational states of the same target molecule (3). However, aptamers that recognize mouse and human protein targets with equal affinities can also be selected, making them suitable for both preclinical and clinical studies (4). Aptamers also have the ability to retain their specific binding ability and inhibitory behavior even after tagging with functional groups, delivery into animals and immobilizing on carrier materials (5).

Aptamers are usually selected from random pool of oligonucleotide sequences libraries, but natural aptamers also exist in riboswitches (6). The process of selecting aptamers from oligonucleotide sequence libraries is termed as SELEX, standing for "Systematic Evolution of Ligands by Exponential enrichment". In 1990 two labs independently developed this technique of selection (7,8). The Gold lab, used the term SELEX for their process of selecting RNA ligands against T4 DNA polymerase and the Szostak lab used the term *In vitro selection* for selecting RNA ligands against various organic dyes. The SELEX procedure is now highly recognized as a powerful tool for obtaining nucleic acid aptamers for almost any target molecule that can bind the nucleic acid with a high affinity and specificity. Since the discovery of aptamers and the SELEX procedure, many aptamers have been selected against a variety of targets molecules ranging from small molecules (9), peptides and amino acids (10,11), antibiotics and aminoglycosides (12), vitamins, carbohydrates and cell membrane proteins (13). Because SELEX is an *in vitro* process there is limitless opportunity for aptamers that recognize more and more target molecules and condition of selection. Therefore, new aptamers for different target molecules continue to be reported.

Aptamers as therapeutics

On the therapeutics front aptamers are new reagents although one aptamer is already in the market as an aptamer-based drug. Aptamers are also in several stages of development as

preclinical, clinical to FDA approved drugs (13). Aptamers have been developed as anticancer (14), antiangiogenesis (15), anticoagulation (16), for diabetes (17), antiviral (18) and antimicrobial (19).

AS 1411 is a 26 nt G-rich DNA aptamer and one of the first reported anticancer aptamers. AS1411 targets nucleolin, a nuclear matrix protein that can also be found on the surfaces of the cancer cells. AS1411 consists only of guanines and thymines. AS1411 was not discovered by the general SELEX procedure but as a part of a screen for antisense oligonucleotides for antiproliferative activity (20). The AS1411 aptamer has been very effective in many preclinical cancer and animal models such as human breast cancer, lung cancer, pancreatic cancer and acute myelogenous leukemia (21). The proposed mechanism of anticancer activity by AS1411 is that internalization of the aptamer by cell surface nucleolin and subcellular inhibition of the transcription factor, nuclear factor-κB (22) also destabilization of the mRNA encoding the anti-apoptotic, B-cell lymphoma protein 2 (BCL2) (23). AS1411 is being developed by Antisoma Research and currently on phase II clinical trials for acute myeloid leukemia.

Another aptamer developed for cancer treatment is the NOX-A-12 aptamer. NOX-A-12 aptamer is in clinical development by NOXXON Pharma AG. It is a spiegelmer selected by a variation of the SELEX procedure. Spiegelmers are selected from a wild type (D-RNA) library using mirror image target (D-amino acids), but they are synthesized as L-RNA in order to bind with the wild type target (L-amino acids) (13). The reason for selecting this type of aptamer is that the L-RNA aptamer that binds to the natural target is resistant to nuclease degradation. Therefore they are stable in human plasma for over 60 hours at 37^{0}C. NOX-12 was selected to bind to chemokine ligand 12, which is a chemokine involved in angiogenesis, cell homing, tumor metastasis and tissue regeneration. The NOX-A-12 aptamer is 45nt L-RNA aptamer conjugated at the 3’ end with polyethylene glycol (PEG). It is currently under phase IIa clinical trial for the treatment of chronic lymphocytic leukemia (CML), multiple myeloma. NOXXON has also developed clinical trials for NOX-A-12 in glioblastoma.

Aptamers are also being developed as anti-coagulation agents. Anticoagulants are a major class of pharmaceutical agents used to prevent blood clotting in clinical procedures and in cardiovascular diseases. Heparin, highly sulfated glycosaminoglycan is currently being used as an anticoagulant, but it has some negative effects such as spontaneous hemorrhage and reduction

of blood platelet. Also heparin produces allergic reactions in some patients. Due to these reasons much attention has been given to discovering novel anticoagulants. One such novel discovery is NU172 DNA aptamer, selected to bind and inhibit thrombin. Thrombin is a serine protease and a key activator of several proteins in the coagulation cascade. NU172 was selected by the SELEX procedure from DNA library and later truncated to 26nt long without additional modifications. NU172 is administered intravenously during cardiovascular surgical procedures to prevent blood clotting. NU172 aptamer is currently undergoing phase II clinical trials to be used for anticoagulation in heart disease treatment by ARCA Biopharma.

A breakthrough in aptamer technology occurred in December 2004, when the FDA approved the first aptamer based drug. Pegaptanib, brand name Macugen, is an anti-vascular endothelial growth factor (VEGF) RNA aptamer. It is an anti-angiogenic therapeutic agent for neovascular (wet) age-related macular degeneration (AMD), a disease in the eye that causes loss of central vision leaving only peripheral or side vision intact (24). The target of Pegatanib is $VEGF_{165,}$ the most abundant VEGF isoform that regulates vascular permeability. Pegatanib binds to the heparin binding domain of the $VEGF_{165}$ and inhibits VEGF binding to its receptor, thereby inhibiting the growth of blood vessels. During selection Pegatanib was only modified at pyrimidine residues by using 2'-fluoro substituted precursors. After selection of the aptamer the purines were stabilized by 2'-O-methyl residues resulting in high nuclease resistance. To increase the half-life and stability of the aptamer in the biological conditions the 5' terminus was also modified by 40 kDa polyethylene glycol (PEG) along with an inverted 3'-3'-deoxythymidine cap (25).

Phase I clinical trials for aptamers in diabetes have also been performed using the spiegelmer, NOX-E36. This aptamer binds to chemokine ligand 2, a cytokine involved in recruiting monocytes, T cells and dendritic cells to the site of injury. NOX-E36 greatly decreases glomerulosclerosis in type 2 diabetes in mouse models (17). NOX-E36 is 40nt aptamer with 3'-terminal PEG9 (26).

Aptamers expressed inside the cells

Aptamers selected by *in vitro* SELEX procedure has been used for inside the cells to serve many purposes (27). There is a new appreciation for the role that can be played by aptamers both *in vitro* and *in vivo*. Aptamers selected by SELEX are being used inside the cell for several

purposes including (1) to antagonize the normal cellular proteins as method of elucidating their biological roles (2) as a decoy of naturally occurring RNA binding proteins to dissect their function (3) to regulate the expression of exogenous genes and (4) to counteract disease related targets for potential biomedical applications.

Binding of an RNA aptamer to its target often inhibits the target's activity *in vitro* (28). Most aptamers have their origins in test tubes; therefore there is no inferential reason as to why they would work in the same way *in vivo*. But, in many instances *in vitro*-selected aptamers retain their binding ability inside the cells. One example is an RNA aptamer designated FC that bind RNA polymerase II holoenzyme from the yeast *Saccharomyces cerevisiae* with dissociation constant (Kd) of 20nM (29). Aptamer FC inhibits *in vitro* transcriptional initiation but not elongation, by RNA Pol II. Also this aptamer does not inhibit *in vitro* transcription by RNA Pol I or RNA Pol III of *S. cerevisiae* by Pol II from *Saccharomyces pombei*. To observe the RNA Pol II inhibition in *S. cerevisiae* by the FC aptamer, DNA encoding the aptamer was cloned downstream of a Pol III dependent RNase P RNA promoter (RPR1) and expressed in yeast cells. The large subunit of RNA Pol II was then placed under the LEU 2 promoter. When these cells were placed in leucine-rich medium, transcription from the LEU2 promoter was suppressed resulting in low Pol II levels, but overall cell growth was not affected. Cells expressing the FC aptamer grew normally in low leucine medium while their growth was drastically inhibited in high leucine medium. Also aptamer expression in otherwise wild type cells did not affect the cell growth. In this example it shows that inhibition of yeast RNA Pol II had a distinct effect only when RNA Pol II concentration was limiting.

One instance where aptamers were used to investigate the function of RNA binding proteins in natural transcripts was a study by Shi *et al.* of the anti SR protein B52 aptamer (30). SR proteins are required in *Drosophila* for constitutive and alternate pre-mRNA splicing. Over expression or deletion of B52 protein results in severe growth defects in *Drosophila*. Shi *et al.* (30) selected an aptamer that binds protein B52 with a K_d of 20-50 nM. They expressed this aptamer in *Drosophila* as a multimeric array of 5 aptamers and observed the growth effects (31). For transgenic flies that carried the aptamer array, but which were otherwise wild type, survival to adulthood was reduced by 50 percent. For flies engineered to over express B52, the developmental defects were largely rescued.

Another example of an aptamer selected *in vitro* that retains its binding activity *in vivo* is an RNA aptamer selected against the nucleocapsid protein of the human immunodeficiency virus-1 (32). When expressed in cells, this aptamer prevented packaging of the viral genomic RNA (33). The same aptamer inhibited the nucleocapsid binding to the stable transactivation response hairpin and psi RNA stem loops of HIV-1 RNA (33).

Aptamers selected to bind with small molecules have also been used as functional units *in vivo*. Grate and Wilson (34) showed that, when inserted in the 5' UTR of the cyclin transcript in the *Sacchromyces cerevisiae*, an aptamer sequence selected to bind with malachite green reduced the rate of cell cycle transit depending on the absence or the presence of the target ligand. The malachite green binding motif of the aptamer which is an internal bulge flanked by short RNA helices, was inserted immediately upstream of the CLB2 start codon. When tetramethylrosamine (a fluorescent malachite green analogue) was added to the aptamer containing yeast strain, progress through the cell cycle was significantly slowed and elongated bud morphology was observed. Quantification of the CBL2 expression at the RNA and protein levels by RT-PCR and western blot analysis, respectively, showed that aptamer ligand interaction regulated the transcript translatability rather than the transcript stability. They also performed one dimensional NMR spectroscopy to demonstrate that ligand binding to the aptamer results in a significant change in the structure of the aptamer with many nucleotides folding to adopt a well-defined conformation. With these results they concluded that translational initiation is blocked by a ligand induced conformational change in the 5'-UTR. Wersturk and Green (28) showed that when RNA aptamers selected to bind with the small antibiotic molecules tobramycin and kanamycin were present in the 5' UTR of an mRNA construct they could repress the translation of that gene in an *in vitro* translation assay. They inserted three copies of the tobramycin binding aptamer in the 5' UTR of an mRNA construct and cap dependent translation in wheat germ extract was near normal when no antibiotic was present, but was reduced to ten percent in the presence of 60 μM tobramycin. No growth inhibition was observed when the 5' UTR had no aptamer or when 60 μM kanamycin was used in place of tobramycin with the tobramycin multi aptamer (28). They translated the mRNA construct containing the aptamer *in vitro* in the presence of [^{35}S] methionine using a wheat germ extract. The protein products were analyzed by SDS-polyacrylamide gel electrophoresis (PAGE) and quantified by densitometry. Wersturk and Green also replaced the aminoglycoside aptamers with one copy of the Hoechst aptamer in the 5'

UTR of a mammalian β-galactosidase RNA in an expression plasmid. Chinese hamster ovary cells (CHO) were transfected with this plasmid. As a control, another vector without Hoechst aptamer was used. The luciferase reporter gene was used to provide an internal control. Addition of the Hoechst dye after 24 h transfection reduced β-galactosidase activity to five to ten percent of that observed without the dye. In the absence of the dye binding aptamer in the 5'UTR neither β-galactosidase nor luciferase activity (from co-transfected control DNA) was affected by the addition of the dye proving that dye itself has no global effect on translation. This technique can be utilized in gene therapy applications. That is activity of an exogenous transfected gene could be regulated through small molecules for which the dosage can be controlled. Aptamers interactions with small molecule targets are also retained in bacterial cells. Wersturk and Green (28) expressed tobramycin and kanamycin aptamers in *E. coli* that were then incubated with the aminoglycosides, tobramycin or kanamycin, respectively. Expressing one copy of the aminoglycoside aptamer allowed bacterial cells to grow at otherwise lethal concentrations of aminoglycosides. Expressing three copies of the aptamer allowed more vigorous growth than expressing one copy at otherwise lethal aminoglycoside concentrations. They concluded that the aptamers rescued the cells from killing by the aminoglycosides because they competed with the ribosome for binding these inhibitors.

One very important aspect of *in vivo* expressed aptamers is their potential biomedical applications. In the previous section on aptamers in therapeutics, aptamers directed against extra cellular targets were discussed. This potential has promoted the development of pharmaceutical companies like Archemix, NexxonPharma AG, Gilead science, Ribozyme Pharmaceutical and others. However, the ability of *in vitro* selected aptamers to function *in vivo* expression adds to the possibilities for medical and other applications. As the following examples suggest, there is substantial promise that aptamers can eventually be used to treat diseases like cancer, inflammatory diseases, sleeping sickness and Acquired Immune Deficiency Syndrome (AIDS).

Curing diseases caused by viruses has been a challenge for decades, especially after the emergence of Human Immunodeficiency Virus (HIV). Although there are some therapeutics for HIV, they are often unsuccessful because of drug resistance conferred by mutations in the viral genome. One of the essential proteins of HIV is its Reverse Transcriptase (RT), which converts the RNA genome into double stranded DNA that can be inserted into the host genome.

It is important to target an essential gene product such as RT for efficient prevention of the disease. Therapeutics against RT is one of the most novel forms of antiviral remedies for HIV today. Aptamers directed against RT inhibits its polymerization activity *in vitro* (35). Aptamers selected to bind RT fold as pseudo-knots inside the cells and bind with RT with K_ds in the low nanomolar range. Recently a new aptamer was discovered that binds RT with a K_d in the low picomolar range (36). The ability of this anti RT aptamer to disrupt the RT activity in *E. coli* has already been assayed (37).

One drawback of antiviral therapeutics is that the therapeutics cannot keep up with the high mutation rate of viruses. In that context aptamers have an attractive solution to this problem, because refinements of aptamers can generate aptamers that can inhibit the mutant viral forms.

Homann and Goringer (38) reported an aptamer that binds with the outer surface of the live *Trypanosoma brucei*, the parasite responsible for sleeping sickness. This aptamer binds a single 42 kDa protein located at the base of the flagella apparatus on the trypanosome. This flagella pocket is responsible for transporting cargo in and out of the parasite. The authors have shown that, after endocytosis of the aptamer, there is a secondary structural core that remains intact in the parasite's lysosome. Also they show, using biotinylated or fluorescently-tagged aptamers, that these aptamers can be used to shuttle materials into the trypanosome. Although this aptamer does not destroy the parasite it can be utilized to deliver materials to kill the parasite.

The examples given above bring out some important aspects of aptamers for their use as therapeutics and as *in vivo* expressed aptamers. One very striking aspect is that *in vitro* selected aptamers retain their binding characteristics even when they are expressed inside the cells. These results emphasize two important factors of *in vivo* expressed aptamers. First, aptamers retain their binding and inhibitory ability inside the cells. Second, it is very important to balance the level of aptamer accumulation, target expression level and cell sensitivity to target expression level. Being very amenable to modification and optimization, aptamers provide an exciting route for future research and application.

Aminoglycoside antibiotics

Structure of aminoglycosides

Aminoglycoside antibiotics are one of the earliest known classes of antibiotics with a broad spectrum activity against gram-negative and gram-positive bacteria, as well as mycobacterium. They are poly cationic molecules with high flexibility. Aminoglycosides have amino sugars, glycosidically linked to aminocyclitols. The aminoglycosides have been classified into two major groups depending on whether the aminocyclitol is of the streptidine or 2-deoxystreptamine class (39). The 2-deoxystreptamine class of aminoglycoside is further categorized depending on the linkage of amino sugars to the non-sugar 2-deoxystreptamine ring. Tobramycin (Figure 1), which belongs to the kanamycin subgroup of antibiotics, has pyranose sugars attached at the 4 and 6 positions of the 2-deoxystreptamine ring. Neomycin-B (Figure 1) along with paromomycin and lividomycin belong to the neomycin subgroup of aminoglycoside antibiotic that has a pyranose sugar attached to the 4 position and a furanose-pyranose pair of sugars attached to the 5 position of the 2-deoxystreptamine ring. Aminoglycosides, being poly cationic molecules, bind various RNA molecules and inhibit their biological activity.

Role of aminoglycosides in bacterial growth inhibition

Aminoglycosides achieve their antibiotic activity by interfering with protein synthesis in prokaryotic cells. The Neomycin class of aminoglycoside antibiotics bind to the 16S ribosomal RNA and inhibit protein synthesis (40). Uptake of aminoglycosides occurs in three phases; first they bind with negatively charged lipopolysaccharides, phospholipids, and negatively charged segments of protein on the cell wall and the plasma membrane of gram-negative prokaryotes because of their polycationic nature at physiological pH (41,42). Bound aminoglycosides displace the Mg^{2+} and Ca^{2+} ions that bridge the lipopolysaccharides in the outer membrane and disrupt membrane integrity. The second phase of aminoglycoside uptake is an energy and concentration dependent process (43). This phase is called as the Energy Dependent phase I (EDPI) (41). This process requires threshold potential (Δp) generated by a proton motive force. The third phase of aminoglycoside uptake is also energy dependent, called Energy Dependent phase II (EDPII), and involves an accelerated linear rate of aminoglycoside transport across the cytoplasmic membrane by a process that uses energy from electron transport and hydrolysis of adenosine triphosphate (ATP). This is supported by the observation that aminoglycoside uptake

during EDPII can be inhibited by cyanide, sulfhydryl reagents and uncouplers of oxidative phosphorylation (42). The binding of aminoglycosides to the ribosome results in interference with translation, incorporation of nonfunctional mis-read proteins into the membrane, and disruption of membrane integrity. This in turn increases the membrane leakiness to aminoglycosides.

Translation of mRNA into protein is a complex process that occurs on the ribosome and requires decoding of the genetic code by selection of the correct amino-acyl-tRNAs. The integrity of aminoacyl-tRNA selection involves selection of the correct amino acyl-tRNA and proofreading by the ribosome. Aminoglycosides disrupt the decoding process by promoting misreading of the genetic code through their interaction with specific sites in the 16S rRNA (44). In the decoding process the anticodon triplet on the tRNA pairs with its cognate codon on the mRNA and protects bases on the 16S rRNA from chemical modification in the same region as the aminoglycosides bind. The decoding site consists of nucleotides 1400-1410 and 1490-1500 that form a stem-loop-stem structure, which is also known as the A site of the *Escherichia coli* ribosome (45). Decoding is accomplished by the interaction of the A site with the backbone of the codon-anticodon helix, thereby protecting the position N1 of A1492 and A1493 from chemical modification (44). The result of aminoglycoside binding by the A-site is dislocation of two conserved adenine residues, A1492 and A1493 to minor groove of the A site. This conformational change turns the A-site into high affinity site to tRNA-mRNA interaction thus reducing the rejection rate for near cognate tRNAs. In this way aminoglycosides inhibit the translocation of the tRNA-mRNA from the A-site to the peptidyl-tRNA site (P-site). Thus aminoglycosides cause a misreading of the genetic code and produce misread proteins. For some time, obtaining a high resolution structure of aminoglycoside bound to the ribosome "A site" was not possible due to the large size of the ribosome. Therefore an alternative approach was adopted of determining the solution structure of a subdomain of the *E. coli* 16S rRNA bound with aminoglycoside using Nuclear Magnetic Resonance (NMR). **Figure 2** shows the NMR solution structures of 27mer A-site RNA alone and **Figure 3** shows the NMR solution structure of 27 mer A site RNA bound with paromomycin (46) , **Figure 4** shows the secondary structure of the A-site RNA, with the bases that are protected by the neomycin class of aminoglycosides indicated by the triangles. The antibiotic binding site is the asymmetric internal loop (shown in blue in figure 2) that is defined by a Watson-Crick base pair C1407-G1494 at its outer limits and

by the non-canonical base pairs U1406-U1495 and A1408-A1493. The upper and lower stems are connected by a continuous interrupted helix with a widened major groove that allows docking of the antibiotics. The antibiotic binding pocket is composed of the base pairs A1408-A1493 and the single bulged adenine A1492. Rings I and II of the aminoglycosides have specific contacts with the RNA. As an example, in the complexes of paromomycin **(Figure 3)**, ring I is stacked upon G1491 and ring II is spans the base pairs U1406-U1495 and C1407-G1494. Ring III of paromomycin is positioned differently. Binding of the aminoglycosides to RNA induces a conformational change in the RNA, displacing the two universally conserved residues A1492 and A1493 toward the minor groove, thus switching the A-site into a higher affinity site for mRNA-tRNA recognition and reducing the rejection rate of near-cognate tRNAs (46). This increased affinity of the A-site for tRNA is believed to result in misreading of the genetic code. This NMR structure of the A-site provided the first structural rationale for the functioning of decoding site. One very important outcome of work of Puglisi *et al*. (47) was the finding that the decoding site is an irregular helix that bind antibiotics by its major groove and makes contact with the anticodon on the tRNA through its minor groove. The first evidence that formation of the codon-anticodon complex includes contact through the 2' hydroxyl group of the codon was finding that the 2' hydroxyl group in the mRNA is required for tRNA binding (48). The additional evidence of rescue of a mutation in the A-site by 2' modifications of the codon resulted in the proposal that minor groove-minor groove interactions between the decoding site and the mRNA stabilize the codon-anticodon duplex (49). In summary, the biochemical and biophysical evidence locates the aminoglycoside binding site on the ribosome as the adenine-rich internal loop at the 3'-end of the helix 44 in the 16S rRNA of the 30S ribosomal subunit, the latter consists of 16S rRNA and 21 proteins. The helix 44 binds aminoglycosides through its major groove and connects with the codon-anticodon complex via its minor groove. Paromomycin, neomycin and other aminoglycosides can also prevent assembly of the 30S subunit resulting in the accumulation of the 21S intermediate that is required for 30S subunit formation. Aminoglycosides bind preferably with prokaryotic ribosomes over eukaryotic ribosomes resulting in selective protein synthesis inhibition of prokaryotes. Therefore these aminoglycosides have been used as antibacterial drugs for a long time.

As with other antibiotics, the challenge of multi drug resistance includes aminoglycosides. The misuse of aminoglycosides has resulted in bacteria that are resistant to their effects. There are

three major mechanisms by which bacteria resist aminoglycosides; which are: 1) inactivation of aminoglycoside drugs by aminoglycoside modifying enzymes, 2) ribosome alteration, and 3) decreased permeability to aminoglycosides. Of these, modifying the ribosome is not very common because the ribosome is the center of the protein synthetic machinery and is well conserved over evolution. But there are reports that modified ribosomes can lead to bacterial resistance. For example, ribosome alterations brought problems in treating tuberculosis (50).Streptomycin is used for *Mycobacterium tuberculosis.* Streptomycin acts by binding to the16S rRNA of *Mycobacterium tuberculosis* and interferes with protein synthesis. All the streptomycin-resistant *Mycobacterium tuberculosis* isolates have point mutations that result in changes in the streptomycin binding site (50). The second way of developing aminoglycoside resistance is by changing permeability for the aminoglycosides. One major mechanism by which microorganisms achieve is this by up regulating the expression membrane efflux pumps (51). Efflux pumps are transport proteins involved in extrusion of toxic substance (including all of antibiotics) from the interior to the exterior of the cell. These are present in gram negative, gram positive and eukaryotic cells. In prokaryotic cells there are five major families of efflux transporters. Those are MF (major facilitator), MATE (Multidrug and Toxic Extrusion), RND (Resistant Nodulation Division), SMR (Small Multidrug Resistance) and ABC (ATP Binding Cassette) (52). Aminoglycosides are exported from *E. coli* by the AcrD pump, which belongs to the RND family (53). Drug efflux promoted by AcrD is mainly determined by a pair of large loops containing more than 300 amino acid residues each, which reside in the periplasmic space (52,53). The third method by which aminoglycoside resistance is achieved is by the action of aminoglycoside modifying enzymes. There are three major classes of aminoglycoside modifying enzymes. This classification was made based on the specific biochemical reaction these enzymes catalyze. They are 1) acetyltransferase (AAC) that transfer the acetyl group of acetyl CoA to an amino group of the aminoglycoside; 2) adenyltransferases (ANT) that transfer the adenosine unit of ATP to a hydroxyl group of an aminoglycoside or 3) phosphotransferases (APH) that transfer a phosphate group of ATP to a hydroxyl group of an aminoglycoside (54). Enzymes of these three classes have been classified into subclasses depending on the position they modified functional group. Acetyltransferases (AAC) modifies amino groups at 1, 2', 3 and 6'. Therefore, further classification of these enzymes would be AAC (3), AAC (6') and so on. The phosphotransferases (APH) are further classified as APH (3'), APH (3"), APH (4), APH (6),

APH (7") and APH (9) depending on the modified hydroxyl group on the aminoglycosides. The adenyltransferases (ANT) are classified as ANT (2"), ANT (3"), ANT (4'), ANT (6) and ANT (9) depending on the modified hydroxyl group on the aminoglycoside. Also, groups of enzymes are further classified into subgroups depending on the individual substrate profile. For an example in the AAC (3) family there are at least 9 members named ACC (3)-I, AAC (3)-II and continuing up to AAC (3)-X. Aminoglycoside resistance is more complicated by the fact that there is more than one gene encoding for one AAC enzyme type. As an example in the enzyme family of AAC (6')-I there are more than 18 specific genes (55). Therefore the battle with aminoglycoside drug resistance in bacteria is complicated.

Aminoglycoside aptamers

Small RNA-aminoglycosides have been well-studied over the past few decades (28). Using thermodynamic and electrostatic experimental evidence, Jin *et al.* (56) demonstrated that aminoglycosides are major groove binders in duplex RNA. They used a combination of spectroscopic, calorimetric, viscometric and computational modeling techniques to characterize binding of the aminoglycoside tobramycin to the polymeric RNA duplex poly(rl).poly(rC), which adopts a distinct A-type conformation that is very common among the natural and synthetic double helical RNA sequences (56). Similarly, like for the ribosomal RNA, aminoglycosides can bind to the hair pin loop structures and internal bulges. An example is aminoglycosides interacting with the Rev Responsive Element (RRE) of the Human Immunodeficiency Virus (HIV) (57). HIV replication depends on the interaction of the viral protein, Rev with the viral RNA, Rev Responsive Element (RRE). RRE has a high affinity core region for the protein, Rev, which is important for this protein-RNA interaction. This core region of the RRE has a noncanonical base pair (G48:G71) that is very important for rev recognition. Aminoglycosides, specially neomycin-B, specifically bind to the RRE and inhibit interaction of the RRE with Rev both *in vitro* and *in vivo* (57). Other than the RRE, aminoglycosides can interact with the Trans-Activating Response Element (TAR element) in HIV-1 RNA (58). The TAR element and Tat protein interactions with the HIV-1 RNA genome are very important for transcriptional initiation of HIV and this interaction is inhibited by the aminoglycoside neomycin-B. Aminoglycosides also bind with other RNA regions like self-splicing group 1 introns (59), the hammerhead ribozyme (60), and site 1 of thymidylate synthase mRNA (61).

Synthetic RNAs have been selected that bind aminoglycosides with high affinity and high specificity. Those are the aminoglycoside aptamers. Aptamers have been selected against the aminoglycosides neomycin-B, tobramycin, kanamycin-A, and paramomycin (62). The predicted secondary structures of some of the *in vitro* selected aptamers and natural aptamers are illustrated in the **Figure 5**. Jiang *et al*. (62) characterized the binding interactions between the aminoglycoside aptamer and the neomycin-B aminoglycoside. The neomycin-B aptamer is a 23 nucleotide long RNA molecule with a secondary structure predicted as shown in **Figure 5**. As illustrated in **Figure 6** in the complex between neomycin-B and the neomycin-B 23mer aptamer, the neamine component (ring I and ring II) of neomycin-B is sandwiched between the major groove floor of the zippered up "G●U" mis-matched nucleotide section and the looped out purine base that flaps over the bound aminoglycoside. Also, distinct hydrogen bonding interactions occur between the neomycin-B and mismatch base edges and the phosphate backbone. These interactions fasten the 2-deoxystreptamine ring I and pyranose ring II in the RNA aptamer binding pocket. Both the tobramycin and neomycin-B aptamers bind their respective ligands, neomycin-B and tobramycin, in a similar fashion in which the 2-deoxystreptamine ring I and attached pyranose rings are captured in the major groove binding pocket consisting of the mismatch base pairs and the bound aminoglycoside is covered by looped out base and held in place by intermolecular hydrogen bond interactions between the charged amine groups of the aminoglycosides and charged residues of the RNA.

Aminoglycoside aptamers are RNA molecules created by *in vitro* selection and evolution techniques to bind with the aminoglycoside antibiotics with high affinity and specificity. Even though aptamers are not of biological origin, determination of the structures of aptamer-ligand complexes aids in understanding the roles of diverse folding topologies of RNA in molecular recognition. Aminoglycoside-aptamer interactions exemplify the structural principles that govern the specific and high affinity interactions that exist in complexes of aminoglycosides with natural RNA. Also the *in vitro* selected aminoglycoside aptamers seem to have very useful applications in treating diseases such as HIV (57). Therefore aptamers selected against aminoglycosides pave the way to exciting new arenas in medicinal chemistry.

Figure 1

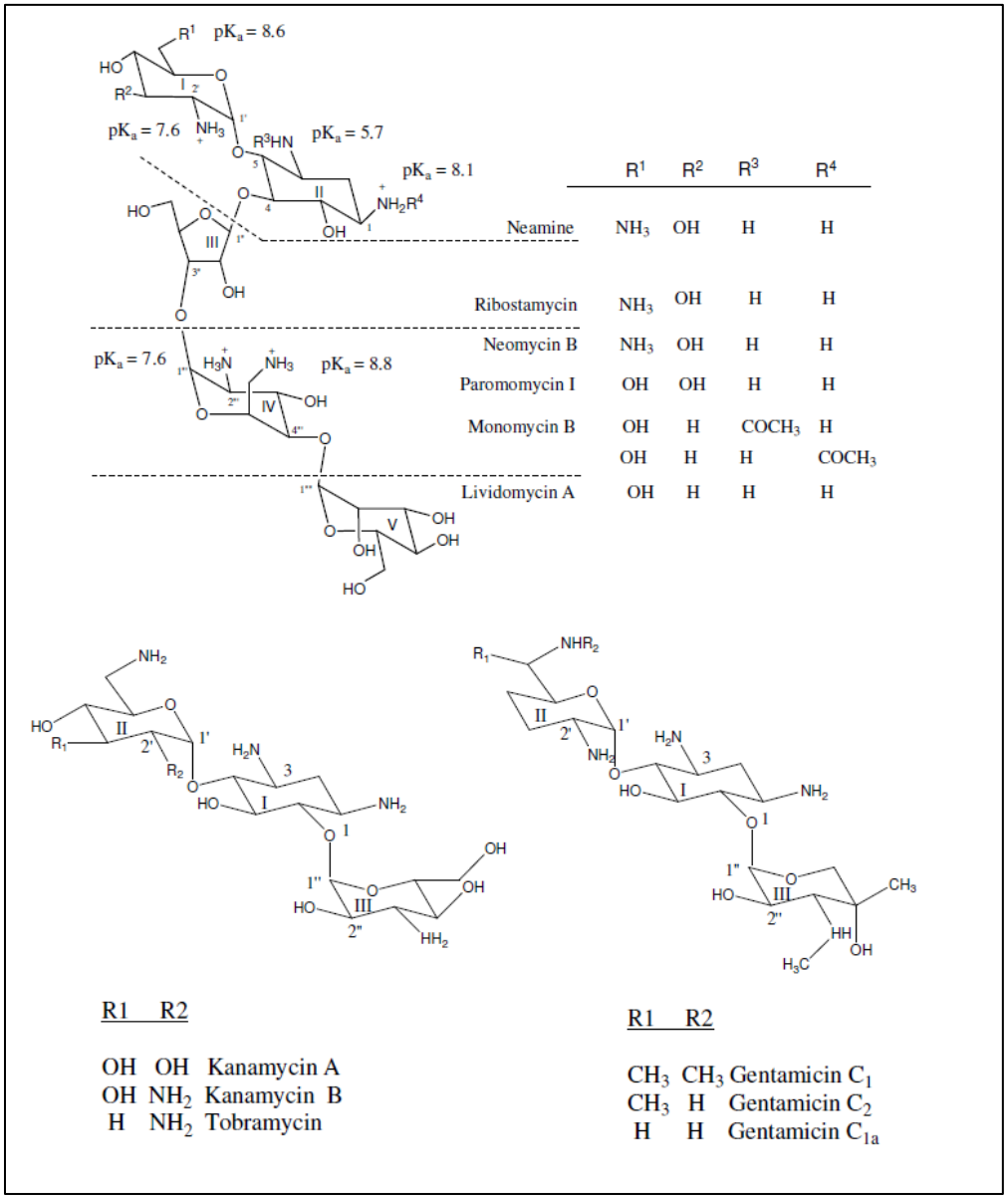

Figure 1. Chemical structures of aminoglycosides and the pKa values of some amine groups. Reprinted from (40) with permission**.**

Figure 2

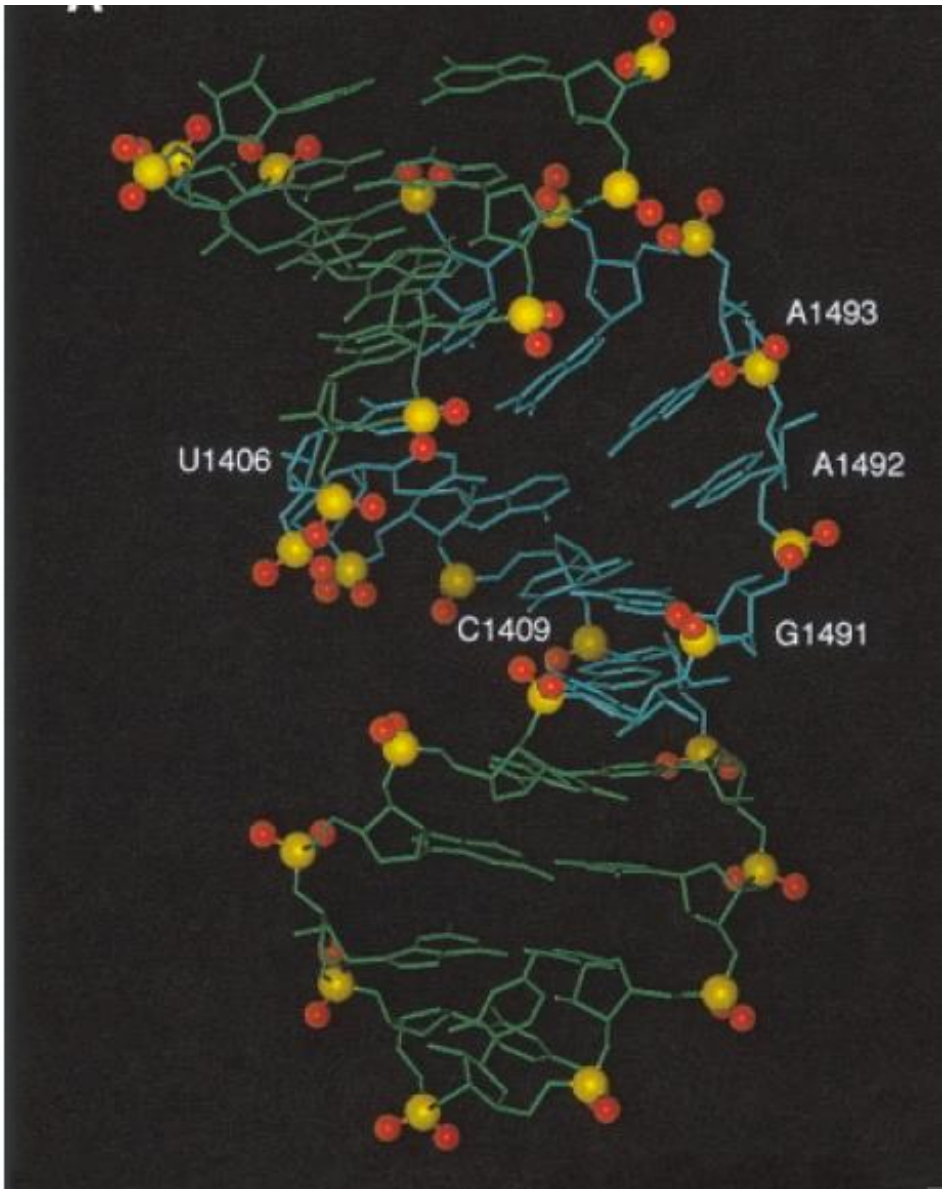

Figure 2. Single representative structure of A-site RNA oligonucleotide. The core of the antibiotic binding site within the RNA (nucleotides U1406 to A1410, and U1490 to U1495) is shown in light blue and RNA residues outside the core are in green. All heavy atoms are displayed. From (40) with permission.

Figure 3

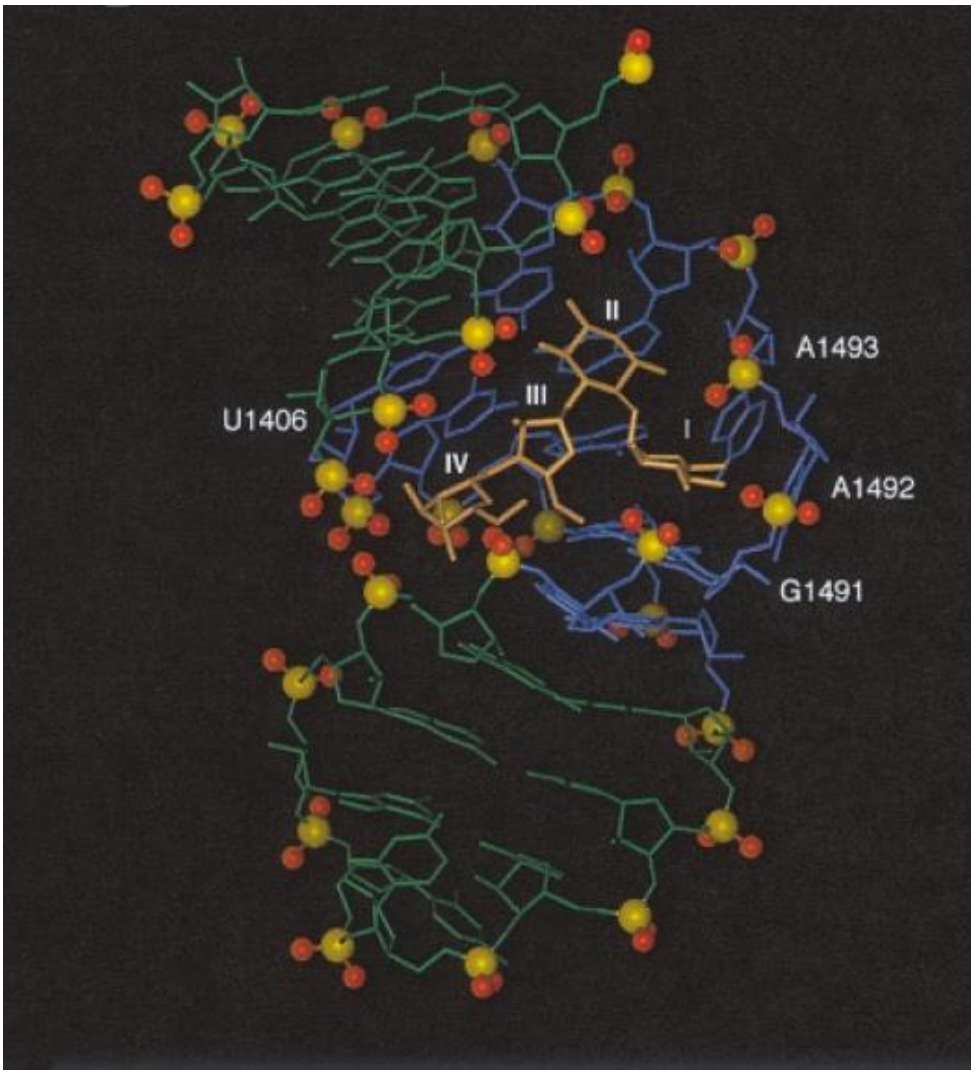

Figure 3. **Single representative structure of A-site RNA in complex with paromomycin.** The core of antibiotic binding site within the RNA is shown in (nucleotide U1406 to A1410 and U1490 to U1495) is shown purple and the residues outside the core is shown in green. Paromomycin is shown in tan. All heavy atoms are displayed. From (40) with permission.

Figure 4

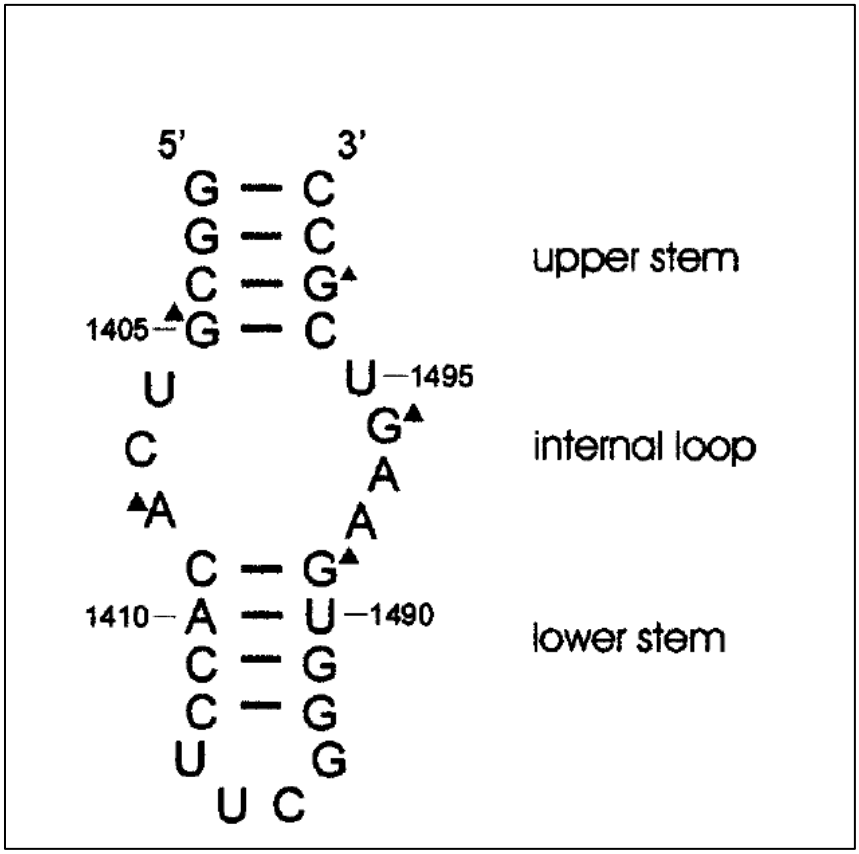

Figure 4. Secondary structure of the A-site RNA oligonucleotide showing the DMS footprints observed in the presence of aminoglycosides and marked with Δ. From (40) with permission.

Figure 5

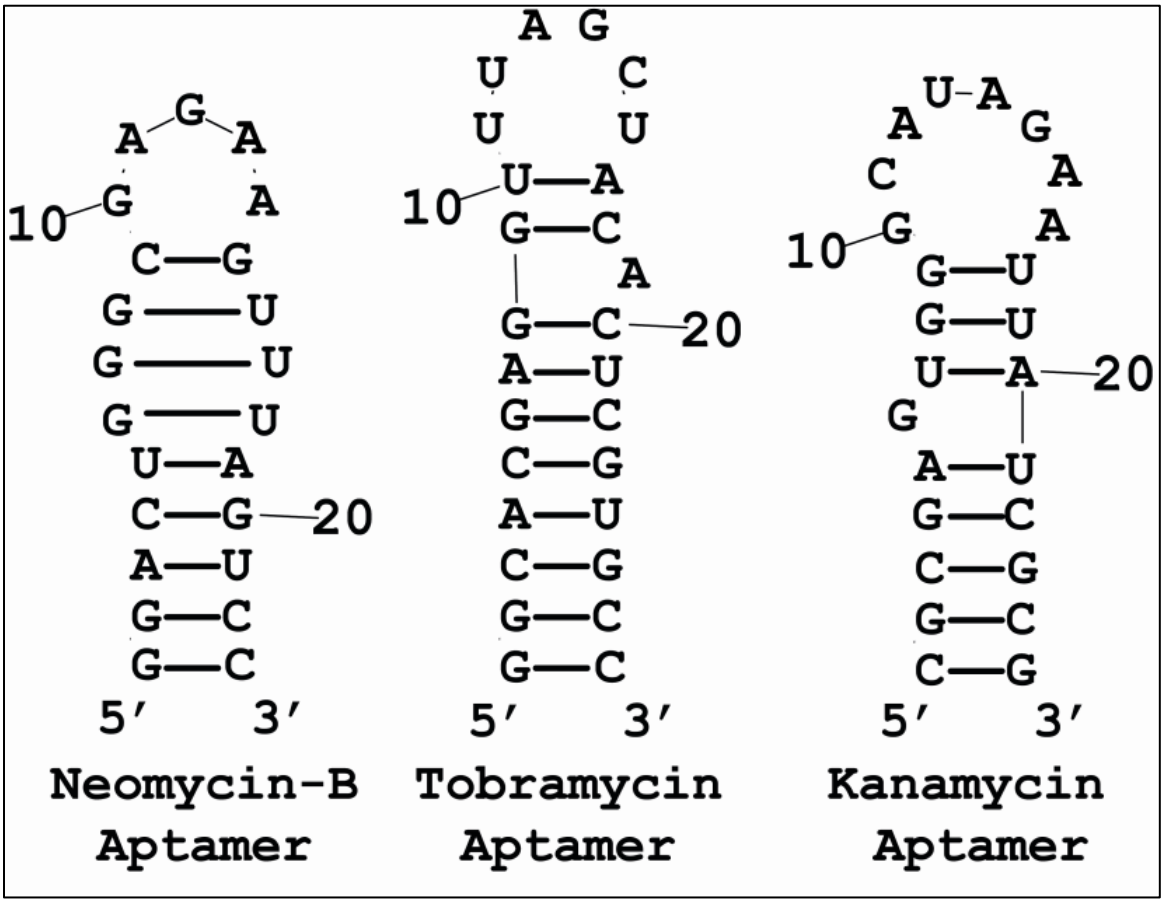

Figure 5. Predicted secondary structures of the some aminoglycoside RNAs. Diagram of secondary structures of RNA aptamers that have been proven to interact with aminoglycosides. These RNA aptamers are *in vitro* selected RNAs to bind with specific aminoglycoside antibiotics. The secondary structures of RNA aptamers shown here were predicted with the RNA Structure 4.6 software and then reconstructed in Adobe Illustrator (63).

Figure 6

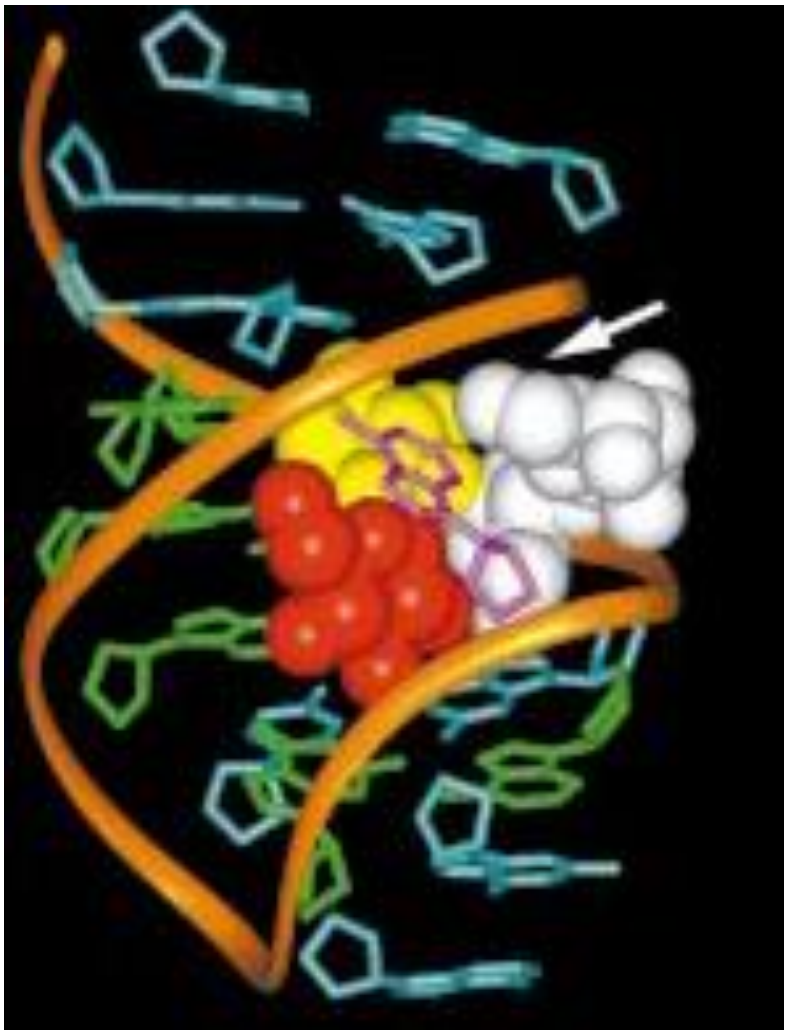

Figure 6. Neomycin-B-RNA complex. The RNA folds are shown in stick and ribbon representation, with the flapped base shown magenta. The bound aminoglycoside antibiotics are shown as space filling models. Ring I and II of the Neomycin-B antibiotic are shown in yellow and red, respectively. Ring III and IV are in white. The white arrow indicates the postulated linkage site of the neomycin-b through its primary amine moiety to the agarose column. From (62) with permission.

Bacterial growth

Bacteria constitute a large group of prokaryotic microorganisms that are usually a few micrometers in length and of a variety of shapes ranging from rods, spheres and spirals (64). Bacteria were among the first life forms on earth (64). Even today, bacteria are present in most habitats on earth. In our study we mainly studied *Escherichia coli*, commonly abbreviated *E. coli*, which is a gram negative, facultative anaerobic rod shaped bacteria. In nature it is mostly found in the lower intestine of warm blooded animals (endotherms). Most *E. coli* strains are harmless, but some strains cause food poisoning in humans (65). The harmless strains are part of the bacterial flora in the gut and give the host the benefit of producing vitamin K_2 (66). This flora can also prevent the effects of pathogenic bacteria by inhibiting the establishment of pathogenic bacteria with in the intestine (67,68). *Escherichia coli* can be grown in laboratory settings very inexpensively. *E. coli* has been used as a model organism in many research studies for over 60 years. It is an important organism in recombinant DNA technology. In 1885 German pediatrician Theodor Escherich found this organism in feces of an individual and named it as *Bacterium coli commune* since it was discovered from in the colon. Later it was named as *Escherichia coli*.

Biology and Biochemistry of *Escherichia coli*.

E. coli is a gram negative, facultative anaerobic and non-sporulating. The cells are typically rod shaped and are about 2.0 μm long and 0.5 μm in diameter with a cell volume of about 0.6-0.7 $\mu m^{3.}$ *E. coli* can survive on a range of substrates (69). Under anaerobic conditions *E. coli* uses mixed acid fermentation and produces lactate, succinate, ethanol, acetate and carbon dioxide. Optimal growth of *E. coli* occurs at 37^0C and some engineered strains can multiply even at temperatures of 49^0C (70). They can grow under aerobic and anaerobic conditions utilizing a wide range of redox pairs, which includes oxidation of pyruvic acid, formic acid, hydrogen and amino acid. The reduction substrates are oxygen, nitrate, fumarate, dimethyl sulfoxide (71). *E. coli* has the capacity to transfer DNA by bacterial conjugation, transduction or transformation to spread genetic material through an existing population. This is called horizontal spread of genetic material.

Cellular structure of *Escherichia coli*

Extracellular structure

Escherichia coli have adhesive fimbriae and a cell wall (72). The cell wall is comprised of an outer membrane that contains lipopolysaccharides, a periplasmic space with a peptidoglycan layer and an inner cytoplasmic membrane. The outer cell wall has an overall negative charge because it contains lipopolysaccharides and phospholipids. *Escherichia coli* cells have fimbriae attached to the cell wall. Fimbriae are protein tubes that extended out from the outer membrane. They are usually short in length and present in high numbers all over the bacterium. Function of the fimbriae is to facilitate the attachment of bacteria to surfaces to other cells such as in animal cells in pathogenesis.

The bacteria cell is surrounded by a lipid membrane also known as the cell membrane or plasma membrane (45). This membrane acts as barrier to hold materials inside the cell and as well encircles the contents of the cell. All the nutrients, proteins, essential components are held in the cytoplasm. *E. coli* do not have membrane bound organelles such as a true nucleus, mitochondria, chloroplasts and lysosomes that are present in the eukaryotic cells, but they have some large intracellular structures. The bacterial cytoplasmic membrane is a phospholipid bilayer with the features of a general cell membrane such as acting as a permeability barrier for most molecules and serving as location for the transporters that determine which molecules get into the cell (64). The cytoplasmic membrane contains electron transport proteins that can generate the proton motive force in bacteria. The *E. coli* membrane also contains the proportions of fatty acids that provide it the fluidity. In the phospholipid bilayer the lipid portion is not very permeable to molecules, therefore the outer membrane contain channels called porins which allows passive transport of many ions, sugars and amino acids. The periplasmic membrane contains the peptidoglycans and many proteins required for signal transduction. The periplasm exists in a gel like state as high concentrations of proteins and lipids are dissolved in it. Important biochemical reactions, such as energy generation, utilize concentration gradients across the membrane. Because *E. coli* lack internal organelles, processes like the electron chain reaction take place between the cytoplasm and the outer membrane (73).

E. coli is a gram negative bacterium, which means that this bacterium does not retain the crystal violet gram stain when washed with absolute ethanol and acetone and can be decolorized

to accept the counter stain (safranine or fuschine) which stain in red or pink. The peptidoglycan layer is responsible for inability of these bacteria to hold the crystal violet staining in gram staining test. Gram positive bacteria retain the crystal violet gram stain and remain the violet colored even after washing with absolute alcohol and acetone.

Gram negative bacteria have a thin single layered peptidoglycan and gram positive bacteria have multilayered thick peptidoglycan layers. Teichoic acid is present in the cell wall of gram positive cells and absent in gram negative cells. An outer membrane and periplasmic space are only present in gram negative bacteria. Cell wall composition is different in the two kinds of bacteria as well. The gram negative bacterial cell wall is 70 Å-120 Å thick, two layered, and the lipid content is 20%-30% (high) whereas the murein content is low as 10%-20%. In gram positive bacteria, the cell wall is 100Å-120Å thick and two layered and the lipid content in the cell wall is low, whereas the murein content is high as 70%-80%. The lipopolysaccharides content is high in gram negative bacteria and low in gram positive bacteria.

Intracellular structure

When compared with eukaryotes, prokaryotes such as *E. coli* have very simple intracellular structures.

Bacterial chromosome and the plasmid

Escherichia coli do not possess a membrane enclosed nucleus like eukaryotes, but have a chromosome residing in the cytoplasm. *Escherichia coli'*s genetic material is a single circular chromosome located in the cytoplasm in an irregular shaped body called a nucleoid. The nucleoid contains the chromosomal DNA with its associated proteins (74). Therefore cellular information transfer processes such as DNA replication, transcription, and protein translation all occur in the same compartment. The bacterial chromosome is not packaged with histones to form chromatin like in eukaryotes but it takes very compact supercoiled structure. Other than the circular chromosome DNA other small independent pieces of DNA exist called as plasmids. Plasmids usually encode traits which are advantageous to *E. coli* but are not essential. Plasmids can be easily transferred between bacterial species and therefore mediate horizontal gene transfer.

Ribosome

E. coli has ribosomes in the cytoplasm that are used for protein synthesis (75,76), but the structure of the bacterial ribosome is different from that of eukaryotes. In *Escherichia coli* the most abundant intracellular structure is ribosome, which is the site for protein synthesis (45). Ribosomes link amino acid molecules in an order specified by the messenger RNA (mRNA) molecules. The ribosome binds an mRNA molecule and uses it as a template to determine the accurate sequence of the amino acids in a particular protein. Amino acids are brought to the ribosome by aminoacylated transfer RNA (tRNA) molecules (45). The ribosome consists of RNA and protein and therefore is a ribonucleoprotein. Each ribosome is divided into two parts, a smaller subunit that interacts with the mRNA and a larger subunit binding with the aminoacylated tRNA. Ribosomes from archea, bacteria and eukaryotes differ in their structures, sequences, sizes and ratios of protein to RNA. These differences aid in antibiotics to target the bacterial ribosomes without affecting the human ribosomes. *E. coli* ribosome is around 20 nm in diameter and composed of 65% ribosomal RNA and 35% ribosomal protein. *E. coli* has the 70S (S= Svedberg unit) ribosome and this 70S ribosome is composed of 30S small subunit and 50S large subunit. The 50S subunit consists of 23S RNA (2900 nucleotides), 5S RNA (120 nucleotides) and 31 proteins. The 30S subunit contains the 16S RNA (consisting of 1540 nucleotides) bound to 21 proteins (75). Proteins are complexed with the rRNA to form the ribosome(75).

Cytoskeleton

Earlier it was thought that prokaryotic bacteria do not possess a cytoskeleton. But with the advances in imaging techniques and structure determination it was concluded that filamentous structures does exists in the cytoplasm (77). The prokaryotic cytoskeleton is the collection of all structural filaments in prokaryotes. Previously bacteria were viewed as bags of cytoplasm, but the discovery of the prokaryotic cytoskeleton (78) and the localization of proteins to specific locations (79) within the cell lead to the idea of more complex cell structure. These subcellular levels of organization have been called as “bacterial hyper structures” (80).

Bacterial growth curve and its phases

Bacterial growth is the division of one bacterial cell into two daughter bacterial cells by binary fission (81). Binary fission is a prokaryotic asexual reproduction method where a cell is

divided in two or more cells with each having a potential to grow into the size of an original cell. Under optimal conditions *E. coli* can grow and divide extremely rapidly, the bacterial population can double with every 20 min. This kind of division occurs without a spindle (82). During prokaryotic cell division, the single chromosomal DNA first replicates and the two products become attached to a different part of the cell membrane. When the cell begins to pull apart, the replicate and the original chromosome are separated and moved to the new two cells (82). With this kind of asexual reproduction the resulting daughter cells are genetically identical. Both resulting cells from this kind of fission might not survive, but if the number of cells surviving exceeds unity on the average, the bacterial population undergoes exponential growth. Therefore bacterial growth in batch culture is modeled into four phases(83), which are: (A) lag phase, (B) exponential or log phase, (C) stationary phase, and (D) death phase. Finer subdivision of the phases are sometimes employed, which are: (A) lag phase, (B) early log phase, (C) log-exponential phase, (D) early stationary phase, (E) stationary phase, (F) early death phase, (G) death phase.

The lag phase is the bacterial growth phase during which the bacteria acclimatize themselves to the culture conditions. In this phase, synthesis of RNA, enzymes and other molecules occur but there is no accumulation of cells. In the exponential phase the characteristic feature is the cell number increments by cell doubling (84). The number of new bacteria appearing per unit time is proportional to the present population. If the growth is not limited, doubling will continue at a constant rate so the number of cells increases and the population doubles regularly over a defined time period. This is exponential growth and plotting the cell number against the time on a log scale produces a straight line. The slope of this line is the specific growth rate of the organism and it gives an idea of number of divisions per cell per time. The calculated rate from the slope of the curve depends on the growth conditions that affect the frequency of cell division and on the probability of daughter cell survival. The duration of the exponential phase depend on the size of the inoculum, capacity of the culturing medium and culture conditions to support the microbial growth. Biomass estimates needs to be plotted over time and the cell count and the dry weight are common methods of determining the biomass. But, exponential growth cannot continue indefinitely without replenishment of nutrients and removal of toxic waste products that accumulate in the medium. Stationary phase is the next phase that *E. coli* enters when grown in batch culture without perfusion to replenish nutrients and

remove waste. In the stationary phase, the bacterial growth and death rates are similar (85). The result is a horizontal portion of the growth curve called the stationary phase. The last phase is the death phase where bacteria die because they run out of nutrients and are killed by the accumulated toxic wastes.

The specific growth rate is defined as the increase in the cell mass per unit time. The specific growth rate is given by the symbol, μ and the most common units are reciprocal hours (h^{-1}). But it can be expressed in reciprocal minutes (min^{-1}) or reciprocal seconds (sec^{-1}) as well. The formula for calculating the specific growth rate is as follows (86):

$$\mu = K' = \frac{\ln(^{mt_2}/_{mt_2})}{t2-t1} \text{ ; t2 > t1}$$

Where,

m_{t1} and m_{t2} are biomasses at different time points (t_1 and t_2) respectively.

μ = specific growth rate

K' = specific growth rate constant

The difference between the growth rate and the specific growth rate is that, the growth rate of a microbial population is a measurement of increase of biomass over time and it is determined from the exponential phase. Growth rate is an important way of expressing ecological success of a strain or a species in adapting to its natural environment or the experimental environment imposed upon it.

The inoculum effect

The inoculum effect is a laboratory phenomenon that is described as a large increment in the minimum inhibitory concentration of the antibiotic when the number of inoculated organisms increases (87). Some bacteria that are susceptible to an antibiotic when the cultures are initiated with low density inoculum will be resistant to the same antibiotic when cultures are inoculated at higher densities (88). The importance of the inoculum effect was first described in the 1940s by several scientists. Fildes and colleagues found an inoculum effect associated with antibacterial activity of mercury (89). Lowell and colleagues determined that when *Streptococcus* were transferred into growth medium containing sulfapyridine with high inoculum densities, these

originally susceptible strains were resistant and grew in that media very well (90).There are several implications of the inoculum effect (87). One implication is that understanding the inoculum effect may provide information about efficacy of an antimicrobial agent against infections involving large number of bacteria, such as in abscesses (87). Another importance of the inoculum effect is in the management of infections that involve high bacterial density and bacteria that express high concentrations of antibiotic degrading enzymes such as β-lactamase (87).

Movement of the molecules in the cell

The mobility of certain molecules inside the cells plays a very important role in well-functioning of the cell. Nenninger *et al*. (91) showed in their study the importance of size of molecules in the cytoplasmic diffusion. The cytoplasm of both eukaryotes and prokaryotes are complex, crowded environments. The movement of molecules within the cytoplasm is constrained by a combination of viscosity, macromolecular crowding and specific interactions of the molecules with the other cell components (e.g. proteins, nucleic acids and the cytoplasmic membrane). Diffusion is regarded as the primary method of intracellular molecule movement and thus it plays an important role in controlling the rates of cell processes. In our study, the mobility of aptamers in the cytoplasm was an important factor in the hypothesis. Aptamers, being small molecules, were hypothesized to be mobile inside the cell.

Terry *et al*. (92) investigated the physical principles behind the mobility of molecules in cells. They discovered that the hydrodynamic radius (STOKES radius) is the deciding factor that drives the mobility of molecules through the plasmodesmata. Plasmodesmata are microscopic channels that transverse the cell walls of plant cells. Even though these plasmodesmata are involved in transport between cells they are composed of cytoplasm (93). Therefore the principles that govern the mobility of molecules through the plasmodesmata are valid for mobility of molecules in the cytoplasm as well. The STOKES radius or hydrodynamic radius is the radius of the hypothetical hard sphere that diffuses at the same rate as the molecule. This radius takes into consideration the shape and hydration effect of the molecule. Therefore a more extended molecule will have a larger STOKES radius than a compact molecule of the same molecular weight. As the STOKES radius of a molecule increases, its mobility decreases. Other

than the hydrodynamic radius, the diffusion coefficient also has an effect on the mobility of molecules inside the cells.

$$R_H = \frac{k_B T}{6\pi\eta D}.$$

Where R_H = STOKES radius, k_B = Boltzmann constant (in JK^{-1}), D = diffusion coefficient (in m^2s^{-1}), T=temperature in Kelvin, η= viscosity

In liquids where there are interactions between solute and solvent molecules, the STOKES radius of a perfect sphere is proportional to the frictional coefficient and inversely proportional to the viscosity η.

Techniques use for determining the mobility of molecules inside cells

To determine the mobility of molecules in the cell cytoplasm, a variety of techniques have been used. One such technique is FRAP, Fluorescence Recovery After Photo bleaching (94,95). In FRAP, fluorescent molecules are photo bleached in a small area of the cell by a laser beam and the consequent diffusion of other surrounding non bleached fluorescent molecules into the bleached area leads to the recovery of the fluorescence that is recorded at a low laser power. The FRAP technique was first used in the 1970s when lipophilic or hydrophilic fluorescent molecules, like fluorescein, coupled with proteins and lipids were commonly utilized. Two very important factors can be inferred from the results of FRAP experiments. One is the mobile fraction of the fluorescent molecules and the mobility of these molecules. FRAP is the most well established method to characterizing the diffusion of fluorescently labeled molecules in liquid crystalline membranes. But under non ideal experimental conditions such as when the signal to noise ratio is low, when there are temporal fluctuations in the illumination or when there is bleaching during the recovery process (96). A more recent development is Pulsed-FRAP, which can be used for protein mobility measurements in the much smaller prokaryotic cells such as *E. coli* (97).

The cloning of green flourescent protein (GFP), from jellyfish *Aequorea victoria* introduced a new era of flourescence tracking. This discovery made it possible to monitor the mobility of proteins in living cells without interference from microinjections. Because of GFP's relatively high photo stability, GFP-tagged molecules can be observed over long periods and the

resolution of light microscopy allows them to be located within the cells. The fusion of GFP to other proteins usually does not affect the function or localization of the proteins and therefore GFP is a very important for detecting mobility of molecules in the cell. Other than these techniques Fluorescence Correlation Spectroscopy (FCS) (95,98) has also been used in experimentation in mobility of molecules in the cells. Fluorescence Correlation spectroscopy gives high resolution spatial and temporal analysis of extremely low concentrated biomolecules. In contrast to other fluorescence techniques in FCS primary parameter of interest is the not fluorescence emission, but the spontaneous intensity fluctuations caused by the minimal deviations of the small system caused by the thermal equilibrium. Therefore by the FCS technique fluctuations in the fluorescence signal is accessible which are caused by any physical parameter. Actually FCS measures the fluctuations in fluorescence intensity that results from diffusion of fluorescent molecules in and out of a small open volume and then uses autocorrelation analysis to detect the correlation of intensity deviation at one point in time to intensity deviation at later point in time. The diffusion coefficient is described by the rate of decay of correlation. Slower the molecule diffuses, longer the correlation continues. FCS technique does not interfere with the steady state of the molecule and also it is a noninvasive technique. But FCS can only function if concentration and volumes are reduced such that only few molecules are detected at the same time. These same techniques have been used to determine the mobility of RNA in the cytoplasm as well.

Mobility of RNA

Mobility of RNA in the cell

The tracking of fluorescently labeled, microinjected and engineered or endogenous RNA demonstrated that ribosomal RNA and poly A RNA move freely and in a non-directional manner with a diffusion coefficient of 0.03-0.1 $\mu m^2 s^{-1}$ within the nucleus (99,100). Ritland and Shav-tel concluded that RNA motion inside the cell is rapid and non-directional. Ido Golding and Edward. C. Cox has reported very significant discoveries regarding the mobility of RNA in the *E. coli* cells (101). In their study they have described a method for tracking down RNA molecules in *E. coli* cells which is sensitive to single copies of mRNA molecules. By their developed tracking method they have observed mobility of RNA molecules in the cytoplasm that is consistent with the known life history of RNA in prokaryotes. The main types of RNA motion

they have observed inside the cell were localized motion consistent with the Brownian motion of an RNA polymer bound to its template DNA and free diffusion. Other than this they also describe polymer chain dynamics that seem to be arising from chain fluctuation and chain elongation due to RNA transcription. Ido Golding and Edward.C.Cox used an mRNA detection system consisting of fluorescence protein GFP fused to the RNA bacteriophage coat protein MS2 and a reporter RNA containing tandem repeats of MS2 binding sites. In addition they also monitored the RNA motion in the entire cell and they observed that the RNA molecule tend to spend more time near the cell pole than the center of the cell, which is due the increased drag experienced by the particles near the cell pole than the center of the cell also called as "hydrodynamic coupling" between the RNA molecule and the cell wall. Also this detection of RNA motion spanning the entire cell enabled them to give a quantitative value to the diffusion coefficient of the RNA-protein hybrids in the cell and the value is 0.03 μm^2/sec. Another important discovery of their study is that they found movement of RNA molecules inside the cell is passive, which is proven by the fact that movement of RNA molecules in the cell is not inhibited by the metabolic poisons.

A remarkable demonstration of this non-directional, rapid movement of RNA came from a set of experiments in which newly synthesized RNA was visualized at the site of the synthesis and then its export to cytoplasm was followed in living cells (99,100). These studies showed that RNA synthesized from genes positioned close to the nuclear envelope diffused away from their synthesis sites in all directions rather than to follow a straight path to nearest nuclear pore. This observation very strongly suggests the non-directional, diffusion based movement of RNA molecules in the nucleus. However this diffusion-based movement of RNA is associated with accessory proteins.

RNA is a very mobile molecule in the cell. The transport of RNA molecules from the nucleus to the cytoplasm is a fundamental cellular process. Compartmentalization in the eukaryotic cell as nucleus and cytoplasm and also the transition from prokaryotic co-transcriptional translation of protein to eukaryotic physical separation of transcription of RNA and translation of proteins required evolution of a nuclear transport system. RNAs are transported from the nucleus to the cytoplasm after their synthesis in the nucleus and also newly synthesized proteins are imported and rapidly dispersed in the nucleus. How proteins and RNA

move within the cell and between the cytoplasm and the nucleus, how they find their targets was unknown for a long time. But with the invention of above mentioned techniques such as FRAP, GFP tagging and using time lapse spectroscopy these questions were answered.

Selective Localization of RNA

Other than its movement from the nucleus to the cytoplasm, localization of RNA is another mode of RNA mobility. It is a long known fact that mRNA for certain proteins is localized in certain localizations of the cytoplasm (102). Known examples of localized RNAs can be divided into two categories. One category is the cellular mRNA transcribed in somatic cells, the localization of which results in synthesis of the encoded proteins at their sites of action (103) and the other category is the maternal mRNAs that are asymmetrically positioned in oocytes and aid in forming the axes of the embryo by establishing the concentration gradient of protein "morphogens" (104). Evidence for these localized mRNAs came from the results of *in situ* hybridization studies. Much attention has since been given to the mechanisms by which the mRNA location occurs. RNAs that are localized in the cell contain specific sequence elements termed "zip codes" (102,105). These zip codes are a class of cis-acting elements that occur within the 3'UTR of the mRNA and they aid in determining the stability, mobility and translational efficiency of the mRNA. Also mRNA zip codes determine the protein synthesis sites in the cell. To identify the proteins that bind the zip code regions, Ross *et al*. (105) performed band shift assays, UV crosslinking and affinity purification. They identified a protein of 68 kDa that binds the proximal half (coding region) of the zip code in β-actin mRNA with high specificity. The zip codes regions are involved in peripheral distribution of the mRNA by interacting with proteins that mediate localization.

β-actin mRNA is transported to peripheral locations in the cell by mechanisms that are not yet well known, although some information is known. One important observation is that actin mRNA movement is energy dependent. This was shown by Lantham *et al*. (106) who demonstrated that an ATP synthesis inhibitor, cordycepin, prevents RNA localization. Also localization does not require ongoing protein synthesis as it occurs at the presence of puromycin or cycloheximide (107). Most importantly the localization is inhibited by disruptors of actin cytoskeleton and not by disruptors of microtubule system, which indicates that localization or anchoring requires the actin cytoskeleton (107).

Mobility of Proteins

It has been long known that RNA and protein move within the cell, especially within the cell nucleus of eukaryotes. Messenger RNA synthesized in the nucleus is quickly transported out of the nucleus to the cytoplasm and the newly synthesized proteins are on the other hand promptly transported in to the nucleus and dispersed. Phair *et al*. tested the mobility of proteins in the mammalian nucleus. They have measured the mobility of three important proteins in the nucleus. Those are nucleosomal binding protein (HMG-17), the pre-mRNA spicing factor SF2/ASF and rRNA processing protein fibrillarin in the nucleus of the living cells using the FRAP method and GFP fusion proteins. They show that these proteins move rapidly and completely into the nucleus after their synthesis. The protein movement is independent of energy indicating that proteins use a passive mechanism for the movement. Elowitz *et al*. had experimented on protein mobility in the cytoplasm of *E. coli* using the similar technique as Phair *et al*. (108). They have made measurements in two different ways, one by photo bleaching the GFP fluorescence and photo activation of red emitting fluorescence state of GFP. They have calculated the diffusion coefficient values for GFP alone and GFP fusion protein in the *E. coli* cytoplasm.

CHAPTER 3: DRAGINS: DRUG BINDING APTAMERS FOR GROWING INTRCELLULAR NUMBERS

Abstract

One of the challenging requirements in cancer disease treatment today is maintaining high enough drug concentrations in order to obtain effective killing of cancer cells. Many attempts have been made to increase the intracellular concentrations of drugs that are based on "push" mechanism. In our novel approach we use a "pull" mechanism, meaning that we express a molecule inside the cell that has been selected specifically to bind with the drug molecule. The molecule expressed inside the cell is an aptamer. Aptamers are short, single stranded nucleic acid molecules ranging from about 15-100 nucleotides long. These small aptamer molecules are mobile inside the cells. Mathematical modeling of the effect of aptamer expression for increasing intra cellular drug concentration showed that this was possible. The initial model was developed for mammalian cells and the initial experimental testing of the hypothesis was done with *Escherichia coli* bacterial cells. Therefore now a new mathematical model for prokaryotic cells has been developed in parallel with the work described here. To test the hypothesis, *E. coli* BL21 strain cells were transformed with plasmids from which aptamers were expressed. The effect of expressing several aminoglycoside aptamers on the toxicity of a range of aminoglycosides was observed over a 12 h period. Then neomycin-B aptamer and the neomycin-B were selected for future studies. The half maximal inhibitory concentration (IC50), which is the concentration of the drug required for 50% growth inhibition, were calculated to be decreased by 2 fold with aptamer expression. The Minimum Inhibitory Concentration (MIC) was also ~2 fold lower for cells with aptamer expression as compared to cells with control RNA expression. To determine the effect of aptamer expression on the intracellular drug concentration we used Cy3-paromomycin. Cells with aptamer expression and cells with control RNA expression were incubated with Cy3-paromomycin and imaged directly or cell lysates were isolated and analyzed for fluorescence content by fluorimetry. Both the images and fluorimetry showed that cells with aptamer expression concentrate more Cy3- paromomycin compared to cells with control RNA expression. In summary, this study gives insight towards a novel approach to increase the intracellular drug concentration by the use of small, mobile RNA aptamers.

Introduction

A major challenge in cancer treatment today is providing a high enough drug concentration in order to obtain an effective killing of cancer cells. Cancer, medically known as malignant neoplasm is a disease which involves unregulated cell growth. Cancer cells have biological mechanisms which allow them to survive and perform unregulated cell growth. One of them is that cancer cells up regulate the expression of multi drug efflux pumps. Cancer cells that survive a drug treatment have elevated levels of drug pump called the Pgp (P-glycoprotein) or MDR (multi Drug Resistant pumps) (109), (110). These drug pumps allow the cells to survive, divide and grow under drug treatments which in turn result in more drug resistant cancer cell population. Therefore, when undergoing chemotherapy cancer patients should be given very high concentrations of drugs in order to get an effective destruction of cancer cells. Most of the cancer drugs (chemotherapy) are cytotoxic reagents, that is providing these drugs in high concentration without targeted delivery, can be harmful to healthy cells as well. Incidentally this is one of the major causes of death in cancer patients. Therefore increasing the effective intra cellular drug concentration is extremely important.

Many efforts have been taken to combat the drug resistance (52). Some of these approaches are to target the pumps by drug or antibodies or to decline pump mRNA level of antisense DNA or RNAi and decrease the pump mRNA by targeting the appropriate mRNA genes and transcriptional factors. Some of these approaches could be successful one day to combat the drug resistance but so far none of them have been effective in war against drug resistance.

By mathematical modeling it was predicted that by having a receptor for the drug inside the cells, intracellular drug concentration can be increased in mammalian cells (111). In that study small RNA aptamer that has high affinity and specific binding to the drug was used as the receptor. Aptamers have been used as intracellular agents to inhibit their targets or to control gene expression (28). But before moving to complex mammalian cells, in this study we tested the effect of intracellular expressed aptamer on bacterial growth at absence and presence of antibiotics and intracellular concentration of labeled antibiotics. Our hypothesis was that aptamers that are selected to bind with aminoglycoside antibiotics are expressed inside the bacterial cells they increase the susceptibility of the bacteria to the aminoglycoside. Here we

used in vitro selected RNA aptamers. The aminoglycoside RNA were cloned in to the bacterial system and the growth of those bacteria was monitored for 12 hour period at the condition of presence of the aminoglycoside and at the absence of the aminoglycoside. Then the IC50 values for aminoglycoside at each condition were calculated. The results show that aminoglycoside binding aptamers lower the IC50 value by 2-5 folds for the aptamer aminoglycoside binding ligands. Then we moved to determine the intra cellular drug concentration by using aminoglycosides modified with fluorescence ligand. The aptamer expressing cells and control RNA expressing cells were incubated with the fluorescent labeled aminoglycosides and then they were directed to fluorescent imaging and fluorescent spectroscopy. These results indicate that the aptamer expressing cells accumulate the fluorescent ligand labeled aminoglycosides more than the non aptamer expressing cells. Other than that now we are testing the predictions from the mathematical modeling.

Materials and methods

Chemicals

Neomycin-B, Paromomycin, Kanamycin-A, Kanamycin-B, Tobramycin were obtained in their sulfate salt forms from the Sigma-Aldrich (Saint Louise, MO). CY3 (Lumiprobe, non sulfonated in 100% DMSO) labeled paromomycin was synthesized in our laboratory. Amberlite Weakly acidic cation exchange resin (Sigma-Aldrich), 9-fluorenyl-methyl chloroformate (FMOC-Cl) (Sigma-Aldrich), Borate buffer (0.37 M H_3BO_3, 0.37 M $Na_2B_4O_7$, pH adjusted to 8.5), H_2O (HPLC grade; Sigma-Aldrich), Acetonitrile (HPLC grade; Sigma–Aldrich), HPLC column: YMC-Pack ODS AM12S05-2536WT AM303 250* 4.6 mm S-5 µM, 12 nm.

Plasmids and Bacterial cells

E. coli (DE3) star chemically competent cells were purchased from Invitrogen (Eugene, OR).

Figure 7

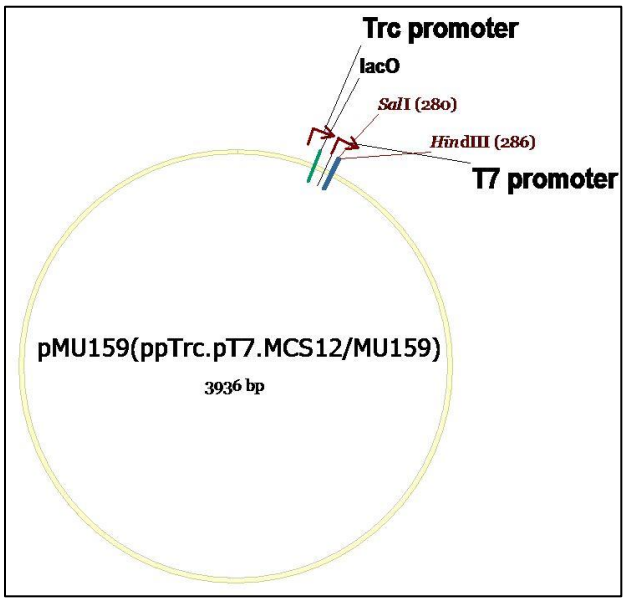

Figure 7. Plasmid map of the control RNA insert. pMU159 (ppTrc.pT7.MCS12/MU159) Ct11a plasmid used as the control RNA and it is the multiple cloning sequences downstream of T7 RNA polymerase promoter. This sequence has same length as aptamer RNA, but does not bind with aminoglycosides as the aptamers.

Figure 8

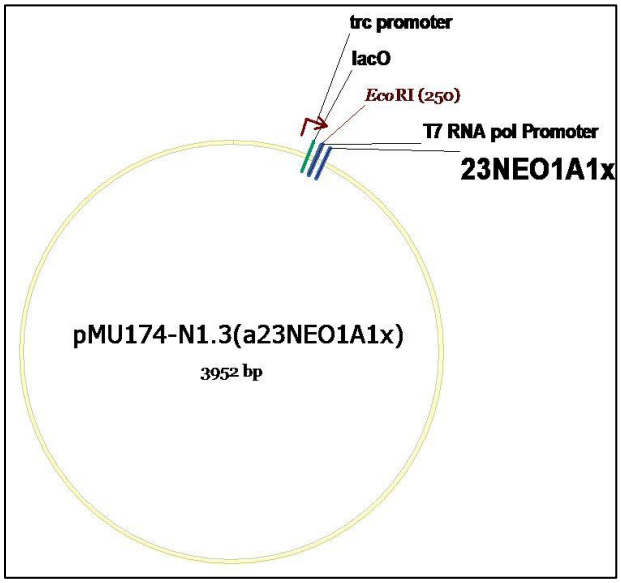

Figure 8. Plasmid map of the Neomycin-B aptamer insert. Neomycin single unit aptamer; 1merppTrc.pT7.a23NEO1Ax1/MU174. N1.3.Neomycin-B aptamer is cloned downstream of T7 RNA polymerase promoter.

Figure 9

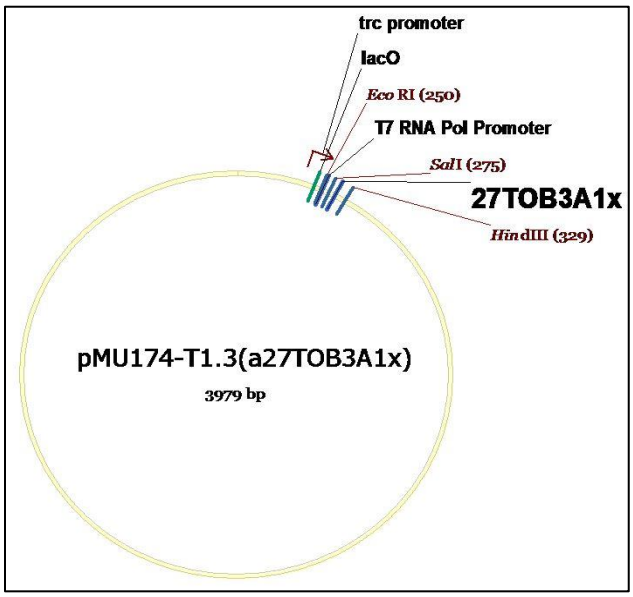

Figure 9. Plasmid map of the tobramycin aptamer insert. Tobramycin aptamer; 1merppTrc.pT7.a27TOB3Ax1/MU174-T1.3. Tobramycin aptamer is cloned downstream of T7 RNA polymerase promoter.

Figure 10

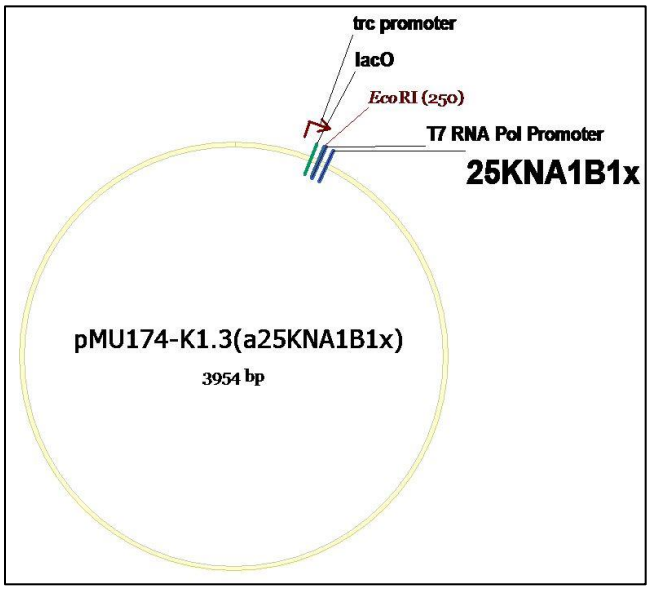

Figure 10. Plasmid map of the Kanamycin aptamer insert. Kanamycin aptamer; 1merppTrc.pT7.a25KNA1Bx1/MU174-K1.3. Kanamycin aptamer is cloned downstream of T7 RNA polymerase promoter.

Table 1. Aptamer RNA sequences

Aptamer Name	Aptamer RNA Sequence
Neomycin single unit aptamer (ppTrc.pT7.a23NEO1Ax1/MU174-N1.3)	5'-GGACUGGGCGAGAAGUUUAGUCC-3'
Tobramycin single unit aptamer (ppTrc.pT7.a27TOB3Ax1/MU174-T1.3)	5'-GGCACGAGGUUUAGCUACACUCGUGCC-3'
Kanamycin single unit aptamer (ppTrc.pT7.a25KNA1Bx1/MU174-K1.3)	5'-CGCGAGUGGGCAUAGAAUUAUCGCG-3'

Equipment

Bacterial growth curves were determined in Synergy2 plate reader (Biotek). Non-tissue culture treated, flat bottom 96-well polystyrene microtest plates were obtained from Falcon. Ninety six well plate sealing regular strength BREATHE-EASY (breathe easier sealing membrane for multi well plates) sealing membranes were purchased from Research Products International Corp. Micropipettes were purchased from Eppendorf and the Pipetmen were from Gilson. The test tubes were 14 ml Polystyrene round bottom tubes from Falcon. The incubator for cell culture was a Max-Q 4000 (Branstead Lab Inc.)

Bacterial growth analysis

E. coli BL21 cells were transformed with above mentioned plasmids and grown for about 16 h at 37^0C in Luria Bertani (LB) with 100 μg/mL ampicillin. Then the cultures were diluted about 100 times and incubated with 1 mM IPTG for 1 h at 37^0C and 250rpm shaking. After the 1 hour induction period incubation with aminoglycosides (neomycin-B, kanamycin-A, kanamycin-B, tobramycin or paromomycin) was started and the bacterial growth was monitored by the plate reader (Biotek, model: Synergy HT) at 37^0C and 250 rpm. The OD600 values were recorded at designated time points (every 1 h or 5 min time points over 12 h or 16 h time span) and the resulting growth curves were analyzed by Microsoft Excel software. By this method the half maximal inhibitory concentration (IC50) of the drugs at the presence and the absence of the aptamer expression was calculated. The Minimum Inhibitory Concentration (MIC) of the Neomycin-B was determined by the serial dilution method. *E. coli* BL21 cells transformed with neomycin-B aptamer and the plasmid containing the control RNA were grown for about 16 h at

37^0C in Luria Bertani (LB) broth with 100 µg/mL ampicillin. Then the cultures were diluted about 10 times and induced with 1 mM IPTG for 1 h at 37^0C and 250 rpm shaking. After the 1 hour induction period both cultures were plated on agar containing a dilution series of Neomycin-B.

Intracellular drug concentration analysis with Cy3-paromomycin

Cy3-paromomycin was used instead of the neomycin-B to determine the intra-cellular drug concentration. *E. coli* BL21 cells transformed with neomycin-B aptamer containing plasmid and the control RNA containing plasmid was primarily grown for about 16 h at 37^0C and 250 rpm shaking in LB media with 100 µg/mL ampicillin. Then 1 mM IPTG was added to both cell cultures and they were incubated for 1 h at 37^0C and 250 rpm shaking. Following the IPTG induction both cell cultures were concentrated by centrifugation at 9300 rcf for 1 min. The cell pellets were dissolved in 0.1 M LiCl, 50 mM K_2HPO_4 , pH 7 then centrifuged at 9300 rcf for 1 min and suspended in 60 µl of 0.1 M LiCl , 50 mM K_2HPO_4 , pH 7. The samples were analyzed by fluorescence spectroscopy using a Varian fluorescence spectrophotomer set at emission maximum of 563 nm and excitation maximum of 510 nm. The emission slit was 5 nm and excitation slit was 10 nm and the PMT voltage was set at high.

Extracellular drug concentration analysis by high performance liquid chromatography (HPLC)

To determine the extra cellular drug concentration in the culture medium, neomycin-B was coupled with 9-fluorenyl-methyl chloroformate (FMOC-Cl). FMOC-Cl has a maximum fluorescence excitation at 260 nm wavelength and maximum fluorescence emission at 315 nm.

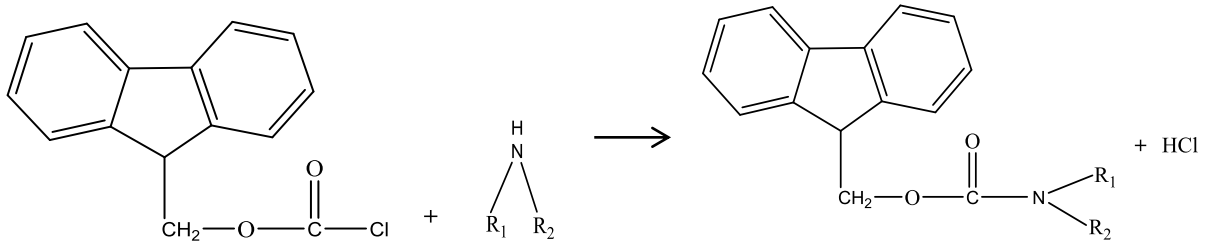

9-fluorenyl-methyl chloro formate (FMOC-Cl) Primary/secondary amine

The coupling reaction with Neomycin-B was performed in 1 mL in the presence of 1 mM FMOC-Cl, 0.185 M borate, pH 8.5. After addition of the sample containing neomycin-B, the mixture was vortexed for 50 sec and the incubated for 15 min in dark at room temperature. The coupling reaction was quenched by adding glycine to a final concentration of 4.76 mM. An YMC-Pack ODS C18 reverse phase column with 4.6 mm diameter was used to separate the reactants and reaction products. The separation was isocratic with a mobile phase of 10:90 = water: acetonitrile ratio and a flow rate of 1 mL/min. In all the experiments 10 µl of sample was injected into the column and column run was performed over a 20 min period at room temperature.

To determine the concentration range of neomycin necessary for its detection, 0.25 and 2.5 µM neomycin-B in water were separated by the HPLC procedure just described. In addition aqueous 2.5 µM kanamycin-A was reacted with 1 mM FMOC-Cl in a final volume of 1 mL and resolved by HPLC as described for neomycin-B.

To establish the background fluorescence in the assay, the analysis was performed on fluorescent reagent, FMOC-Cl with glycine and without glycine, which is the coupling reaction quenching reagent. Other control experiments to detect the background fluorescence that were performed to test for fluorescent compounds produced when FMOC-Cl was incubated with and without the 0.185 M borate buffer of pH 8.5. To establish the effect of the cell culture medium on the detection of neomycin B by this method, the same HPLC analysis was performed on 40% Luria Broth (LB) and 5 µM Neomycin-B in 40% LB.

Extraction of neomycin-B from the LB culture media by cation exchange chromatography

The cation exchange column was 2 cm in height and 1.5 cm in diameter and filled with an Amberlite resin. The Amberlite (CG50, Type1, Hydrogen form, Sigma-Aldrich) is a weakly acidic cation exchange resin (Sigma-Aldrich). After packing the column the resin was washed with 50 mL double distilled sterile water and then 5 mL of 5 µM Neomycin-B was passed through the column over a period of about 1 h to test the extraction conditions. The neomycin-B was eluted with three 1 mL aliquots of 1 M NH_4OH. After the addition of each 1 mL of 1 M NH_4OH, the column was incubated for 30 min to allow equilibrate. Five hundred microliter aliquots of the column elutions were used for the coupling reaction with the FMOC-Cl and

HPLC analysis. A sample of 0.5 mL of 4.1 μM Neomycin-B in 1 M NH4OH was reacted with 0.5 mL of FMOC-Cl and used as a positive control for the HPLC separation.

To determine if the cation exchange column could be used to extract neomycin-B from LB and neomycin-B mixture and for its successful analysis by fluorescence detection through HPLC, 5 mL of 5 μM neomycin-B in 100% LB was passed through the same cation exchange column, eluted, reacted with 1 mM FMOC-Cl and analyzed by HPLC analysis. As a positive control, 100% LB was also reacted with FMOC and resolved by HPLC.

Results and discussion

Effect of DRAGINS on aminoglycoside inhibition of cell proliferation

A Decrease in the IC50 value was observed for neomycin-B with neomycin-B aptamer expressing cells as compared with the control.

If aptamers increase the intracellular drug concentration then cell growth inhibition should be observed with a lower extracellular concentration of the drug in the presence of the intracellular aptamer as compared to cells expressing control RNA. To test the hypothesis that aptamers increase the intracellular drug concentration of a drug, BL21 *E. coli* cells were used as a model and aminoglycosides as the model drug. Aminoglycosides inhibit the growth of *E. coli*. We observed the growth of *E. coli* BL21 when incubated with antibiotic drugs and the effect aptamer expression on this growth by two methods of analysis: determination of the minimum inhibitory concentration (MIC) and determination of the 50% inhibitory concentration (IC 50) for each aminoglycoside. *E. coli* that expressed a control RNA of similar length to the aptamer RNA but did not bind aminoglycosides were used as the control. To determine the IC50, a range of aminoglycosides were tested against *E. coli* that expressed the cognate aptamer. To verify that aptamer expression was not toxic to cells we included a control condition of cells with and without aptamer expression that were cultured in the absence of antibiotics (Fig.11).

By this test we evaluated the effect of the aptamer alone on bacterial growth. The results of these experiments (Fig. 11) showed that aptamer expression does not have an effect on bacterial growth.

To test the effect of aptamer expression on aminoglycoside toxicity, a range of aminoglycosides of different concentrations were incubated with cells that expressed aptamers and cells that expressed control RNA to observe the growth pattern of the cells (Fig. 12).

Initially several RNA aptamers selected to bind with the specific aminoglycoside were expressed in *E. coli* and then incubated with the specific aminoglycoside and approximate IC50 values were estimated (Table. 2).

Once the neomycin aptamer and neomycin-B were selected as the aptamer-aminoglycoside pair, more concentrations of neomycin-B were analyzed with cell cultures with aptamer expression or with control RNA expression (Fig.14).

Figure 11

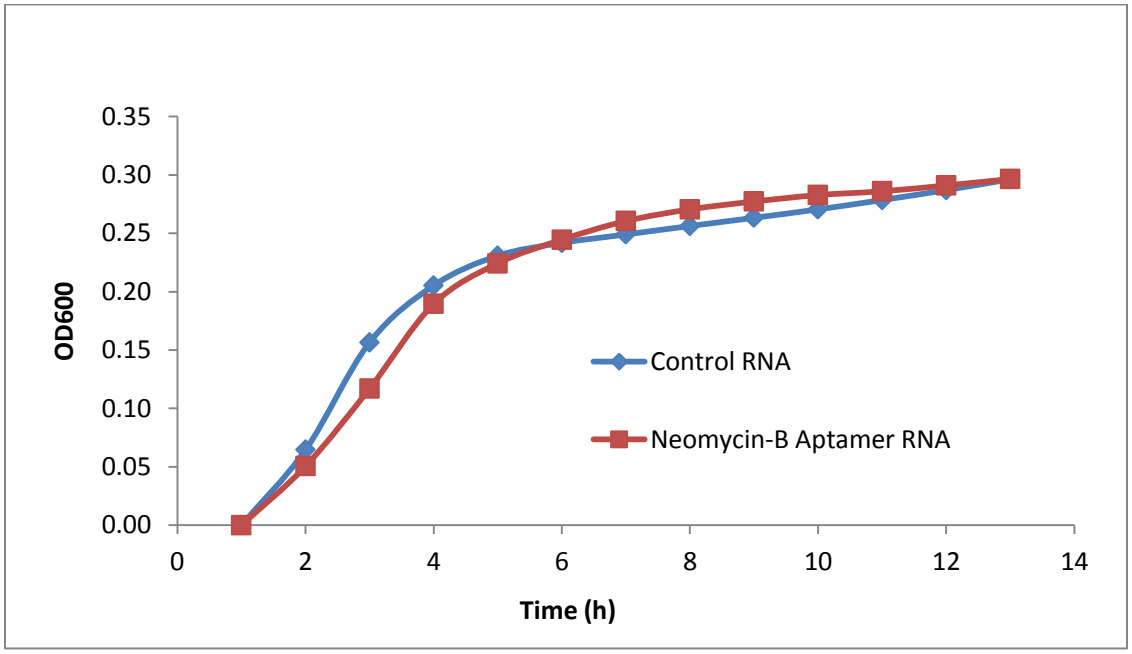

Figure 11. Comparison of bacterial growth in cells with aptamer expression and cells with control RNA expression without the inclusion of antibiotic.

Figure 12

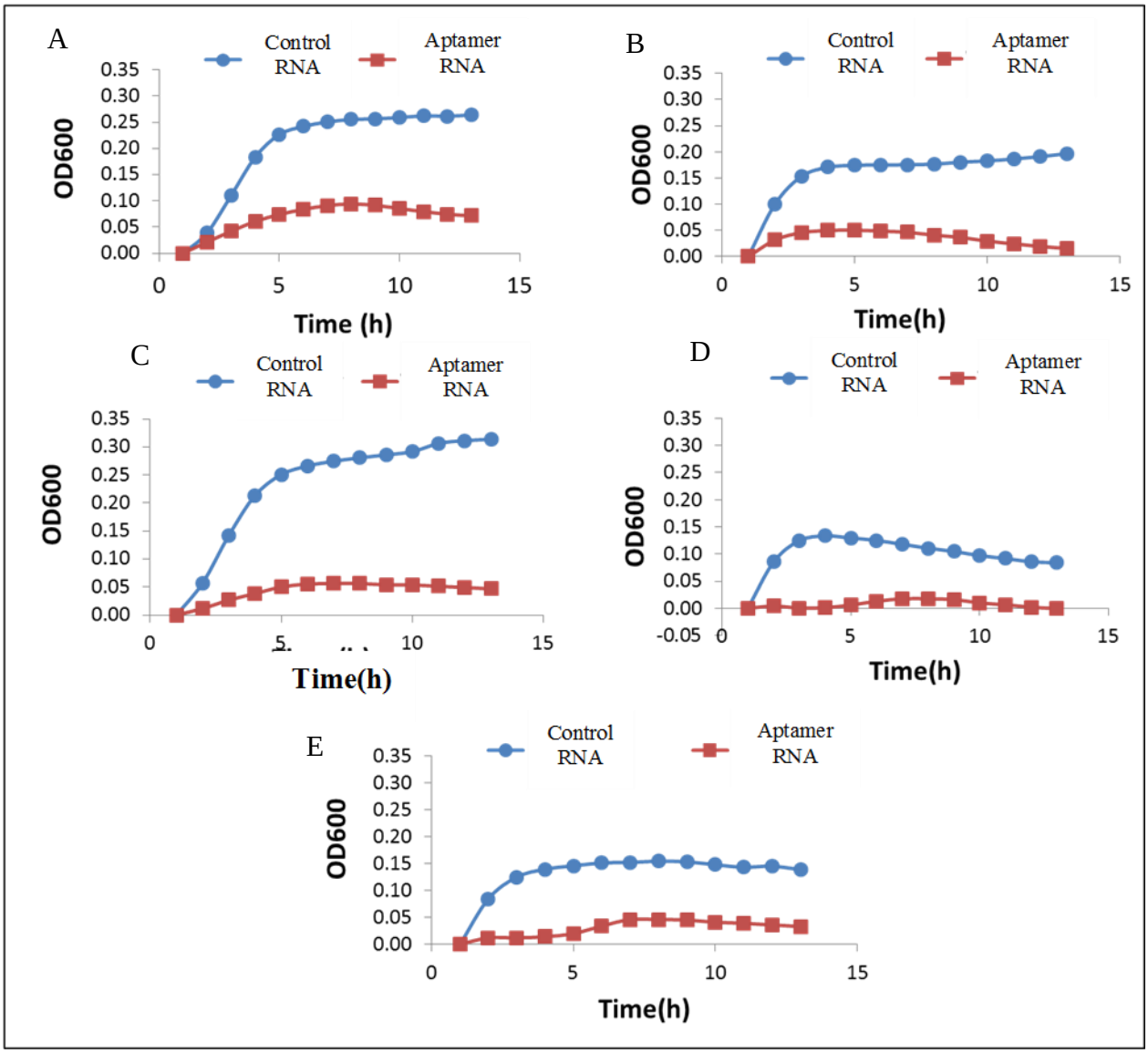

Figure 12. Comparison of bacterial growth with aptamer and control RNA expression. Cells that expressed the neomycin-B aptamer (red closed squares) **(A)** 7.5 μM kanamycin-A, **(B)** 5 μM kanamycin-B, **(C)** 7.5 μM paromomycin, **(D)** 5 μM neomycin-B and **(E)** 5 μM tobramycin. In all cases, control cells with control RNA expression is shown in blue closed circles.

Table 2. Approximate IC50 values for neomycin-B with the neomycin aptamer

	IC50 value (μM)					
	Lag phase		Log phase		Stationary phase	
	Cells with aptamer	Cells with control RNA	Cells with aptamer	Cells with control RNA	Cells with aptamer	Cells with control RNA
Kanamycin-A	1	18.7	7.0	91.0	5.9	40.0
Kanamycin-B	1	1	4.0	28.7	3.8	24.0
Paromomycin	5.0	1	4.1	12.4	4.6	5.0
Neomycin-B	4.7	1	5.8	74.7	4.5	12.4
Tobramycin	4.4	1	3.4	22.3	4.1	8.9

The results from the initial experiments showed that incubation with aminoglycosides resulted in decrease in the growth rate, extension of the lag phase and a decrease of cell density in the stationary phase for cells that expressed aptamers compared with cells that expressed the control RNA. This allowed crude estimates of IC50 for each phase of the cell cycle (Table 1). The aptamer-aminoglycoside pair that showed the best difference in IC50 values and MIC values among the cells expressing the aptamers and cells expressing the control RNA was selected for further experimentation. Therefore, the neomycin aptamer with neomycin-B was selected as this aptamer-aminoglycoside pair because they showed the most consistent separation in IC50 values and MIC values between the cells expressing the aptamer and cells expressing the control RNA. Further experiments were performed to determine the IC50 for neomycin-B inhibition of cell proliferation of cells that expressed control RNA compared to cells that expressed the neomycin-B RNA aptamer (Fig. 13).

Figure 13

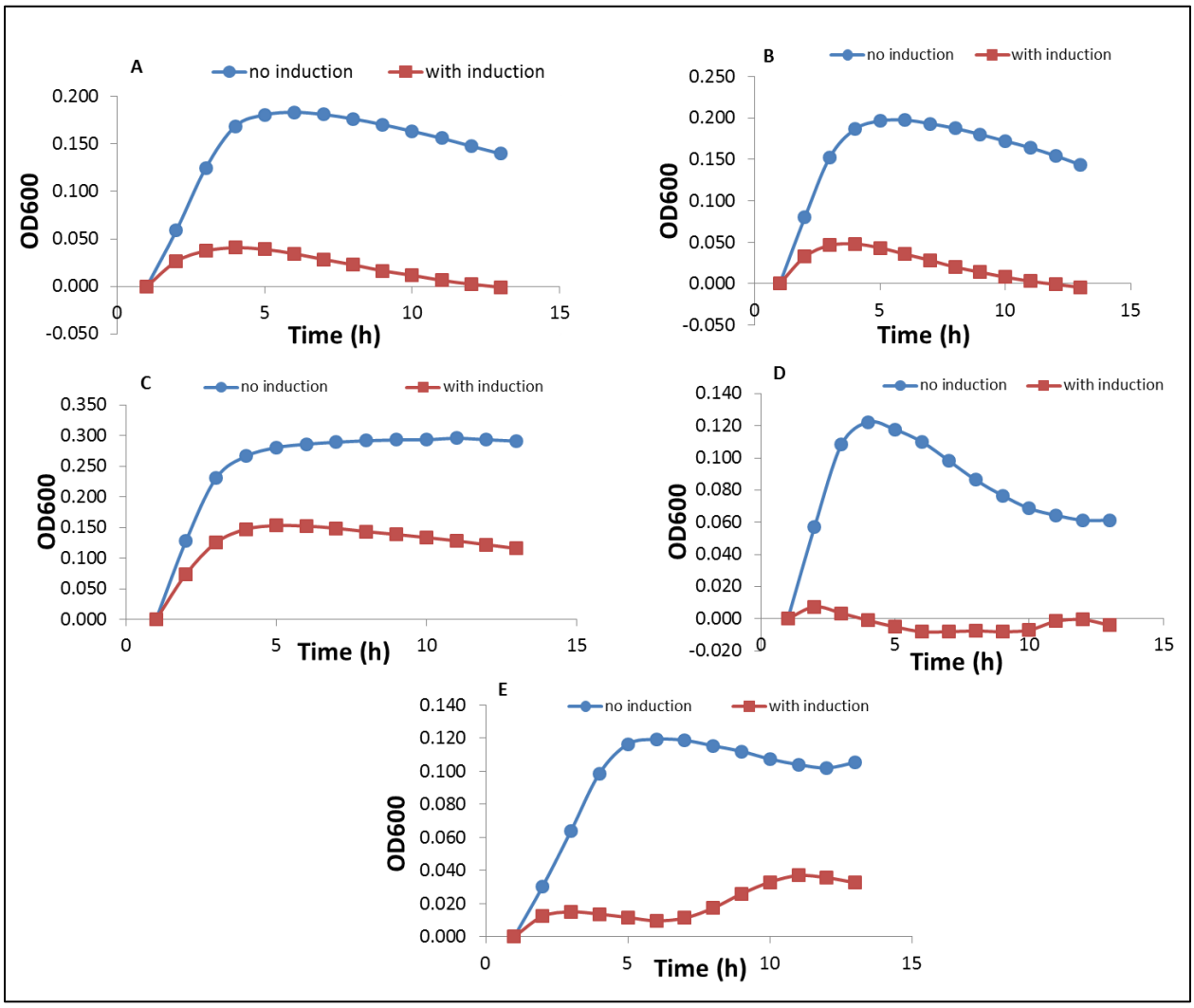

Figure 13. Comparison of bacterial growth with and without IPTG induction for cells that express neomycin-B aptamers. These results show that when the neomycin-B aptamer is expressed (induced by IPTG) decreases the growth of bacteria in the presence of aminoglycosides**.** aptamer (closed squares) **(A)** 7.5 μM Kanamycin-A, **(B)** 5 μM Kanamycin-B, **(C)** 7.5 μM Paromomycin**, (D)** 5 μM Neomycin-B, **(E)** 5 μM Tobramycin**.** In all cases cells without IPTG induction is shown in closed circles.

Figure 14

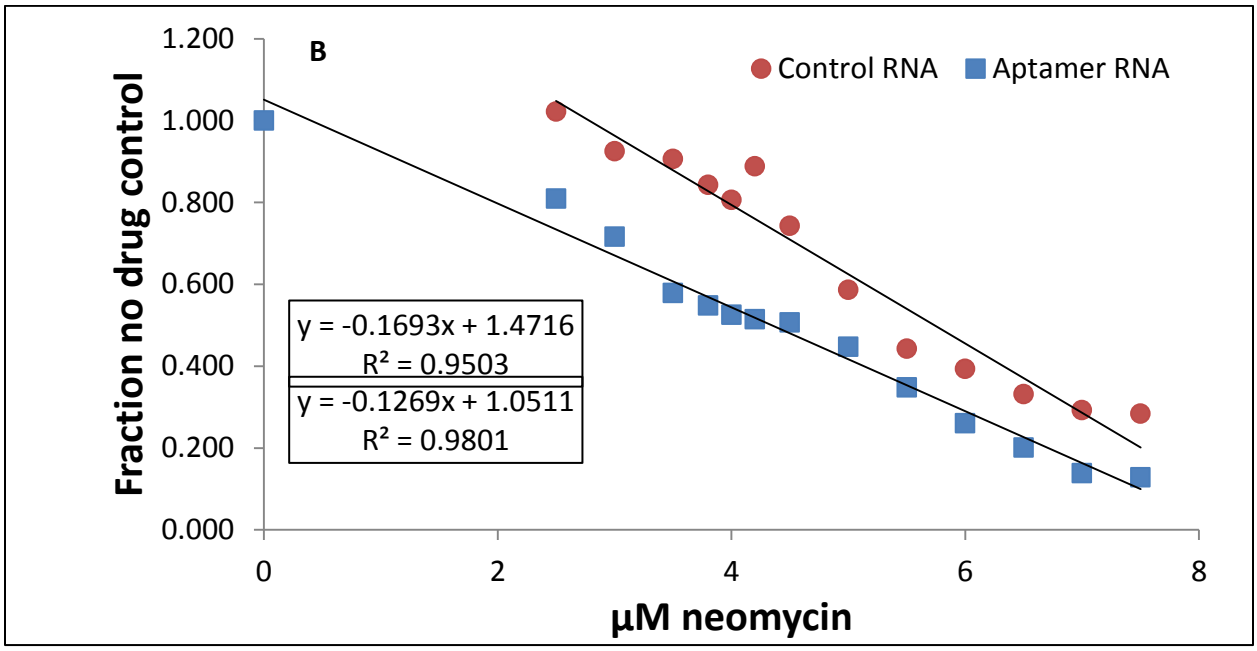

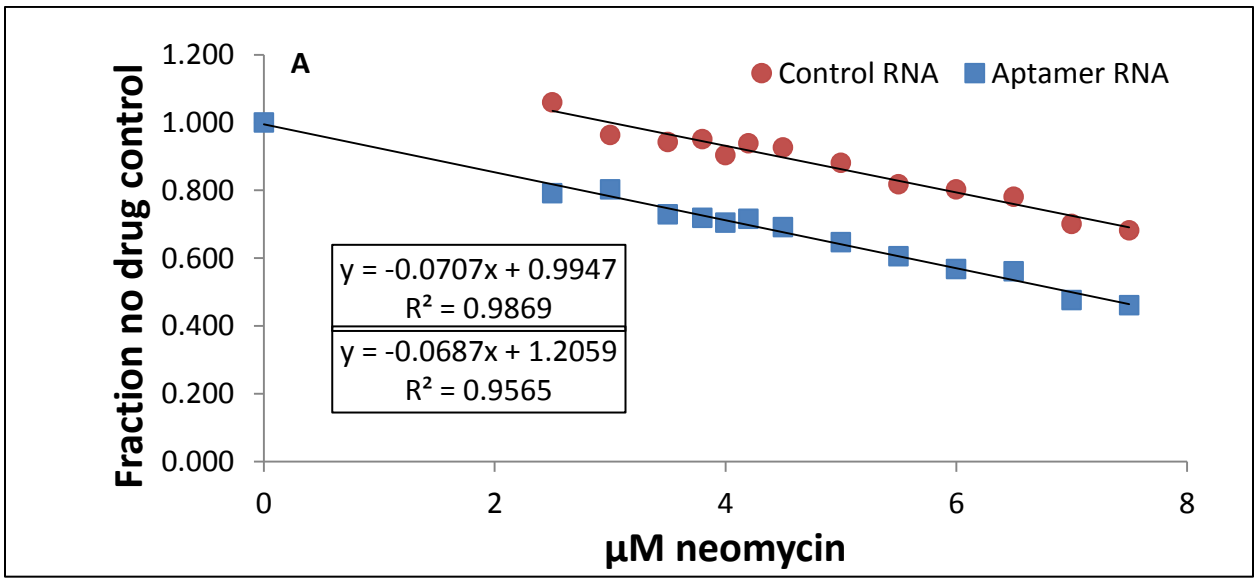

Figure 14. Comparison of bacterial growth with neomycin aptamer expression. The final cell densities were normalized to the no-drug control sample for cells that expressed the neomycin aptamer (closed squares) and with cells that expressed the control RNA (closed circles). **(A)** 1 h time point (**B)** 6 h time point.

From these data, more accurate estimates were made of IC50 values than the estimates shown in Table 1. These values are shown in Table.2. Neomycin-B molecules inside the cell at the presence of the aptamer can exists in two forms, one is as free neomycin-B and other is the neomycin-B bound to the aptamer. Of these two forms only free neomycin-B that is not bound with the aptamer can be utilized for cell killing by interacting with the ribosome. Therefore the results in figure 12, 13 and 14 demonstrate that the free drug concentration inside the cell increases when the neomycin-B aptamer is expressed which leads to cell killing.

Table 3. IC50 values for neomycin aptamer with neomycin-b

	Aptamer expressing cells (μM)	With control RNA expressing cells (μM)
Lag phase	2.5	5
Log phase	3.6	4.7
Stationary phase	4.0	6.2
6hour time point	2.3	5.9

A Decrease in the minimum inhibitory concentration (MIC) was observed for neomycin-B with neomycin-B aptamer expressing cells as compared with the control.

Another approach to test the hypothesis of that aptamers increase the intracellular drug concentration is to calculate the minimum inhibitory concentration or the MIC value. The MIC is the minimum concentration of a drug required to inhibit the growth after an overnight incubation. MIC values were calculated for cells that expressed aptamers and cells that expressed the control RNA, (Fig.15) & (Table 4).

Table 4. **Minimum inhibitory concentration values for neomycin-B for cells with neomycin aptamer expression and cells with control RNA expression.**

Neomycin-B concentration (μg/mL)	Cells with control RNA expression	Cells with aptamer expression
12.5	No growth	No growth
6.25	No growth	No growth
3.12	No growth	No growth
1.56	Growth	No growth
1.00	Growth	No growth
0.78	Growth	Growth
0.50	Growth	Growth
0.39	Growth	Growth
0.19	Growth	Growth
0.09	Growth	Growth

Table 5. Controls in the minimum inhibitory concentration experiments

Plate	LB+ Agar	Neomycin-B 1mg/mL	Cells	Growth Conditions
1	+	-	-	No growth
2	+	+	-	No growth
3	+	+	+	No growth
4	+	-	+	Growth

Figure 15

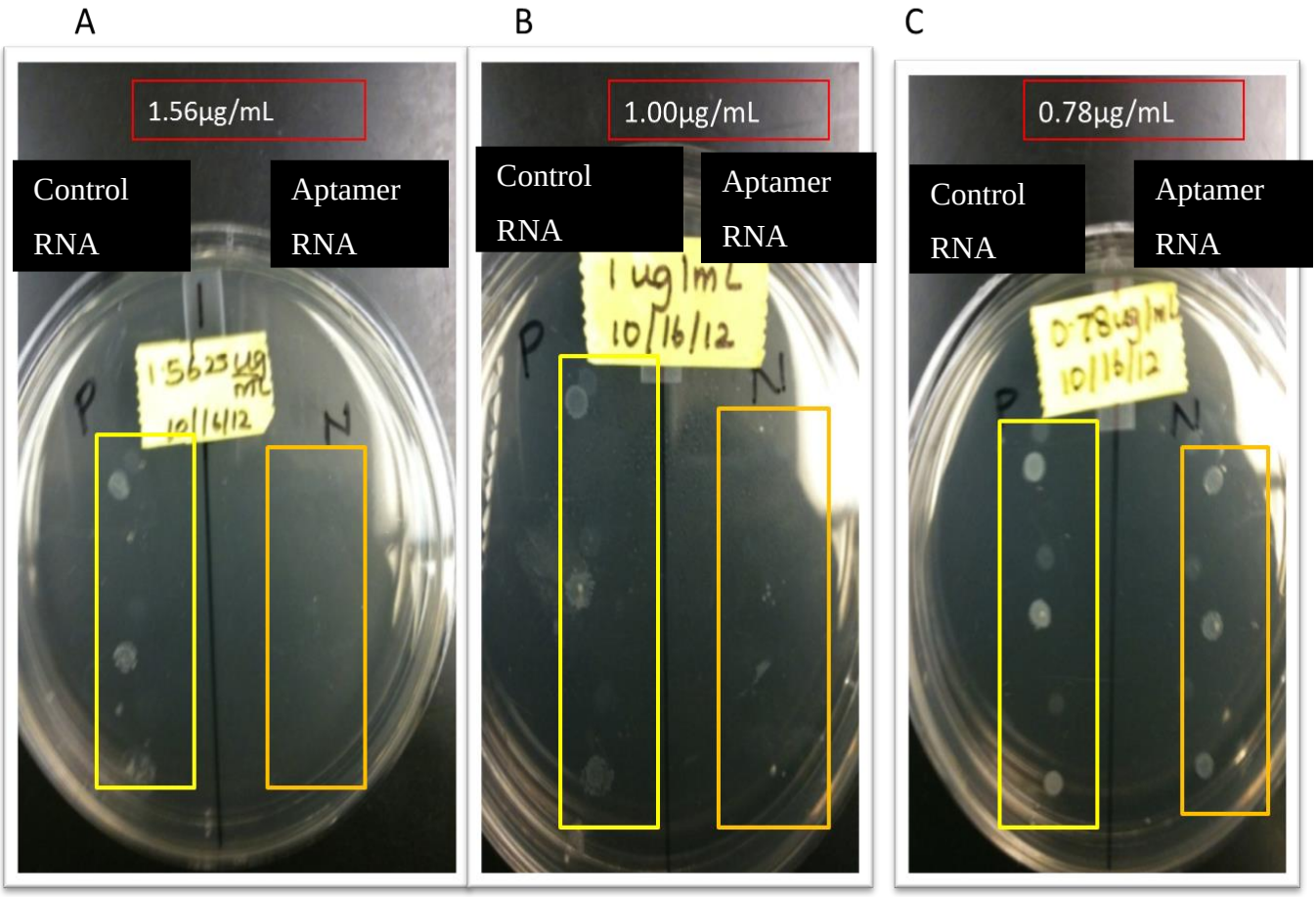

Figure 15. Comparison of visible bacterial growth on agar plates with aptamer expression and with control RNA expression A) Cells neomycin-B aptamer and cells expressing control RNA was spotted on agar plate with 1.56 µg/mL neomycin-B, **(B)** Cells expressing neomycin-B aptamer and cells expressing control RNA were spotted on agar plates with 1.00 µg/mL neomycin-B. **(C)** Cells expressing neomycin-B aptamer and cells expressing control RNA were spotted on agar plates with 0.78 µg/mL neomycin.

Effect of DRAGINS on intracellular drug concentrations

The previously described results showed that DRAGINS affect the growth of bacterial cells because aptamer expressing cells have lower IC50 and MIC values than the control RNA expressing cells. This suggests that the intracellular concentration of neomycin-B was increased in cells that expressed aptamers. To test this conclusion, I used a direct test of the effect of DRAGINS on the intracellular drug concentration, which was to measure the cell uptake of paromomycin labeled with Cy3 that was analyzed by fluorescence imaging and fluorescence spectroscopy. I also attempted to determine the extracellular drug concentrations with condition using High Performance Liquid Chromatography (HPLC) to analyze the aminoglycoside modified by chemical linkage to a fluorescent moiety. In these experiments described in this section I used cells that expressed neomycin-B aptamer and as the control I used cells that expressed control RNA, which is of the same length as the aptamer, but does not bind with the aminoglycoside drug as the aptamer.

Effect of aptamer expression on the Intracellular Cy3-paromomycin concentration

Increase in fluorescence signal was observed for cells with aptamer expression after incubating with Cy3-paromomycin as compared to controls. To verify the hypothesis that aptamers increase the intracellular drug concentration, Cy3- paromomycin was used instead of neomycin-B as neomycin-B does not have any chromophores or fluorophores for its ready detection. First an imaging approach was taken to determine the effect of aptamers on intracellular Cy3-paromomycin levels (Figs. 16 & 17). For this initial experiment 3μM of Cy3-paromomycin was selected as this concentration was used in our growth analysis experiments.

As evident by these results, aptamer expressing cells have more Cy3-paromomycin intracellular drug molecules than the cells expressing control RNA. To verify the results, I performed the same experiment with more controls to account for background fluorescence coming from cells, the background fluorescence coming from Cy3-paromomycin without any cells, and the filter used in these experiments.

It is clear from the above results that aptamer expressing cells have higher intracellular drug concentrations than the cells expressing the control RNA, because the fluorescence image of letter “L” written by cells expressing the aptamer incubated with Cy3-paromomycin is more intense than the rest of the fluorescence images of letter “L” written by the cells expressing the

control RNA incubated with Cy3-paromomycin, cells that were not incubated with Cy3-paromomycin or the just the filters used in these experiment.

But this approach is more of a qualitative analysis. For a more quantitative approach I used fluorescence spectroscopy with Cy3-paromomycin. I determined the internal fluorescence intensity for three different concentrations of Cy3-paromomycin (Fig. 18). In these experiments I introduced a new control which is named as “zero time incubation”. In this sample cells were grown in a similar fashion as the rest of cell cultures. Cy3-paromomycin was introduced just before precipitating the cells for their analysis. This sample was done to account for the any adhered Cy3-paromomycin to the cell surface.

The results showed that cells expressing the neomycin-B aptamer have higher fluorescence emission at 563nm, the Cy3 fluorescence maximum, compared with cells expressing the control RNA and when the back ground fluorescence coming from cells and adhered fluorescent molecules were subtracted from the fluorescence spectrum of cells expressing the aptamer and cells expressing the control RNA this difference was much clearer.

Figure 16

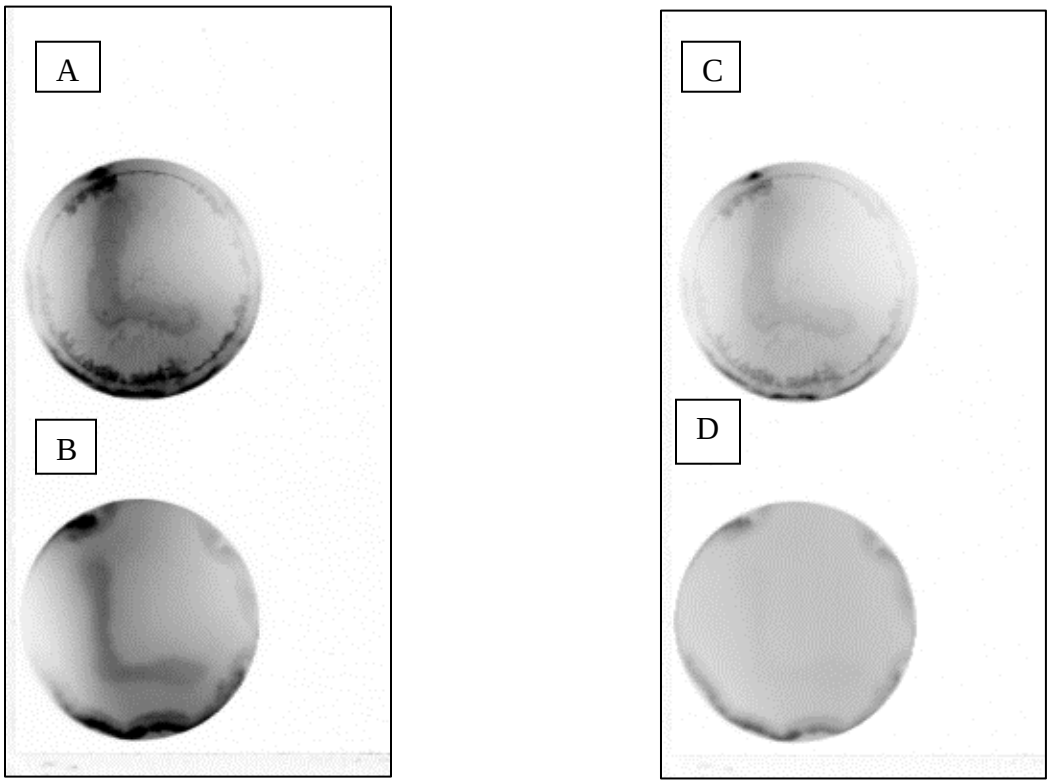

Figure 16. Comparison of intracellular Cy3-paromomycin in cells expressing the neomycin-B aptamer and cells expressing the control RNA. **(A)** Fluorescence image of cells with aptamer expression taken at 400pmt voltage. **(B)** Fluorescence image of cells with aptamer expression taken at 300pmt voltage. **(C)** Fluorescence image of cells expressing the control RNA taken at 400pmt voltage. **(D)** Fluorescence image of cells expressing the control RNA taken at 300pmt voltage.

Figure 17

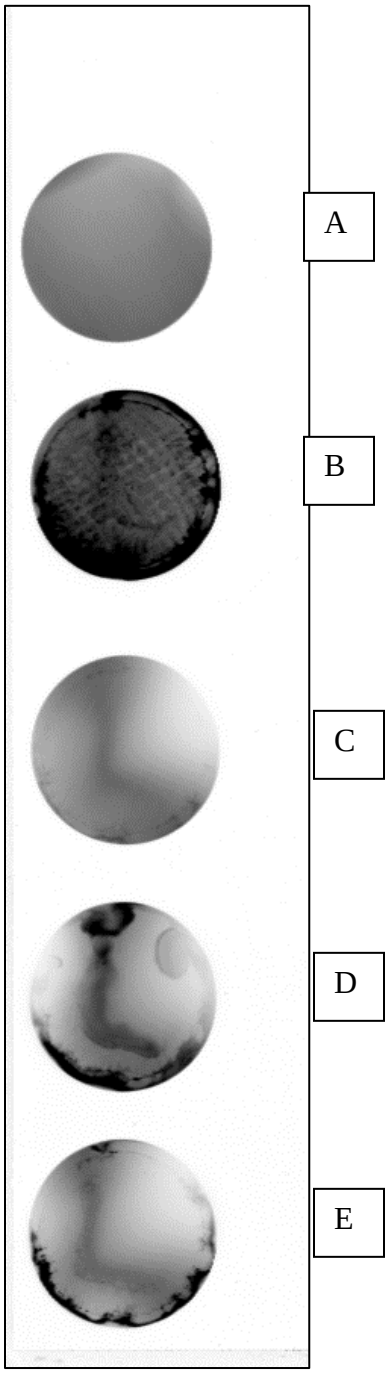

Figure 17. Fluorescence images of cells with and without expressed neomycin-B aptamer and the controls for the images. **(A)** Fluorescence image of just the filter **(B)** 3μM Cy3 labeled paromomycin, **(C)** cells with neomycin-B aptamer without any antibiotic incubation, **(D)** cells expressing the neomycin-B aptamer incubated with 3μM Cy3-paromomycin, **(E)** cells expressing the control RNA incubated with Cy3-paromomycin. All images obtained with 400pmt voltage.

Figure 18

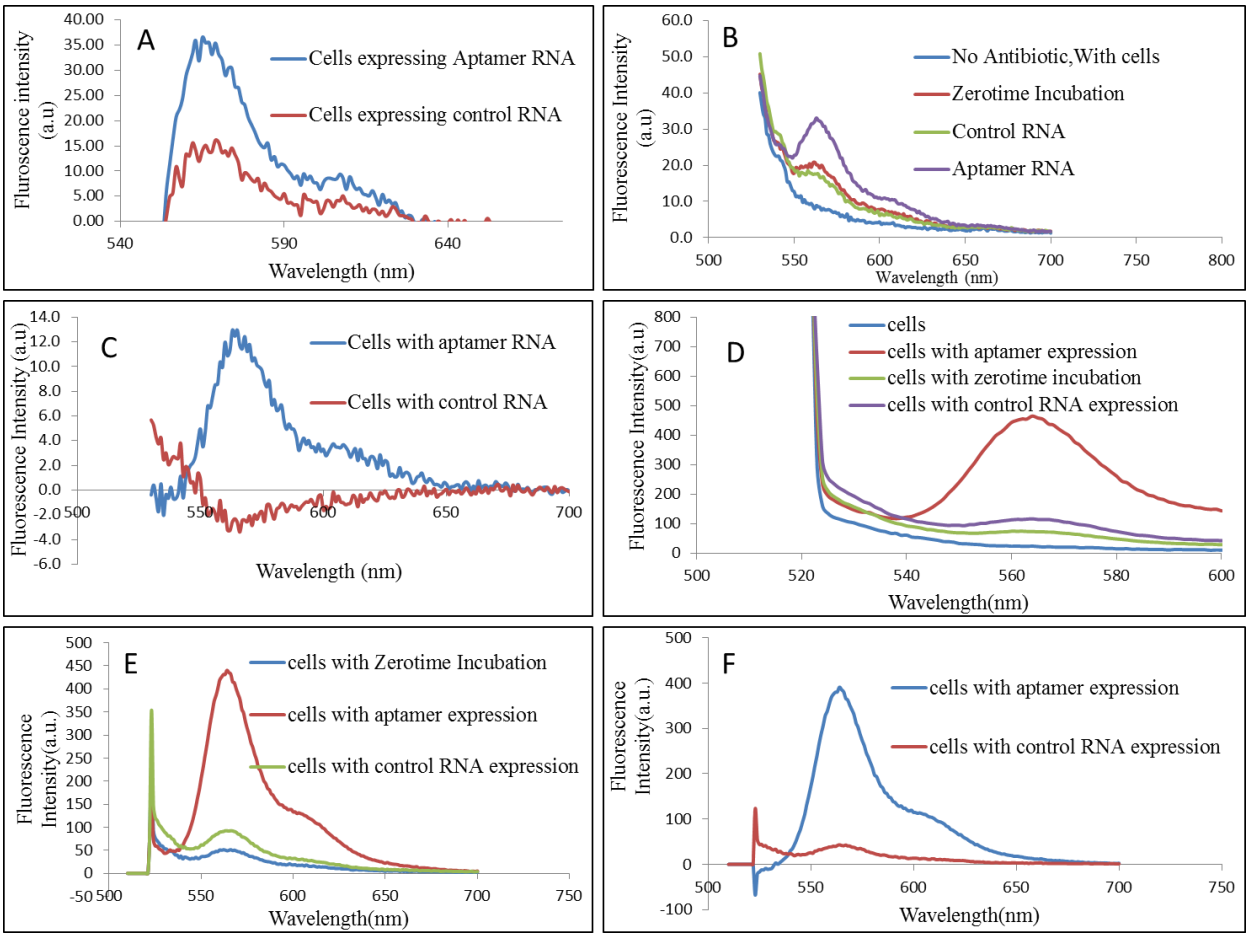

Figure 18. Fluorometry of cells with and without expressed neomycin-B aptamer and the controls. **(A)** 3µM Cy3-paromomycin incubated with cells with aptamer expression and cells with control RNA expression after the no antibiotic control was subtracted from both. **(B)** 5µM Cy3-paromomycin incubated with aptamer expressing cells and cells expressing the control RNA with controls of no antibiotic and zero time incubation. **(C)** 5µM Cy3-paromomycin incubated with aptamer expressing cells and cells expressing the control RNA after the no antibiotic control and zero time incubation control subtracted from both. **(D)** 7µM Cy3-paromomycin incubated with aptamer expressing cells and cells expressing the control RNA with controls of no antibiotic and zero time incubation. **(E)** 7µM Cy3-paromomycin incubated with aptamer expressing cells and cells expressing the control RNA after no antibiotic control subtracted from others. **(F)** 7µM Cy3-paromomycin incubated with aptamer expressing cells and

cells expressing the control RNA after no antibiotic control and zero-time incubation control subtracted from both.

To verify that the increase in intracellular Cy3- paromomycin in cells expressing the neomycin-B aptamer was due to the paromomycin moiety and not Cy3, I performed several other control experiments. Cy3 and paromomycin of the similar concentrations were mixed in the same culture tube and incubated with the cells. Other cell cultures were incubated with Cy3 and or paromomycin (Fig. 19).

As shown by these results, when neomycin-B aptamer expressing cells were incubated with Cy3- paromomycin the fluorescence at 563nm, which is the CY3 fluorescence emission maximum, was highest. This result indicates that cells expressing neomycin-B apatmer have the highest intracellular concentration of Cy3-Paromomycin. In another test that aptamer expression causes the increase in intracellular Cy3-paromomycin concentration, experiments to observe Cy3-paromomycin uptake by the cells were performed with and without IPTG to induce aptamer or control RNA expression (Fig.20).

Figure 19

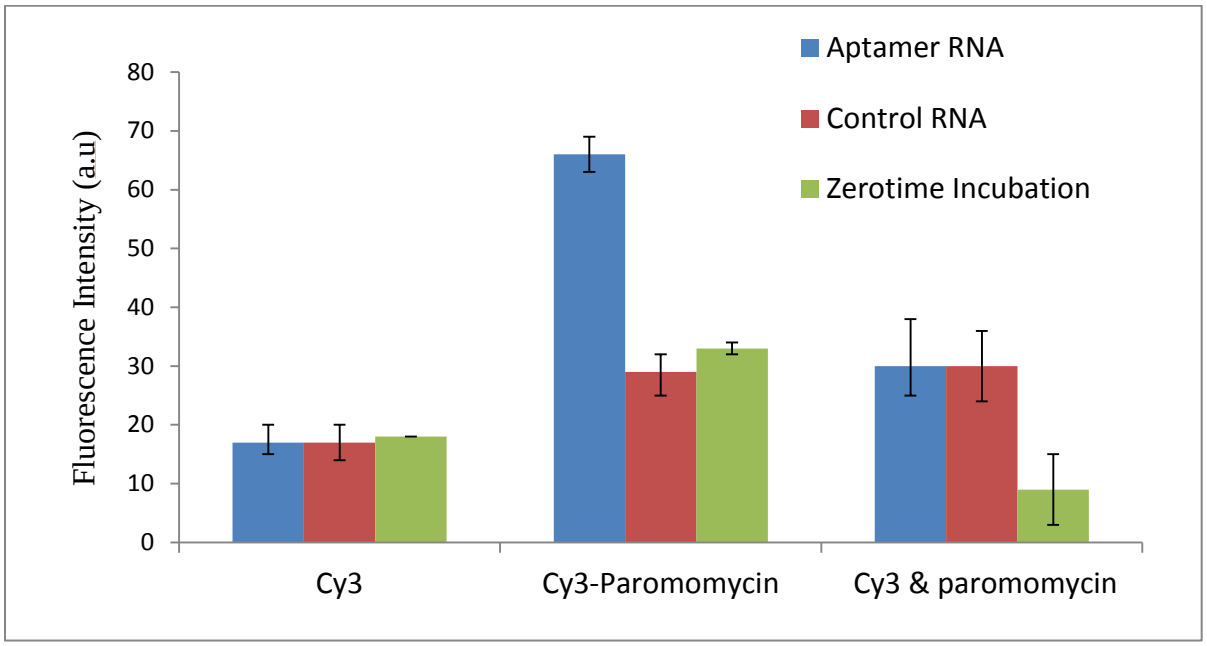

Figure 19. Fluorometry of aptamer expressing cells and control RNA expressing cells incubated with CY3 labeled paromomycin, CY3, CY3 and paromomycin.

IPTG induces the aptamer RNA and control RNA synthesis, therefore cell cultures incubated with IPTG will have higher levels of plasmid-expressed RNA than in the absence of IPTG. In this experiment, cells incubated with IPTG and expressing the neomycin-B aptamer showed the highest fluorescent emission peak around 563nm indicating that these cells have the highest intracellular Cy3-paromomycin (Fig.20).

Figure 20

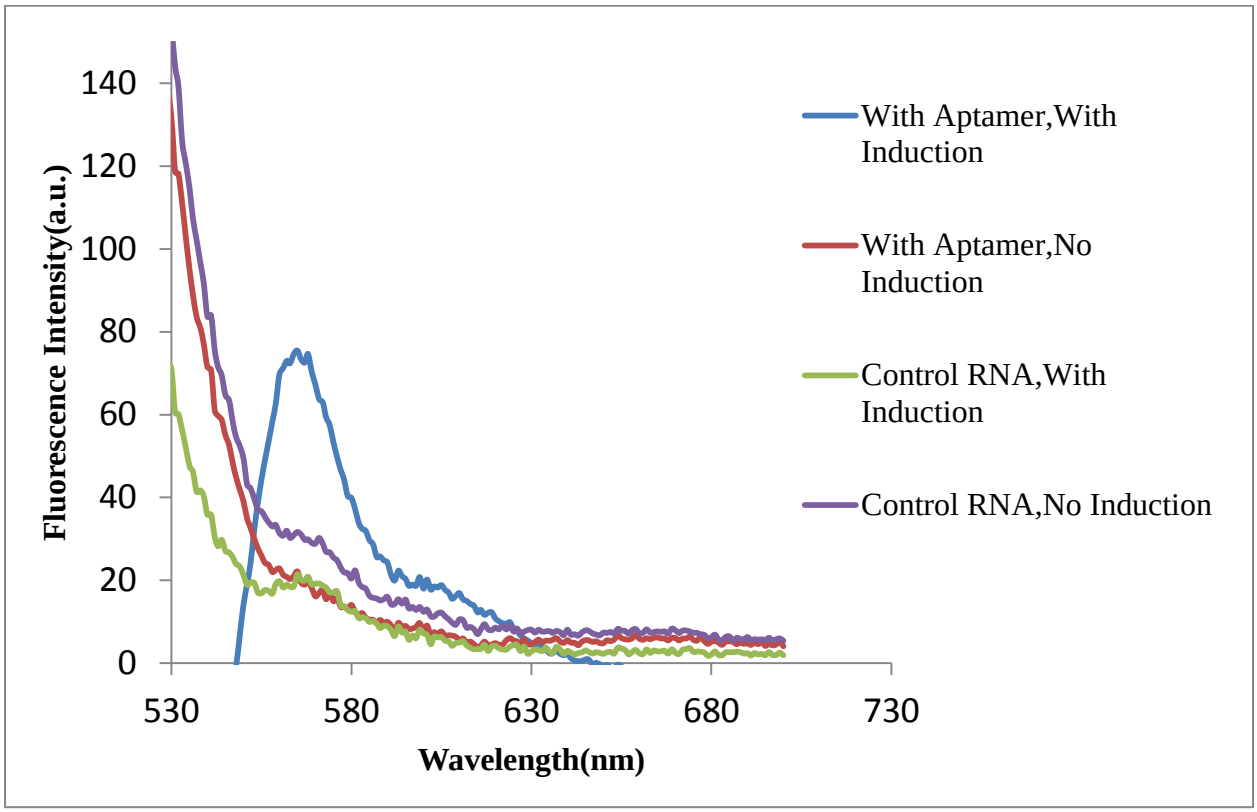

Figure 20. Fluorescence spectra of aptamer expressing cells and cells expressing control RNA with and without IPTG induction. Aptamer expressing cells and cells expressing the control RNA was incubated with Cy3-paromomycin and directed to fluorescence spectroscopy.

Measuring the extracellular neomycin-B concentration

To determine the concentration range of FMOC-neomycin-B that can be detected by this method 0.25µM and 2.5µM of neomycin-B were tested by modifying with FMOC-Cl and analyzed by HPLC.

Figure 21

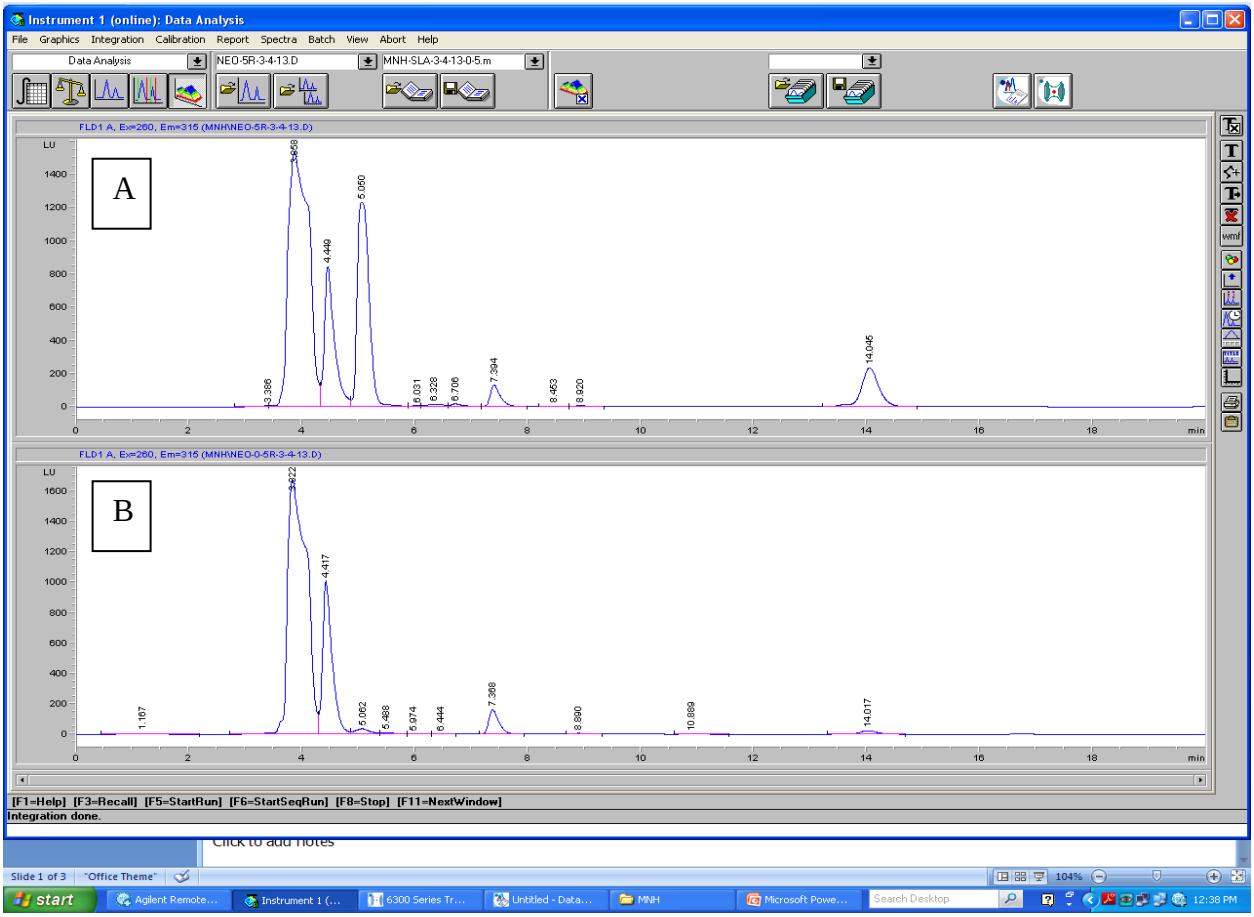

Figure 21. HPLC chromatograms obtained by C18 RP column and 90:10=Acetontrile: Water isocratic elution. (A) 2.5µM Neomycin-B **(B)** 0.25µM Neomycin-B.

As evident from the chromatogram 2.5 µM neomycin-B (aq) around 14 minutes retention time and when the neomycin-B was diluted 10 times to a concentration of 0.25 µM, then the peak around 14 minutes retention time was observed but with much less intensity. Thus, this result shows that 2.5 µM neomycin-B can be detected by this method. To verify the peak that I observed at around 14 min is due to neomycin-B rather than a system artifact, 2.5 µM kanamycin-A **(**aq) was analyzed in the same way by HPLC. Kanamycin-A is an aminoglycoside with similar properties to neomycin-B.

Figure 22

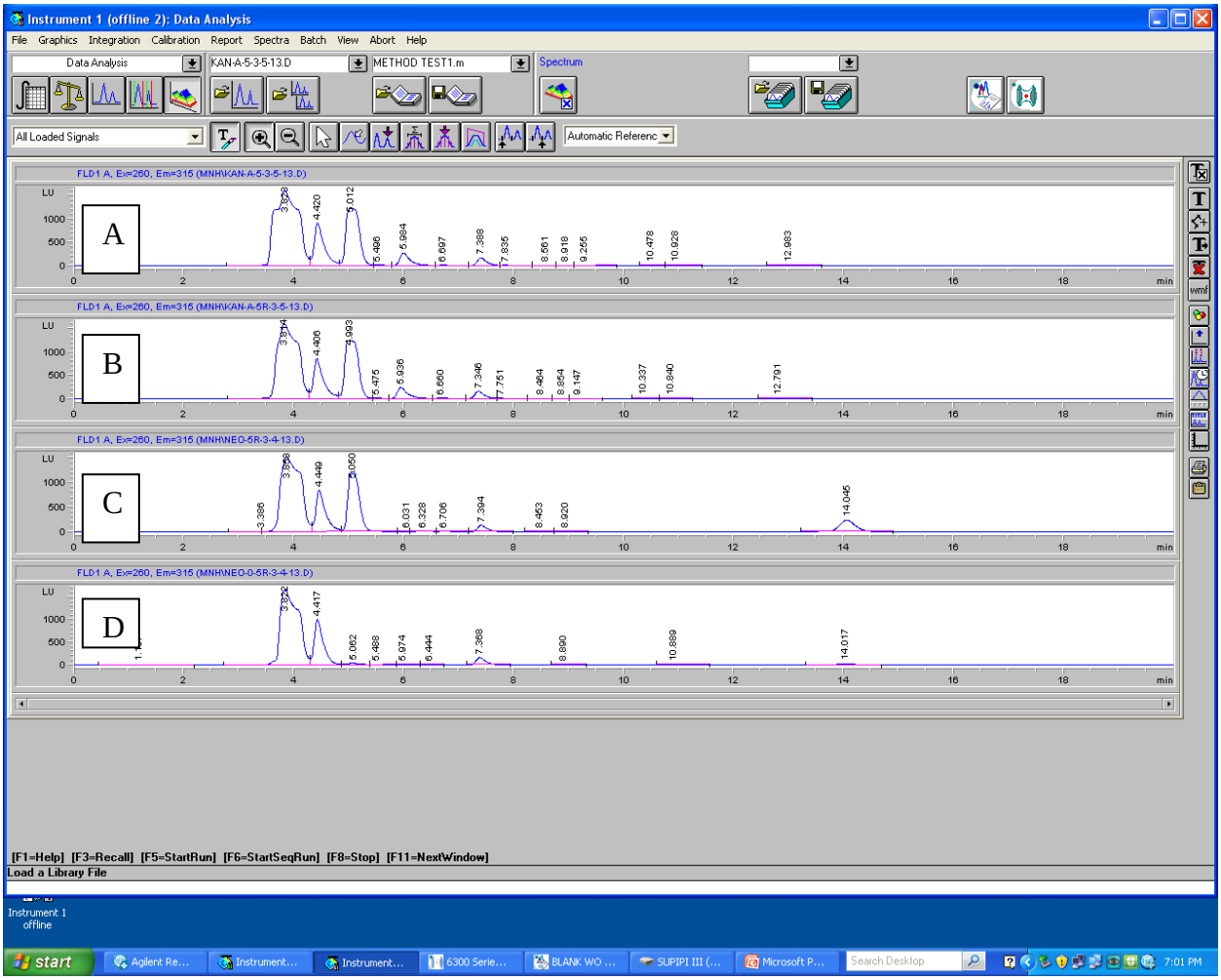

Figure 22. HPLC chromatograms obtained by C18 RP column and 90:10=Acetontrile: Water isocratic elution. (A) 2.5 µM Kanamycin-A **(B)** 2.5 µM Kanamycin-A **(C)** 2.5 µM Neomycin-B **(D)** 0.25µM Neomycin-B.

In the kanamycin-A chromatogram peak around 5 min retention time could be observed in repeated experiments. But the peak observed at 14 min for Neomycin-B was absent. Therefore the kanamycin-A peak of 5 min and neomycin-B peak of 14 min are unique to the each aminoglycoside. This is evident that the 14 min retention time peak is due to neomycin-B.

The next step was to observe whether this method can be used to detect neomycin-B in culture medium. All bacterial cell cultures for this project were grown in Luria Broth (LB), this culture media was incubated with FMOC-Cl and analyzed by HPLC. For the FMOC-Cl reaction, the sample was diluted to 40% LB. The chromatograms of 40% LB and 2.5 µM neomycin-B were compared (Fig. 23).

Figure 23

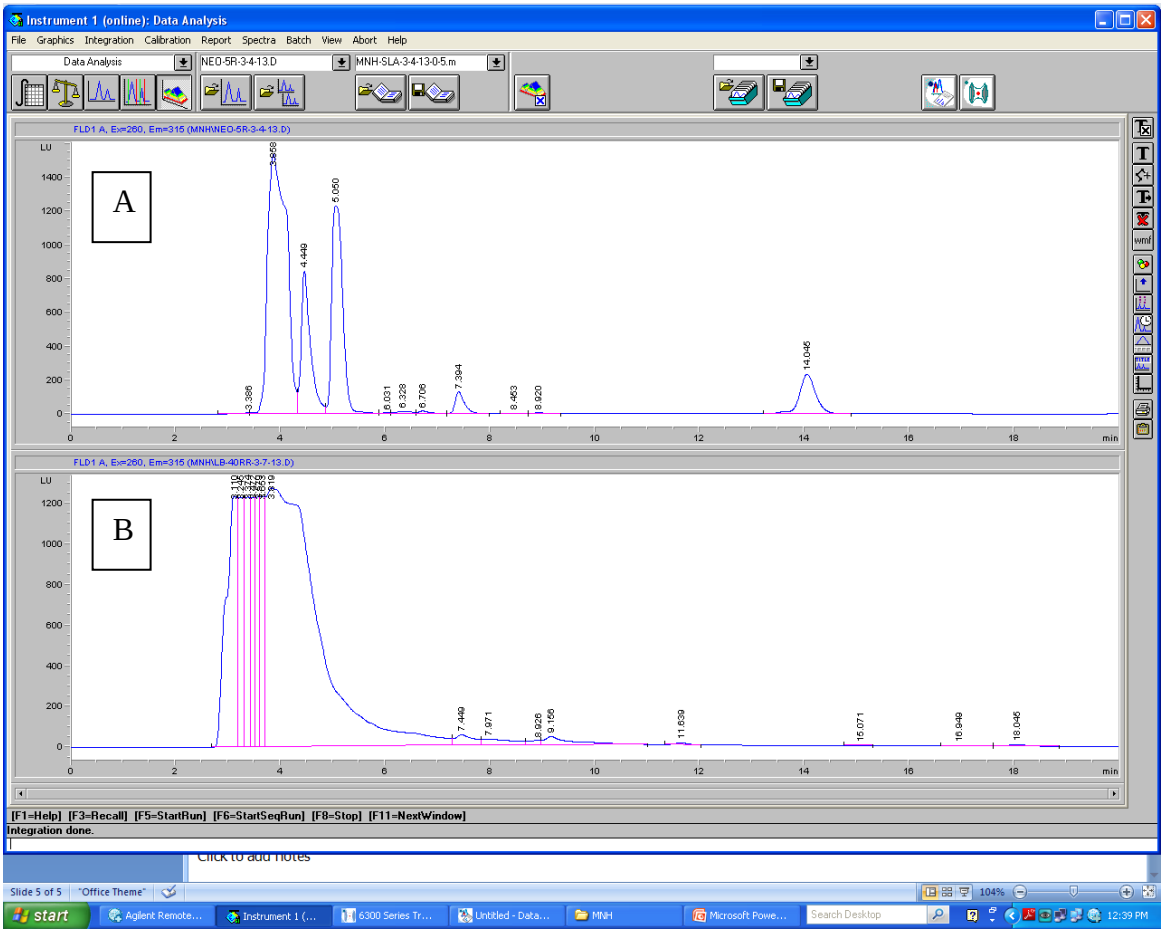

Figure 23. HPLC chromatograms obtained by C18 RP column and 90:10=Acetontrile: Water isocratic elution. (A) 2.5µM Neomycin-B **(B)** 40% LB.

The chromatogram of 40% LB did not have any peaks around the retention time of 14 min, which is the position of the neomycin-B peak. Therefore it seems the LB does not interfere in the detection of neomycin-B. I then analyzed a 2.5µM Neomycin-B in 40% LB (Fig. 24).

As been evident by the chromatogram the peak that I observed around 14 min retention time is for 2.5µM neomycin-B (aq) is not visible in 2.5µM neomycin-B in 40% LB. It appears from this chromatogram that the presence of LB interferes with the ability to detect neomycin-B.

Figure 24

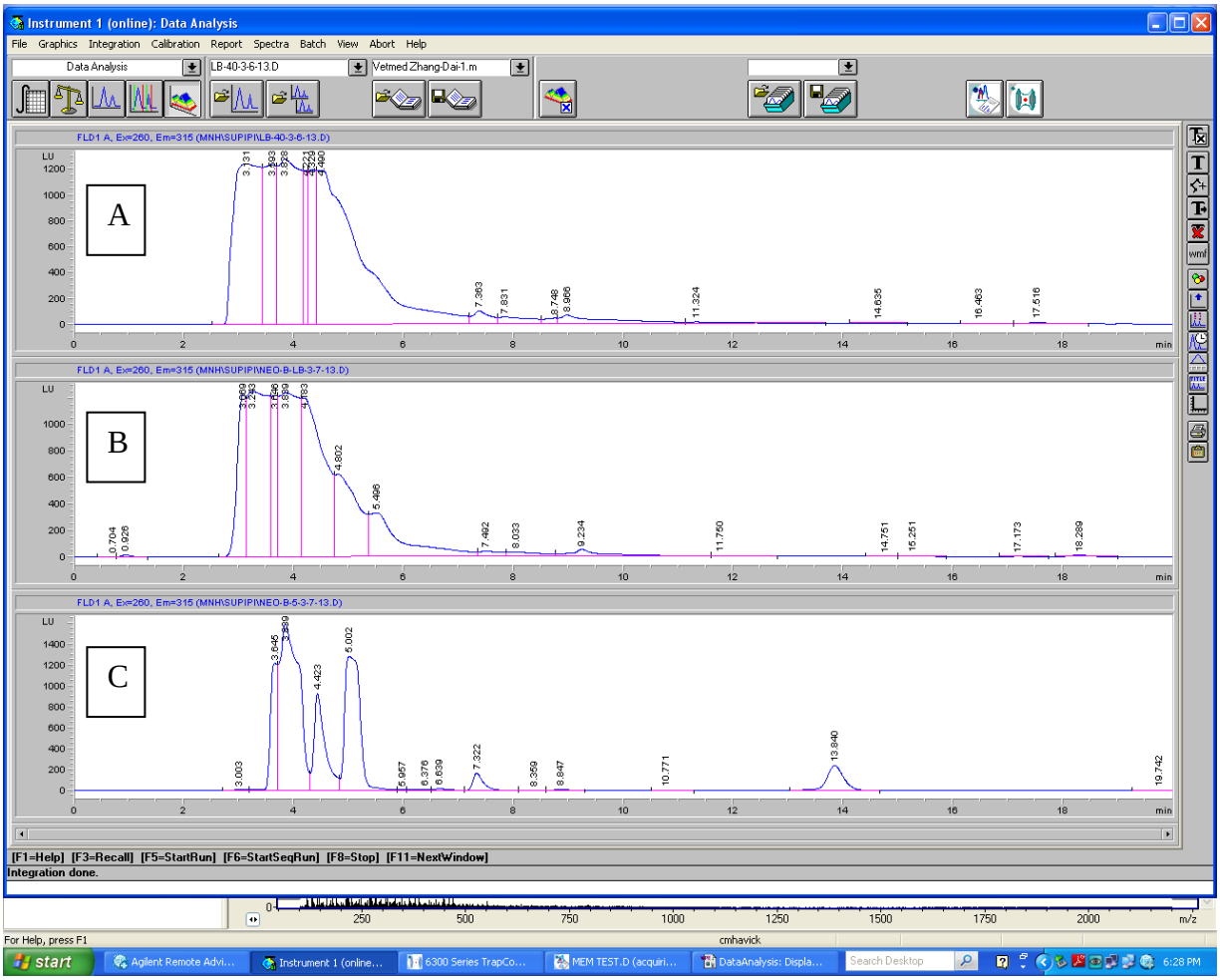

Figure 24. HPLC Chromatograms of (A) 40% LB **(B)** 2.5µM Neomycin-B in 40% LB **(C)** 2.5µM Neomycin-B.

To establish the background fluorescence coming from the other components of the coupling reaction the same reaction and HPLC analysis was performed on the fluorescent agent, FMOC-Cl incubated with and without glycine, which was the quenching reagent for the coupling reaction, or with and without the borate buffer (Fig. 25).

The resulting chromatograms show that the other components in the reaction mixture do not create a peak that migrates in the same position as FMOC-Cl-neomycin-B.

Figure 25

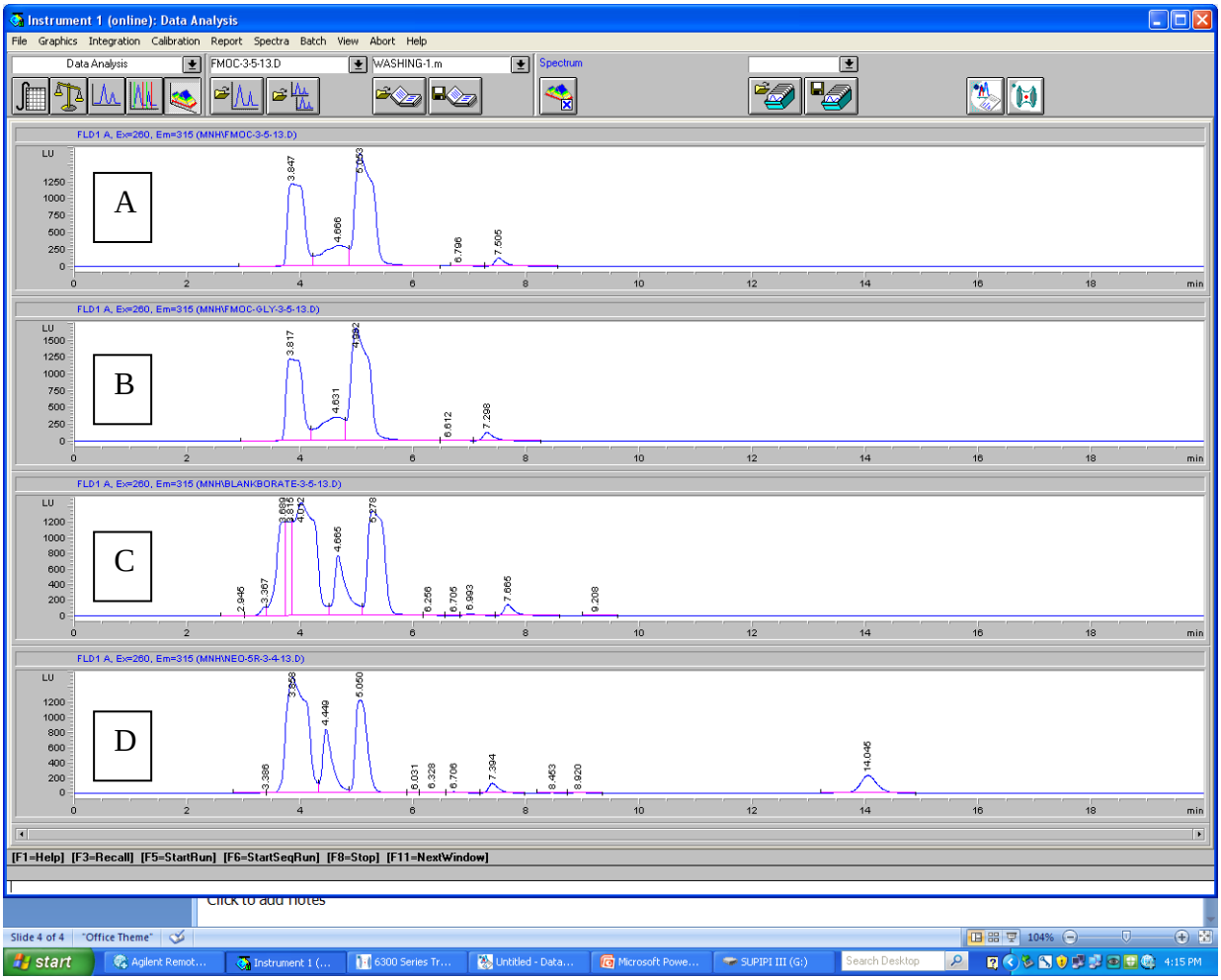

Figure 25. HPLC Chromatograms of (A) 1mM FMOC-Cl with 0.1M Glycine with 0.185M borate buffer **(B)** 1mM FMOC-Cl without glycine and borate buffer **(C)** 1Mm FMOC-Cl with 0.185M borate buffer and without glycine **(D)** 2.5µM Neomycin-B.

To verify that the fluorescent reagent that I used, FMOC-Cl, was not a limiting reagent for the coupling reaction I carried out experiments that reacted 2.5 µM Neomycin-B in 40% LB with 2 mM, 10 mM and 1M FMOC-Cl and analyzed these samples by HPLC (Fig. 26).

Figure 26

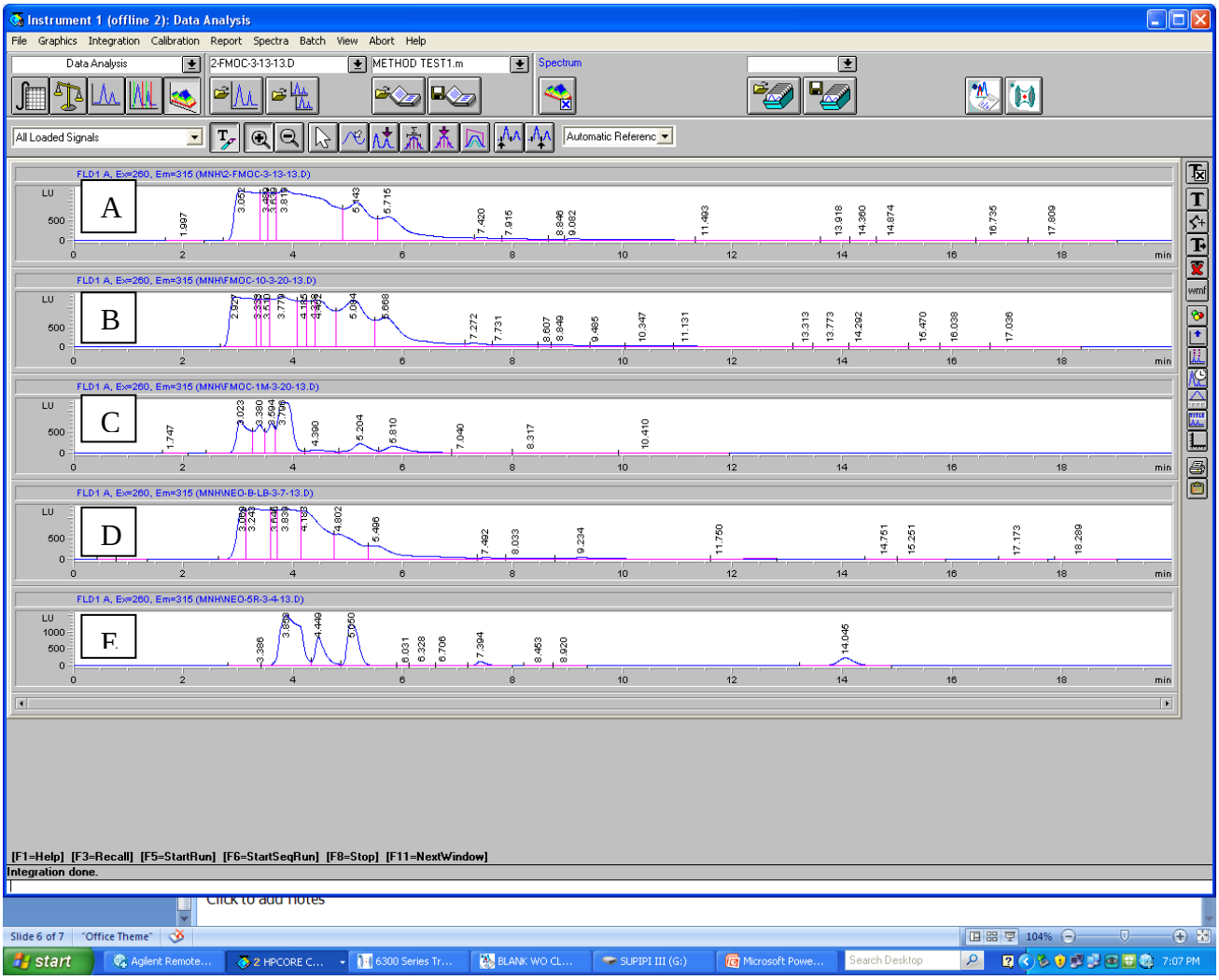

Figure 26. HPLC Chromatograms of 2.5µM Neomycin-B and 40% LB coupled with (A) 2mM FMOC-Cl **(B)** 10Mm FMOC-Cl **(C)** 1M FMOC-Cl and **(D)** 2.5µM Neomycin-B in 40% LB **(F)** 2.5µM Neomycin-B.

The results showed that increasing the FMOC-Cl concentration does not result in the neomycin-B peak becoming visible in the neomycin-B and LB mixture. Therefore, it is unlikely a limitation.

Because the reason for the loss of the Neomycin-B peak from the neomycin-B and LB mixture seemed to be due to LB interference, the neomycin-B was extracted from the mixture of neomycin-B and LB by the use of cation exchange chromatography.

Figure 27

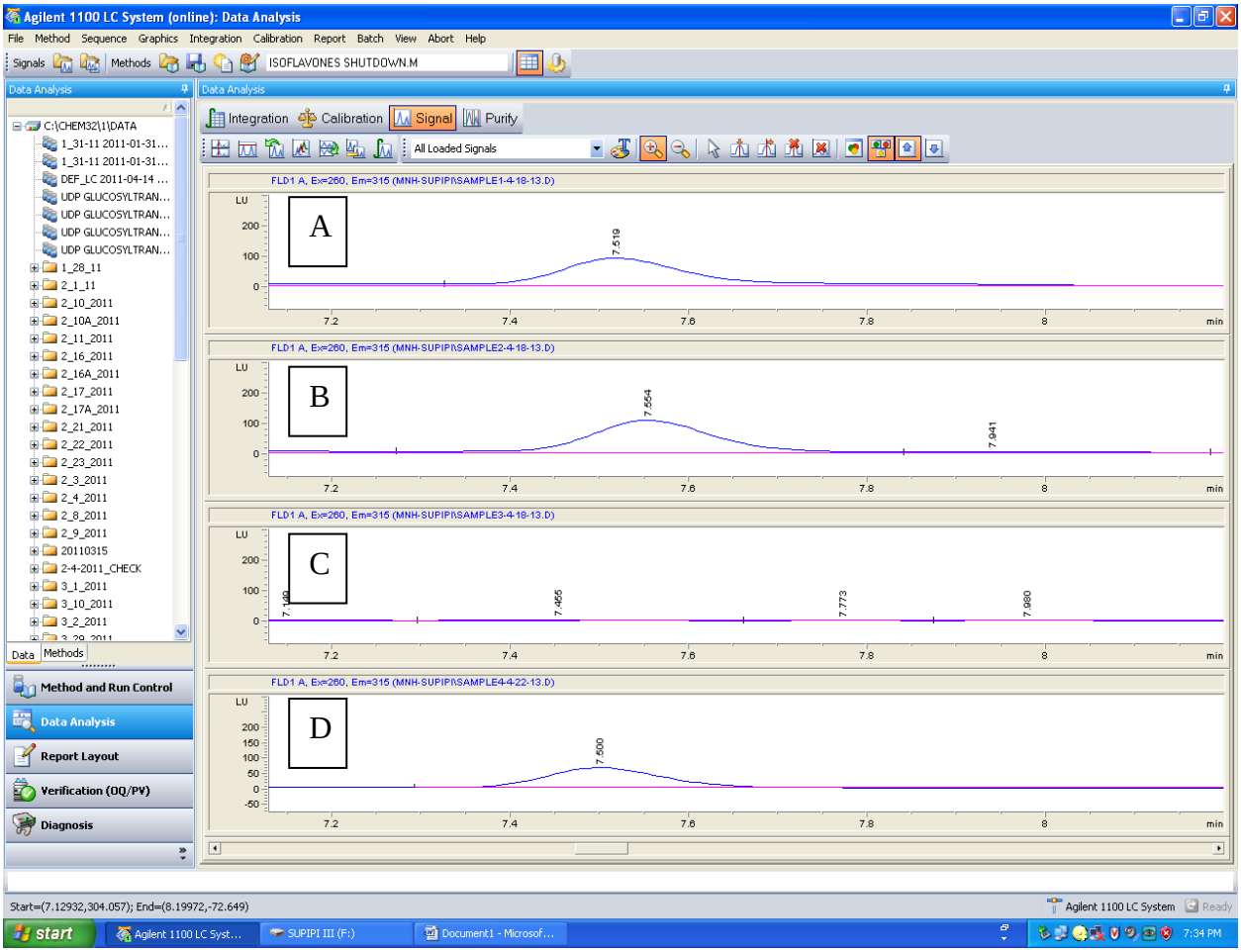

Figure 27. HPLC Chromatograms of cation exchange column 1M NH_4OH elutions of 5µM Neomycin-B (aq) (A) first 1M NH_4OH elution **(B)** second 1M NH_4OH elution **(C)** third 1M NH_4OH elution **(D)** Positive control: 4.1µM Neomycin-B in 1M NH_4OH.

To determine the ability of cation exchange chromatography to extract neomycin-B from bacterial cultures with LB, 5µM of neomycin-B was passed down the cation exchange column, eluted by three separate 1M NH_4OH elutions, reacted with FMOC-Cl, then analyzed by HPLC.

The resulting chromatograms showed that the elution 1 and 2 with 1M NH_4OH had the same peak around 7 min retention time which is visible in the positive control of 4.1 µM Neomycin-B in 1M NH_4OH that had not been run through the cation exchange column. Therefore it was decided that neomycin-B can be extracted from the cation exchange column and the FMOC derivative can be detected by HPLC. The next step was to determine how LB alone would appear on the chromatogram after passing through the cation exchange column, reaction with FMOC-Cl and resolution by HPLC. To serve that purpose 100% LB was applied to the column and then eluted consecutively three times with 1M NH_4OH.

Figure 28

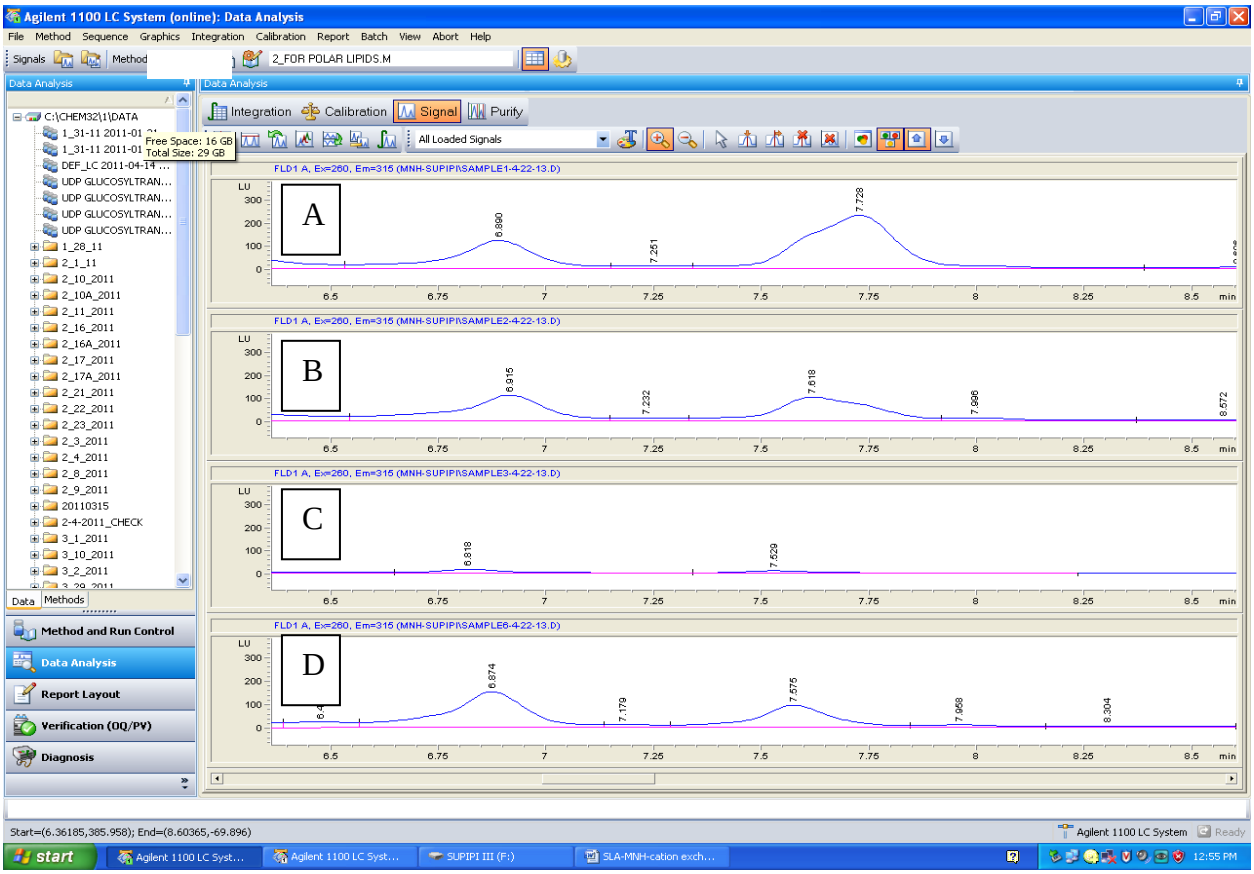

Figure 28. HPLC Chromatograms of cation exchange 1M NH_4OH elutions of 100% LB (A) first 1M NH_4OH elution **(B)** second 1M NH_4OH elution **(C)** third 1M NH_4OH elution **(D)** positive control: 50% LB in 1M NH_4OH.

Chromatograms of the first two elutions of 50% LB in 1M NH_4OH, showed a peak at around 8 min retention time (Fig. 24). This peak was close to the FMOC-neomycin-B peak and could interfere with the latter. A mixture of 5 µM Neomycin-B and 50% LB was then through the cation exchange column and eluted three consecutive times with 1M NH4OH. The eluted samples were reacted with FMOC-Cl and analyzed by HPLC.

Figure 29

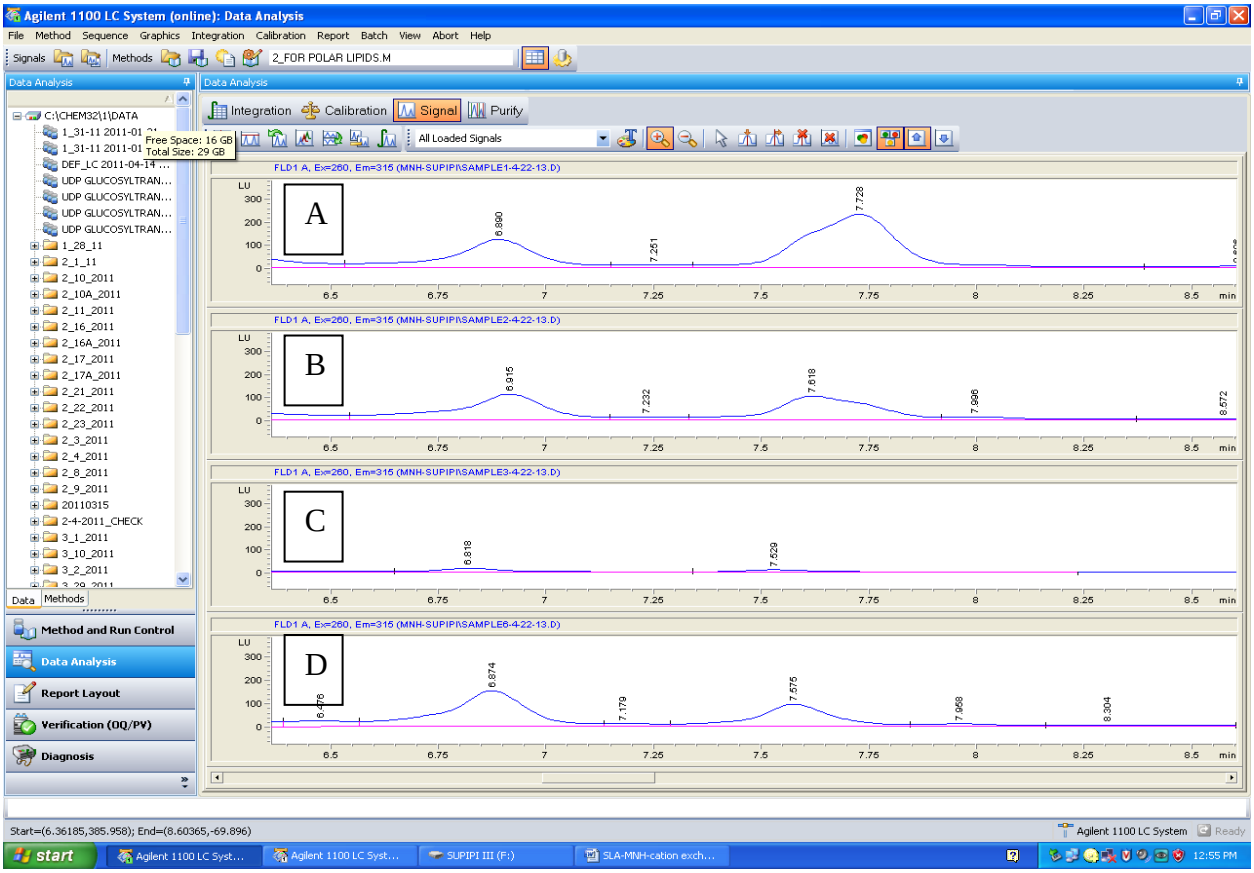

Figure 29. HPLC Chromatograms of cation exchange with 1M NH_4OH elutions of 5µM Neomycin-B in 100% LB (A) first 1M NH_4OH elution **(B)** second 1M NH_4OH elution **(C)** third 1M NH_4OH elution **(D)** Positive control: 4.1µM Neomycin-B in 50% LB with 1M NH_4OH.

The three 1M NH4OH elutions contained two peaks around 6.8 min and 7.7 min, whereas the positive control sample that was not run through the cation exchange column also contained the peaks around 6.8 min and 7.5min. These 6.8 min and 7.5 min peaks are the characteristic peaks observed for 100% LB passed through the cation exchange column and resolved by HPLC and also its positive control sample that was not run through the cation exchange column which is 50% LB in 1M NH_4OH (Fig. 24). As demonstrated from these results the chromatogram of LB-FMOC and LB-neomycin-B-FMOC cannot be distinguished from each other. This result indicates extracting the Neomycin-B from the Neomycin-B and LB mixture was not successful. This could be because LB and aminoglycosides might have molecules with a very similar polarity and they both elute around the same retention time in the HPLC and also elute together from the cation exchange column as well.

Conclusions and future directions

The results presented here show the ability of *in vivo* expressed aminoglycoside aptamers to increase aminoglycoside concentrations inside the cells. First we observed the effect of expressing aptamers inside the cells. This shows that expressing aptamers inside the cells do not affect the growth of *E. coli* bacterial cells in the absence of their ligands. Then we analyzed the neomycin-B aptamer expressed by cells that were incubated with different concentrations of aminoglycosides. The results showed that aptamer expression decreased the growth bacteria in the presence of a range of aminoglycoside concentrations when compared with control *E. coli* that expressed control RNA that did not bind aminoglycosides. In addition we also tested the effect of aptamer expression by varying the presence or absence of IPTG, which induces the RNA aptamer expression. Cells incubated with IPTG in which the neomycin-B aptamer was expressed grew more slowly than cells in the absence of IPTG in which the aptamers were not induced when incubated with aminoglycosides. Using the neomycin-B aptamer and the neomycin-B we determined the IC50 and MIC values, which both decreased by about 2-fold for cells with the aptamer expression compared to cells with control RNA expression.

If the increased effectiveness of neomycin-B cell killing was due to the proposed mechanism as defined by the mathematical model, then it is predicted that the intra cellular aminoglycoside concentration should increase with aptamer expression. We used Cy3-paromomycin to measure relative intracellular concentrations of aminoglycoside with and

without aptamer expression. Cells that expressed control RNA or aptamer were incubated with Cy3-paromomycin and the spectra of these cell lysates were determined. These results also showed that the cells with aptamer expression contained more the Cy3-paromomycin compared with cells that expressed the control RNA. To confirm that the increased cellular content of Cy3-paromomycin was due to aptamer recognition of the paromomycin and not to the Cy3 tag, we compared the effect of aptamer expression on the intracellular content of Cy3-paromomycin, Cy3 or a mixture of Cy3 and paromomycin. The results showed an increase in intracellular fluorescence only for aptamer-expressing cells that had been incubated with Cy3-paromomycin. Finally fluorometric analysis was done for aptamer expressing cells and control RNA expressing cells with and without IPTG induction. These results indicate that aptamer-expressing cells (IPTG induced) accumulate higher intracellular concentrations of Cy3-paromomycin compared with cells that are not induced by IPTG.

Our next specific aim was to determine if the presence or absence of aptamers caused an effect on the extracellular drug concentration. For that purpose, HPLC detection of fluorescent ligand labeled aminoglycoside was used. First we investigated the neomycin-B concentration range that can be detected with this method. It was evident from the results that the concentration range of neomycin-B used in the experiments could be detected by HPLC. Kanamycin-A was used as a control to determine if the peaks observed for neomycin-B might be due to neomycin-B or an artifact of sample preparation. The results showed that neomycin-B and kanamycin-A chromatogram were separated by HPLC to give distinctive peaks. Both aminoglycosides had been modified with FMOC-Cl. Because the bacterial culture was done in LURIA broth (LB) media we tested whether neomycin-B could be detected in the presence of LB. The HPLC chromatograms for 40% LB showed distinct peaks for the contents of LB, but neomycin-B could not be detected against this background. This could be because the some component in LB was interfering with the neomycin-B separation in the chromatographic column. Then control experiments were performed to see whether the fluorescent reagent used, FMOC-Cl, was limiting. It was concluded that no interfering fluorescence was coming from the other contents in the reaction mixture other than LB. Therefore it was decided to extract the neomycin-B from the LB, neomycin-B mixture by the use of cation exchange chromatography. In order to determine the feasibility of the extracting neomycin-B from LB by the cation exchange chromatography first neomycin-B was passed through the cation exchange column and resolved by the

established HPLC method. This concludes that neomycin-B could be extracted from the cation exchange column with the established conditions and the elutions could be analyzed by the HPLC by the used method. Then LB alone was passed through the cation exchange column and then resolved by the HPLC method. The three consecutive 1M NH_4OH elutions gave the same distinctive peaks on HPLC as the LB that was not passed through the cation exchange column proving that LB could be extracted from the cation exchange column and could be resolved by the established HPLC method. Then mixture of LB and neomycin-B was passed through the cation exchange column and the elutions of the column were directed to established HPLC method along with positive control of neomycin-B and LB mixture that was not passed through the cation exchange column. The chromatograms of the 100% LB and the neomycin-B, LB mixture show the same peaks. This result proves that cation exchange column cannot be used to extract neomycin-B from the LB, neomycin-B mixture. Therefore we can use another method such as aminoglycoside modified with fluorescence ligand as cy3-paromomycin with HPLC or fluorescence spectroscopic detection for extracellular drug concentration variation determination.

In 2009 our group collaborated with Boushaba and Levine, mathematicians in the Department of Mathematics at Iowa State University, to evaluate if aptamers could concentrate drugs inside cells. Our data shows that aptamer expression works as predicted by the mathematical modeling.

With these results it is evident that aptamer expressing cells are inhibited in their growth more by aminoglycoside antibiotics compared to cells expressing the control RNA. This effect is evidenced by lower IC50 and MIC values of the aptamer expressing cells than cells expressing control RNA. These results also confirmed that the aptamer expressing cells also have higher intracellular free drug number than cells expressing control RNA. From the results of experiments with Cy3-paromomycin, it could be concluded that cells expressing the neomycin-B aptamer have more Cy3-paromomycin in the intracellular environment than the cells expressing the control RNA. These results demonstrate that cells with aptamer expression accumulate higher total intracellular drug concentrations (both bound with aptamer and unbound) than cells expressing the control RNA.

In our project we assume mobility of the aptamers plays an important role. Therefore it is important to observe the effect of the aptamer mobility. To test the effect of aptamer mobility for

increasing the intracellular drug concentration we can use single unit aptamers attached to longer RNA molecules that does not affect the aptamer's characteristic properties and binding ability. Another experiment that can be performed in order to serve the same purpose is to use aptamers attached with SHINE-DALGARNO sequence (ribosome binding sequence) and then ribosome binding will increase the apparent molecular weight of the aptamer thereby decreasing the mobility of the aptamer molecule. Other than this, it is important to test the effect of the multi-drug efflux pumps. According to the model, the aptamers work against the drug efflux pumps. AcrD is the drug efflux pump that is expressed by *E. coli* cells to export the aminoglycoside antibiotics. Therefore bacterial growth assays and intracellular drug concentration determination assays can be performed with cells expressing aptamers and cells expressing control RNA with cells engineered to over express AcrD pump and also with cells in which the AcrD is deleted. These experiments could give a more clear understanding of the mechanism by which aptamers increase intracellular drug numbers with regard to action of multi drug efflux pumps.

References

1. Keefe, A.D., Pai, S. and Ellington, A. (2010) Aptamers as therapeutics. *Nat. Rev. Drug Discov.*, **9**, 537-550.

2. Nimjee, S.M., Rusconi, C.P. and Sullenger, B.A. (2005) Aptamers: an emerging class of therapeutics. *Annu.Rev. Med.*, **56**, 555-583.

3. Proske, D., Blank, M., Buhmann, R. and Resch, A. (2005) Aptamers-basic research, drug development, and clinical applications. *Appl. Microbiol. Biotechnol.*, **69**, 367-374.

4. Marro, M.L., Daniels, D.A., McNamee, A., Andrews, D.P., Chapman, T.D., Jiang, M.S., Zining, W., Smith, J.L., Patel, K.K. and Gearing, K.L. (2005) Identification of potent and selective RNA antagonists of the IFN-ç-inducible CXCL10 chemokine. *Biochemistry*, **44**, 8449-8460.

5. Dhar, S., Kolishetti, N., Lippard, S.J. and Farokhzad, O.C. (2011) Targeted delivery of a cisplatin prodrug for safer and more effective prostate cancer therapy in vivo. *Proc. Natl. Acad. Sci., USA*, **108**, 1850-1855.

6. Tucker, B.J. and Breaker, R.R. (2005) Riboswitches as versatile gene control elements. *Curr. Opin. Struct. Biol.*, **15**, 342-348.

7. Tuerk, C. and Gold, L. (1990) Systematic evolution of ligands by exponential enrichment: RNA ligands to bacteriophage T4 DNA polymerase. *Science*, **249**, 550-510.

8. Ellington, A.D. and Szostak, J.W. (1990) In Vitro selection of RNA molecules that bind specific ligands. *Nature*, **346**, 818-822.

9. Mannironi, C., Di-Nardo, A., Fruscoloni, P. and Tocchini-Valentini, G.P. (1997) In vitro selection of dopamine RNA ligands. *Biochemistry*, **36**, 9726-9734.

10. Takahashi, T., Tada, K. and Mihara, H. (2009) RNA aptamers selected against amyloid [small beta]-peptide (A[small beta]) inhibit the aggregation of A[small beta]. *Mol. Biosyst.*, **5**, 986-991.

11. Vinkenborg, J.L., Mayer, G. and Famulok, M. (2012) Aptamer-based affinity labeling of proteins. *Angew. Chem. Int. Ed. Engl.*, **51**, 9176-9180.

12. Jiang, L., Majumdar, A., Hu, W., Jaishree, T.J., Xu, W. and Patel, D.J. (1999) Saccharide–RNA recognition in a complex formed between neomycin-b and an RNA aptamer. *Structure*, **7**, 817-827.

13. Ni, X., Castanares, M., Mukherjee, A. and Lupold, S.E. (2011) Nucleic acid aptamers: clinical applications and promising new horizons. *Curr. Med. Chem.*, **18**, 4206-4214.

14. Chang, Y.M., Donovan, M.J. and Tan, W. (2013) Using aptamers for cancer biomarker discovery. *J. Nucleic Acids*, **2013**, 817-824.

15. Biesecker, G., Dihel, L., Enney, K. and Bendele, R.A. (1998) Derivation of RNA aptamer inhibitors of human complement C5. *Immunopharmacology*, **42**, 219-230.

16. Mayr, F.B., Knobl, P., Jilma, B., Siller-Matula, J.M., Wagner, P.G., Schaub, R.G., Gilbert, J.C. and Jilma-Stohlawetz, P. (2010) The Aptamer ARC1779 blocks von willebrand factor-dependent platelet function in patients with thrombotic thrombocytopenic purpura ex vivo. *Transfusion*, **50**, 1079-1087.

17. Ninichuk, V., Clauss, S., Kulkarni, O., Schmid, H., Segerer, S., Radomska, E., Eulberg, D., Buchner, K., Selve, N., Klussmann, S. *et al.* (2008) Late onset of Ccl2 blockade with the spiegelmer mNOX-E36-3'PEG prevents glomerulosclerosis and improves glomerular filtration rate in db/db mice. *Am. J. Pathol.*, **172**, 628-637.

18. Givera, L., Bartelb, D.P., Zapp, M.L., Green, M.R. and Ellington, A.D. (1993) Selection and design of high-affinity RNA ligands for HIV-l rev. *Gene*, **137**, 19-24.

19. Bruno, J.G., Carrillo, M.P. and Phillips, T. (2008) In vitro antibacterial effects of anti lipopolysaccharide DNA aptamer–C1qrs complexes. *Folia Microbiol.*, **53**, 295-302.

20. Ireson, C.R. and Kelland, L.R. (2006) Discovery and development of anticancer aptamers. *Mol. Cancer Ther.*, **5**, 2957-2962.

21. Bates, P.J., Laber, D.A., Miller, D.M., Thomas, S.D. and Trent, J.O. (2009) Discovery and development of the G-Rich oligonucleotide AS1411 as a novel treatment for cancer. *Exp. Mol. Pathol.*, **86**, 151-164.

22. Girvan, A.C., Teng, Y., Casson, L.K., Thomas, S.D., Juliger, S., Ball, M.W., Klein, J.B., Pierce, W.M.J., Barve, S.S. and Bates, P.J. (2006) AGRO100 inhibits activation of nuclear factor-kappaB (NF-kappaB) by forming a complex with NF-kappaB essential modulator (NEMO) and nucleolin. *Mol. Cancer Ther.*, **5**, 1790-1799.

23. Soundararajan, S., Chen, W., Spicer, E.K., Courtenay, L.J. and Fernandes, D.J. (2008) The nucleolin targeting aptamer AS1411 destabilizes Bcl-2 messenger RNA in human breast cancer cells. *Cancer Res.*, **68**, 2358-2365.

24. Ng, E.W.M., Shima, D.T., Calias, P., Cunningham, E.T., Guyer, D.R. and Adamis, A.P. (2006) Pegaptanib, a targeted anti-VEGF aptamer for ocular vascular disease. *Nat. Rev. Drug Discov.*, **5**, 123-132.

25. Ruckman, J., Green, L.S., Beeson, J., Waugh, S., Gillette, W.L., Henninger, D.D., Claesson-Welsh, L. and Janjic, N. (1998) 2'-Fluoropyrimidine RNA-based aptamers to the 165-amino acid form of vascular endothelial growth factor (VEGF165): inhibition of receptor binding and VEGF-induced vascular permeability through interactions requiring The exon 7-encoded domain. *J. Biol. Chem.*, **273**, 20556-20567.

26. Kulkarni, O., Pawar, R.D., Purschke, W., Eulberg, D., Selve, N., Buchner, K., Ninichuk, V., Segerer, S., Vielhauer, V., Klussmann, S. *et al.* (2007) Spiegelmer inhibition of CCL2/MCP-1 ameliorates lupus nephritis in MRL-(Fas)lpr mice. *J. Am. Soc. Nephrol.*, **18**, 2350-2358.

27. Burke, D.H. and Nickens, D.G. (2002) Expressing RNA aptamers inside cells to reveal proteome and ribonome function. *Brief. Funct. Genomic. Proteomic.*, **1**, 169-188.

28. Werstruck, G. and Green, M.G. (1998) Controlling gene expression in living cells through small molecule-RNA interactions. *Science*, **282**, 296-298.

29. Thomas, M., Chedin, S., Carles, C., Riva, M., Famulok, M. and Sentenaci, A. (1997) Selective targeting and inhibition of yeast RNA polymerase II by RNA aptamers. *J. Biol. Chem.*, **272**, 27980-27986.

30. Shi, H., Hoffman, B.E. and Lis, J.T. (1997) A Specific RNA hairpin loop structure binds the RNA recognition motifs of the drosophila SR protein B52. *Mol. Cell Biol.*, **17**, 2649-2657.

31. Shi, H., Hoffman, B.E. and Lis, J.T. (1999) RNA aptamers as effective protein antagonists in a multicellular organism. *Proc. Natl. Acad. Sci., USA*, **96**, 10033–10038.

32. Kim, S.J., Kim, M.Y., Lee, J.H., You, J.C. and Jeong, S. (2002) Selection and stabilization of the RNA aptamers against the human immunodeficiency virus type-1 nucleocapsid protein. *Biochem. Biophys. Res. Commun.*, **291**, 925-931.

33. Kim, M.Y. and Jeong, S. (2004) Inhibition of the functions of the nucleocapsid protein of human immunodeficiency virus-1 by an RNA aptamer. *Biochem. Biophys. Res. Commun.*, **320**, 1181-1186.

34. Grate, D. and Wilson, C. (2001) Inducible regulation of the *S. cerevisiae* cell cycle mediated by an RNA aptamer–ligand complex. *Bioorg. Med. Chem.*, **9**, 2565-2570.

35. Tuerk, C., MacDougal, S. and Gold, L. (1992) RNA pseudoknots that inhibit human immunodeficiency virus type 1 reverse transcriptase. *Proc. Natl. Acad. Sci., USA*, **89**, 6988-6992.

36. Kensch, O., Connolly, B.A., Steinhoff, H.J., McGregor, A., Goody, R.S. and Restle, T. (2000) HIV-1 reverse transcriptase-pseudoknot RNA aptamer interaction has a binding affinity in the low picomolar range coupled with high specificity. *J. Biol. Chem.*, **275**, 18271-18278.

37. Nickens, D.G., Patterson, J.T. and Burke, D.H. (2003) Inhibition of HIV-1 reverse transcriptase by RNA aptamers in *Escherichia coli*. *RNA*, **9**, 1029-1033.

38. Homann, M. and Goringer, H.U. (1999) Combinatorial selection of high affinity RNA ligands to live african trypanosomes. *Nucleic Acids Res.*, **27**, 2006-2014.

39. Willis, B. and Arya, D.P. (2006), Clemson University, Clemson,SC.

40. Schroeder, R., Waldsich, C. and Wank, H. (2000) Modulation of RNA function by aminoglycoside. *EMBO J.*, **19**, 1-9.

41. Taber, H.W., Mueller, J.P., Miller, P.F. and Arrow, A.S. (1987) Bacterial uptake of aminoglycoside antibiotics. *Microbiol. Rev.*, **5**, 439-457.

42. Bryan, L.E. and Elzen, H.M.V. (1976) Streptomycin accumulation in susceptible and resistant strains of *Escherichia coli* and *Pseudomonas aeruginosa*. *Antimicrob. Agents Chemother.*, **9**, 928-938.

43. Bryan, L.E. and Kwan, S. (1983) Roles of ribosomal binding, membrane potential, and electron transport in bacterial uptake of streptomycin and gentamicin. *Antimicrob. Agents Chemother.*, **23**, 835-845.

44. Moazed, D. and Noller, H.F. (1987) Interactions of antibiotics with functional sites in 16S ribosomal RNA. *Nature*, **327**, 389-394.

45. Berg, J.M., Tymoczko, J.L. and Stryer, L. (2006) *Biochemistry*. 6th ed. W.H.Freeman and Company, New York.

46. Fourmy, D., Recht, M.I. and Puglisi, J.D. (1998) Binding of neomycin-class aminoglycoside antibiotics to the A-site of 16S rRNA. *J. Mol. Biol*, **277**, 347-362.

47. Fourmy, D., Recht, M.I., Blanchard, S.C. and Puglisi, J.D. (1996) Structure of A-site of *Escherichia coli* 16S ribosomal RNA complexed with an aminoglycoside antibiotic. *Science*, **274**, 1367-1370.

48. Potapov, A.P., Alonso, F.J.T. and Nierhaus, K.H. (1995) Ribosomal decoding process at the codons in the A or P sites depend differently on 2'-OH groups. *J. Biol. Chem.*, **270**, 17680-17684.

49. Yoshizawa, S., Fourmy, D. and Puglisi, J.D. (1999) Recognition of the codon-anticodon helix by ribosomal RNA. *Science*, **285**, 1722-1725.

50. Meier, A., Kirschner, P., Bange, F.C., Vogel, U. and Böttger, E.C. (1994) Genetic alterations in streptomycin-resistant *Mycobacterium tuberculosis*: mapping of mutations conferring resistance. *Antimicrob. Agents Chemother.*, **38**, 228-233.

51. Poole, K. (2005) Efflux-mediated antimicrobial resistance. *J. Antimicrob. Chemother.*, **56**, 20-51.

52. Webber, M.A. and Piddock, L.J.V. (2002) The Importance of efflux pumps in bacterial antibiotic resistance. *J. Antimicrob. Chemother.*, **51**, 9-11.

53. Rosenberg, E.Y., Ma, D. and Nikaido, H. (2000) Aminoglycoside efflux pump AcrD of *Escherichia coli* Is an aminoglycoside efflux pump. *J. Bacteriol.*, **182**, 1754-1758.

54. Hare, R.S. and Miller, G.H. (1984) Mechanisms of aminoglycoside resistance. *The Antimicrobic Newsletter*, **1**, 77-84.

55. Wright, G.D. and Thompson, P.R. (1999) Aminoglycoside phosphotransferases: proteins, structure and mechanism. *Front. Biosci.*, **4**, 9-21.

56. Jin, E., Katritch, V., Olson, W.K., Kharatisvili, M., Abagyan, R. and Pilch, D.S. (2000) Aminoglycoside binding in the major groove of duplex RNA: the thermodynamic and electrostatic forces that govern recognition. *J. Mol. Biol*, **298**, 95-110.

57. Werstruck, G., Zapp, M.L. and Green, M.R. (1996) A non-canonical base pair with in the human immunodeficiency virus rev-responsive element is involved in both rev and small molecule recognition. *Chem. Biol.*, **3**, 129-137.

58. Wang, S., Huber, P.W., Cui, M., Czarnik, A.W. and Mei, H.Y. (1998) Binding of neomycin to the TAR element of HIV-1 RNA induces dissociation of tat protein by an allosteric mechanism. *Biochemistry*, **37**, 5549-5557.

59. Ahsen, U.V., Davies, J. and Schroeder, R. (1991) Antibiotic inhibition of group 1 ribozyme function. *Nature*, **353**, 368-370.

60. Stage, T.K., Hertel, K.J. and Uhlenbeck, O.C. (1995) Inhibition of the hammerhead ribozyme by neomycin-b. *RNA*, **1**.

61. Tok, J.B.H., Cho, J. and Rando, R.R. (1998) Aminoglycoside antibiotics are able to specifically bind the 5¢-untranslated region of thymidylate synthase messenger RNA. *Biochemistry*, **38**, 199-206.

62. Jiang, L., Majumdar, A., Hu, W., Jaishree, T.J., Xu, W. and Patel, D.J. (1999) Saccharide–RNA recognition in a complex formed between neomycin-b and an RNA aptamer. *Structure*, **7**, 817-827.

63. Ilgu, M. (2012), Iowa State University, Ames, IA.

64. Madigan, M.T. and Martinko, J.M. (2006) *Biology of microorganisms* 11th ed. Pearson education, Inc., New Jersey.

65. Vogt, R.L. and Dippold, L. (2005) *Escherichia coli* O157:H7 outbreak associated with consumption of ground beef, June–July 2002. *Public Health Reports*, **120**, 174-178.

66. Bentley, R. and Meganathan, R. (1982) Biosynthesis of vitamin K (Menaquinone) in bacteria. *Microbiol. Rev.*, **46**, 241-280.

67. Hudault, S., Guignot, J. and Servin, A.L. (2001) *Escherichia coli* strains colonising the gastrointestinal tract protect germ free mice against *Salmonella typhimurium* infection. *Gut*, **49**, 47-55.

68. Reid, G., Howard, J. and Gan, B.S. (2001) Can bacterial interference prevent infection? *Trends Microbiol.*, **9**, 424-428.

69. Kubitschek, H.E. (1990) Cell volume increase in *Escherichia coli* after shifts to richer media. *J. Bacteriol.*, **172**, 94-101.

70. Fotadar, U., Zaveloff, P. and Terracio, L. (2005) Growth of *Escherichia coli* at elevated temperatures. *J. Basic Microbiol.*, **45**, 403-404.

71. Ingledew, W.J. and Poole, R.K. (1984) The respiratory chains of *Escherichia coli*. *Microbiol. Rev.*, **48**, 222-271.

72. Alcamo, I.E. (2001) *Fundamentals of microbiology*. 6th ed. Jones & Bartlett Learning, Boston.

73. Harold, F.M. (1972) Conservation and transformation of energy by bacterial membranes. *Bacteriological Reviews*, **36**, 172-230.

74. Thanbichler, M., Wang, S.C. and Shapiro, L. (2005) The bacterial nucleoid: a highly organized and dynamic structure. *J. Cell Biochem.*, **96**, 506-521.

75. Brimacombe, R., StofJIer, G. and Wittmann, H.G. (1978) Ribosome structure. *Ann. Rev. Biochem.*, **47**, 217-249.

76. Poehlsgaard, J. and Douthwaite, S. (2005) The bacterial ribosome as a target for antibiotics. *Nat. Rev. Microbiol.*, **3**, 870-881.

77. Graumann, P.L. (2004) Cytoskeletal elements in bacteria. *Curr. Opin. Microbiol.*, **7**, 565-571.

78. Shih, Y.L. and Rothfield, L. (2006) The bacterial cytoskeleton. *Microbiol. Mol. Biol. Rev.*, **70**, 729-754.

79. Gitai, Z. (2005) The new bacterial cell biology: moving parts and subcellular architecture. *Cell*, **120**, 577-586.

80. Norris, V., Blaawen, T.D., Cabin-Flaman, A., Doi, R.H., Harshey, R., Janniere, L., Jimenez-Sanchez, A., Jin, D.J., Levin, P.A., Mileykovskaya, E. *et al.* (2007) Functional taxonomy of bacterial hyperstructures. *Microbiol. Mol. Biol. Rev.*, **71**, 230-253.

81. Koch, A.L. (2002) Control of the bacterial cell cycle by cytoplasmic growth. *Crit. Rev. Microbiol.*, **28**, 61-77.

82. Stewart, E.J., Madden, R., Paul, G. and Taddei, F. (2005) Aging and death in an organism that reproduces by morphologically symmetric division. *PLoS Biol.*, **3**, 295-300.

83. Jacques, M. (1949) The growth of bacterial cultures. *Annu. Rev. Microbiol.*, **3**, 371-384.

84. Prats, C., Lopez, D., Giro, A., Ferrer, J. and Valls, J. (2006) Individual-based modelling of bacterial cultures to study the microscopic causes of the lag phase. *J. Theor. Biol.*, **241**, 939-953.

85. Hecker, M. and Volker, U. (2001) General stress response of *Bacillus subtilis* and other bacteria. *Adv. Microb. Physiol.*, **44**, 545-555.

86. Levasseur, M., Thompson, P.A. and Harrison, P.J. (1993) Physiological acclimation of marine phytoplankton to different nitrogen sources. *J. Phycol.*, **29**, 587-595.

87. Brook, I. (1989) Inoculum effect. *Rev. Infect. Dis.*, **11**, 361-368.

88. Francisco, S. and Carmen, P. (1990) Implications of the inoculum effect. *Rev. Infect. Dis.*, **12**, 369-373.

89. Flides, P. (1940) The mechanism of The anti-bacterial action of mercury. *Brit. J. Exp. Pathol.*, **21**, 67-73.

90. Kenny, G.E. and Cartwright, F.D. (1993) Effect of pH, inoculum size, and incubation time on the susceptibility of *Ureaplasma urealyticum* to erythromycin in vitro. *Clin. Infect. Dis.*, **17**, 215-218.

91. Nenninger, A., Mastroianni, G. and Mullineaux, C.W. (2010) Size dependence of protein diffusion in the cytoplasm of *Escherichia coli*. *J. Bacteriol.*, **192**, 4535-4540.

92. Terry, B.R. and Robards, A.W. (1987) Hydrodynamic radius alone governs the mobility of molecules through plasmodesmata. *Planta*, **171**, 145-157.

93. Robards, A.W. and Lucas, W.J. (1975) Plasmodesmata. *Annu. Rev. Plant. Physiol.*, **26**, 7580-7610.

94. Reits, E.A.J. and Neefjes, J.J. (2001) From fixed to FRAP: measuring protein mobility and activity in living cells. *Nature Cell Biol.*, **3**, 145-148.

95. Politz, J.C., Browne, E.S., Wolf, D.E. and Pederson, T. (1998) Intranuclear diffusion and hybridization state of oligonucleotides measured by fluorescence correlation spectroscopy in living cells. *Proc. Natl. Acad. Sci., USA*, **95**, 6043-6048.

96. Jonsson, P., Jonsson, M.P., Tegenfeldt, J.O. and Hook, F. (2008) A method improving the accuracy of fluorescence recovery after photobleaching analysis. *Biophys. J.*, **95**, 5334-5348.

97. Mika, J.T., Krasnikov, V., Bogaart, G.V.D., Haan, F.D. and Poolman, B. (2011) Evaluation of pulsed-FRAP and conventional-FRAP for determination of protein mobility in prokaryotic cells. *PLoS ONE*, **6**, 371-376.

98. Gradl, G. and Sterrer, S. (2000) Mobility of molecules and particles within the cytoplasm of a living cell.

99. Shav-Tal, Y., Darzacq, X., Shenoy, S.M., Fusco, D., Janicki, S.M., Spector, D.L. and Singer, R.H. (2004) Dynamics of single mRNPs in nuclei of living cells. *Science*, **304**, 1797-1800.

100. Politz, J.C., Tuft, A., Prasanth, K.V., Baudendistel, N., Fogarty, K.E., Lifshitz, L.M., Langowski, J., Spector, D.L. and Pederson, T. (2005) Rapid, diffusional shuttling of poly(A) RNA between nuclear speckles and the nucleoplasm. *Mol. Biol. Cell*, **56**, 1239-1249.

101. Golding, I. and Cox, E.C. (2004) RNA dynamics in live *Escherichia coli* cells. *Proc. Natl. Acad. Sci., USA*, **101**, 11310-11315.

102. Singer, H.R. (1993) RNA zipcodes for cytoplasmic addresses. *Curr. Biol.*, **3**, 719-721.

103. Lawrence, J.B. and Singer, H.R. (1986) Intracellular localization of messenger RNAs for cytoskeletal proteins. *Cell*, **45**, 407-415.

104. Johnston, S.D. (1995) The intracellular localization of messenger RNAs. *Cell*, **81**, 161-170.

105. Ross, A.F., Oleynikov, Y., Kislauskis, E.H., Taneja, K.L. and Singer, H.R. (1997) Characterization of a beta-actin mRNA zipcode-binding protein. *Mol. Cell Biol.*, **17**, 2158-2165.

106. Latham, V.M.J., Kislauskis, E.H., Singer, H., R. and Ross, A.F. (1994) 13-Actin mRNA localization is regulated by signal transduction mechanisms. *J. Cell Biol.*, **126**, 1211-1219.

107. Sundell, C.L. and Singer, R.H. (1990) Actin mRNA localizes in the absence of protein synthesis. *J. Cell Biol.*, **111**, 2397-2403.

108. Elowitz, M.B., Surette, M.G., Wolf, P.E., Stock, J.B. and Leibler, S. (1999) Protein mobility in the cytoplasm of *Escherichia coli*. *J. Bacteriol.*, **181**, 197-203.

109. Gottesman, M.M., Fojo, T. and Bates, S.E. (2002) Multidrug resistance in cancer: role of ATP-dependent transporters. *Nat. Rev. Cancer*, **2**, 48-58.

110. Moitra, K., Lou, H. and Dean, M. (2011) Multidrug efflux pumps and cancer stem cells: insights into multidrug resistance and therapeutic development. *Clin. Pharmacol. Ther.*, **89**, 491-502.

111. Boushaba, K., Levine, H. and Hamilton, M.N. (2009) A mathematical feasibility argument for the use of aptamers in chemotherapy and imaging. *Math. Biosci.*, **220**, 131-142.